ANALYSIS OF A NATURAL GAS COMBINED CYCLE POWERPLANT MODELED FOR CARBON CAPTURE WITH VARIANCE OF OXY-COMBUSTION CHARACTERISTICS

by

MATTHEW JOSEPH BRESHEARS

A THESIS

Submitted in partial fulfillment of the requirements
for the degree of Master of Science in the
Department of Mechanical Engineering
in the Graduate School of
The University of Alabama

TUSCALOOSA, ALABAMA

2011

ABSTRACT

The world's ever growing demand for energy has resulted in increased consumption of fossil fuels for electricity generation. The emissions from this combustion have contributed to increasing ambient levels of carbon dioxide in the atmosphere. Many efforts have been made to curb and reduce carbon dioxide emissions in the most efficient manner.

The computer process modeling software CHEMCAD was used to model a natural gas combined cycle powerplant for carbon capture and sequestration. Equipment for two proven carbon capture techniques, oxy-combustion and post-combustion amine scrubbing, were modeled. The necessary components modeled included an air separation unit, powerplant, amine scrubbing unit, and a carbon dioxide compression and drying unit. The oxygen concentration in the oxidizer supplied to the powerplant was varied from ambient air, 21%, to nearly pure oxygen, 99.6%. Exhaust gas recirculation was incorporated to maintain a constant combustion temperature. At ambient conditions no air separation unit was necessary and all carbon capture was provided by the amine scrubbing unit. At concentrations ranging from 22 – 99% both oxy-combustion and amine scrubbing techniques are used at inversely varying degrees. At 99.6%, no amine scrubbing unit was necessary. As the oxygen concentration was varied operational parameters were investigated with the goal of identifying optimum operational conditions.

Across the varying oxygen concentrations, the First Law efficiency losses ranged from 3.3 – 13.6%. The optimal operational point occurred when ambient air was supplied and exhaust gas recirculation was utilized for flame temperature control. A Second Law efficiency of 52.2% was maximized at an oxygen concentration of 22%. This corresponds to a 2.28% reduction in

Second Law efficiency. An exergy analysis of each component identified the air separation unit as the component where the most improvements are possible. At 99% oxygen concentration, the Second Law efficiency of the air separation unit was 3%. Through modeling a natural gas combined cycle powerplant for carbon capture and varying the oxy-combustion characteristics, valuable information was gained in the understanding of operational losses associated with carbon capture.

ACKNOWLEDGMENTS

Many people have contributed, in many ways, to the completion of this thesis. Without their support and encouragement, completion would not have been possible. I would first like to thank Dr. Clark Midkiff for his wisdom, guidance, and continual support. In serving as my faculty advisor, he has provided both professional guidance and invaluable friendship. Additionally, I would like to thank Dr. Keith Woodbury and Dr. Derek Williamson for serving on the thesis committee. I am extremely grateful for both the knowledge I have received in their courses, as well as their willingness to commit the necessary time for committee service.

Without a doubt, my family has been greatly influential in the completion of this work. My parents, Dean and Joan Breshears, and siblings, Jamie, Jonathan, Sarah Beth, and Rachel, have been all a person could ask for. I am extremely grateful for their encouragement, support, and unwavering love.

I would also like to extend a special thanks to Dr. Stephen Ritchie for his assistance in obtaining the CHEMCAD software. Additionally, I would like to thank my classmate Alan Hewitt for his friendship and occasional technical assistance.

Finally, I would like to thank the many faculty and staff at the University of Alabama, especially in the Mechanical Engineering Department, for the invaluable education I have received.

LIST OF ABBREVIATIONS AND SYMBOLS

ASU	Air separation unit
atm	Atmospheres (pressure unit)
CO_2	Carbon dioxide
EGR	Exhaust gas recirculation
EIA	US Energy Information Administration
EOR	Enhanced Oil Recovery
EPA	Environmental Protection Agency
GJ	Gigajoule
HRSG	Heat recovery steam generator
IEA	International Energy Agency
IPCC	Intergovernmental Panel on Climate Change
kg	Kilogram
kWh	Kilowatt hour
m^3	Cubic meters
MEA	Monoethanolamine
MJ	Megajoule
mol.	Mole
MPa	Megapascal
MW	Megawatt
NAAQS	National Ambient Air Quality Standards

NEED	National Energy Education Development Project
NETL	National Energy Technology Laboratory
NGCC	Natural gas combined cycle
NOAA	National Oceanic and Atmospheric Administration
N_2	Nitrogen
NO_x	Nitrogen oxides
ppb	Part per billion
ppm	Part per million
psi	Pound per square inch
s	Second
T	Short ton

CONTENTS

LIST OF TABLES

LIST OF FIGURES

CHAPTER 1

INTRODUCTION

Since the start of the industrial revolution, mankind has become increasingly dependent on hydrocarbon fuels for the generation of electricity. Currently, 85% of the entire energy needs of the United States are supplied by fossil fuels (Turns, 2000). The increasing combustion of fossil fuels and associated carbon dioxide (CO_2) emissions are creating concerns about climate change. Because of this, interest in efficiently reducing the amount of CO_2 emitted into the atmosphere is growing. A significant source for these emissions is the power generation industry. While coal provides the lion's share of the fuel needs for electricity generation, natural gas is growing in popularity and supply. According to the National Energy Education Development Project (NEED), natural gas provides 21% of The United States' electricity needs (NEED, n.d.). With this consideration in mind, natural gas power generation stations provide a large venue for the possible reduction of CO_2 emissions.

Technology is currently available that allows CO_2 emissions from natural gas combustion to be captured. Multiple techniques have been successfully applied, however, resulting energy penalties have proven to be significant. Two methods considered to be the most promising include post-combustion flue gas scrubbing with an amine solution and oxy-combustion. Investigations into amine scrubbing have shown that total efficiency losses can range from 5.5 – 11% (A. Cormos, Gaspar, Padurean, C. Cormos, & Agachi, 2010). Oxy-combustion efficiency losses can range from 4.8 – 8.5% (Jensen, Musich, Ruby, Steadman, & Harju, 2005). In order for techniques for carbon capture to be effective, the minimum equipment and operational costs

must be implemented. Previous works have only compared carbon capture methods in a mutually exclusive manner, for example, either amine scrubbing or oxy-combustion. With the goal of achieving the optimal means of preventing CO_2 from entering the atmosphere, a combination of both techniques may be viable. Neglecting the impact of capital costs and combining oxy-combustion with post-combustion amine scrubbing will provide a more integrated method for finding the optimum operational conditions.

1.1. Objective

The objectives of this work include: (1) to accurately model a natural gas combined cycle (NGCC) powerplant, (2) accurately model an air separation unit (ASU) that can produce oxygen purities varying from 22% to 99.6%, (3) accurately model an amine CO_2 scrubber, as well as, a CO_2 drying and compression unit, (3) using these models, analyze the operational characteristics of the powerplant and associated carbon capture and sequestration equipment as oxygen concentrations vary from ambient air, 21%, to 99.6% oxygen, (4) perform a First Law efficiency analysis, identifying the optimum operational oxygen concentration, and finally (5), identify, using an exergy analysis and corresponding and Second Law analysis, the portion of the system where the most efficiency improvements can be achieved.

1.2. Organization of Thesis

This thesis is divided into five chapters. Chapter 1, the introduction, describes the current status of electricity generation in the United States and the increasing awareness of CO_2's effect on climate change. Chapter 2 provides the background and fundamental information relevant to carbon capture. Issues discussed include the thermodynamic fundamentals and description of NGCC powerplants, combustion, CO_2 as an emission and its associated effects, CO_2 separation and storage, as well as the available techniques for carbon capture. Chapter 3 describes the

methodology of this study. The process simulation software CHEMCAD and specific modeling components developed for process analysis are described in detail. Chapter 3 is also provided to validate the models developed for this study with results from previous modeling works. Chapter 4 discusses the results of the parameter study, including the effects that varying oxygen purities with oxy-combustion from 21% to 99.6% have on energy requirements for carbon capture. Chapter 5 draws conclusions for operational considerations when capturing carbon, and makes recommendations for future study.

CHAPTER 2

BACKGROUND

The combined cycle powerplant has become more popular in recent years due to its flexibility in power production and relatively inexpensive capital costs. It combines two thermodynamic cycles, the Brayton and the Rankine, to generate power efficiently. A typical plant will combine one or more gas turbines, exhaust heat recovery steam generators (HRSG), steam turbines, and generators to create electricity. Figure 2.1 displays a thermodynamic layout of a combined cycle powerplant.

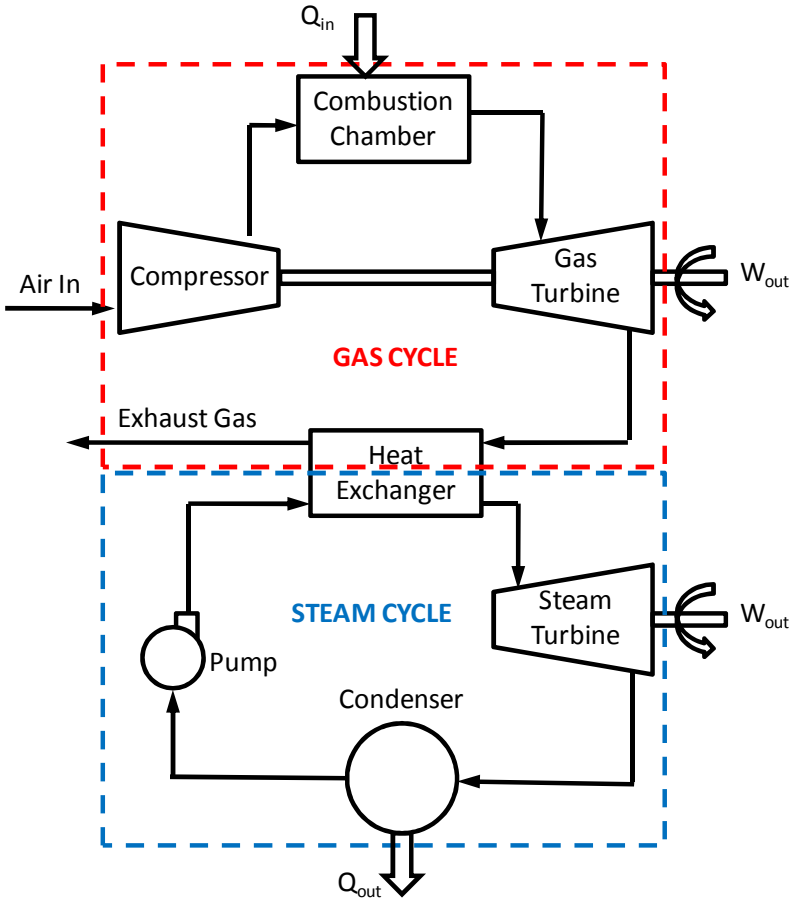

Figure 2.1. Thermodynamic layout of a combined cycle powerplant (Çengel & Boles, 2008).

As seen in Figure 2.1, fuel is burned with air in the gas turbine. The rotation of the turbine produces work. The hot exhaust gases from the gas turbine are used to create steam for the steam cycle. This steam is then used to get more work from a steam turbine. Both rotating shafts on the gas and steam turbines are connected to generators that produce electricity. Additionally, if steam is desired for other processes, some of the steam generated from the HRSG can be removed from the steam cycle. Combined cycle powerplants are usually manufactured with standard components, which are combined to meet specific user needs. These plants can be fueled by a variety of fuels, including natural gas, fuel oils, as well as gasified coal.

2.2. Brayton Cycle / Gas Turbine

Gas turbines operate using the principles of the Brayton cycle. The ideal cycle operates on four internally reversible processes. Figure 2.2 displays a graphical representation of the four thermodynamic states of the Brayton cycle on P - v and T - s diagrams.

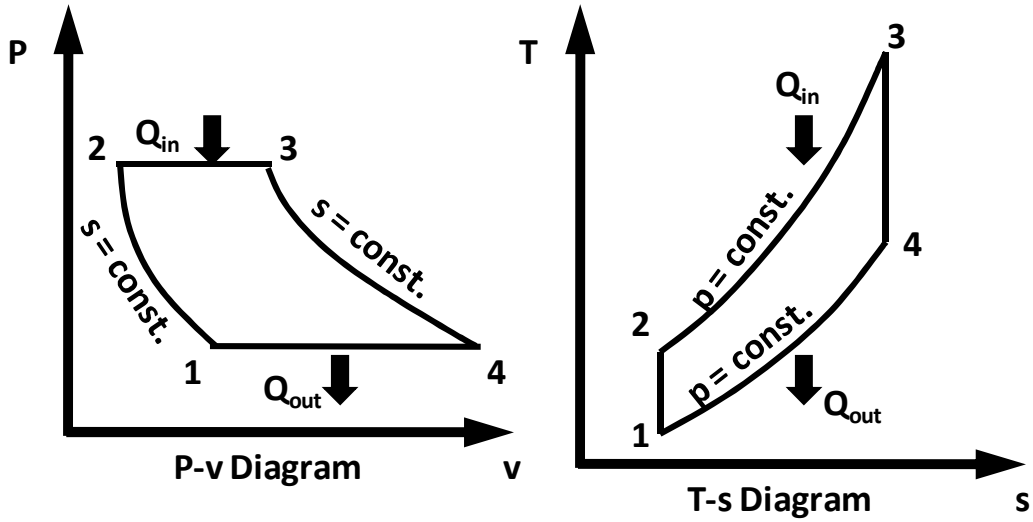

Figure 2.2. Thermodynamic states of the Brayton cycle (Brayton Energy, n.d.).

As depicted in Figure 2.2, the idealized Brayton cycle has four states. At the first state the working fluid has particular properties including temperature, pressure, volume, and entropy.

From state 1 to 2, the fluid undergoes an isentropic, or constant entropy, compression. This increases both the pressure and temperature of the fluid. In a gas turbine, this is carried out by a compressor. From state 2 to 3, the fluid undergoes an isobaric, or constant pressure, heat addition. This heat is added by combustion of fuel with the working fluid, in a gas turbine. From state 3 to 4, the fluid goes through an isentropic expansion. The hot expanding gases create rotation in the turbine. This rotation and expansion not only provide the rotational work for the compressor, but also allow useful shaft work to be produced. From state 4 to 1, fluid in an idealized Brayton cycle undergoes isobaric cooling, where it returns to the properties at state 1, for the cycle to be repeated. Because a gas turbine usually operates on an open cycle, the hot fluid is exhausted from the turbine and new ambient fluid enters the cycle at state 1.

While the ideal Brayton cycle is internally reversible, gas turbines have operational irreversibilities. Both the compression and expansion phases in a gas turbine are not isentropic. Additionally, pressure drops will occur during the heat addition and removal processes. Therefore, efficiencies will never reach that of the ideal cycle. It does, however, provide a model with which comparisons can be made. Assuming constant specific heats, thermal efficiency of the Brayton cycle is given by Equation 2.1.

$$\eta_{th} = \frac{w_{net}}{q_{in}} = 1 - \frac{q_{out}}{q_{in}} = 1 - \frac{c_p(T_4 - T_1)}{c_p(T_3 - T_2)} \tag{2.1}$$

Because the processes from stage 1 to 2 and 3 to 4 are isentropic, $P_2 = P_3$ and $P_4 = P_1$, yielding Equation 2.2.

$$\frac{T_2}{T_1} = \left(\frac{P_2}{P_1}\right)^{(k-1)/k} = \left(\frac{P_3}{P_4}\right)^{(k-1)/k} = \frac{T_3}{T_4} \tag{2.2}$$

When these equations are substituted into the equation for thermal efficiency and reduced, the resulting equation for thermal efficiency for the Brayton cycle is given by Equation 2.3

$$\eta_{th,Brayton} = 1 - \frac{1}{r_p^{(k-1)/k}} \tag{2.3}$$

where,

$$r_p = \frac{P_2}{P_1}$$

and *k* is the specific heat ratio. From these equations, we can see that in order to improve efficiencies in a gas turbine, three variables can be changed. These include, increasing the temperature at which gases enter the turbine (T_3), lowering the temperature at which gas is exhausted from the turbine (T_4), or increasing the pressure ratio (r_p).

2.2. Rankine Cycle / Steam Turbine

The steam turbine in a combined cycle powerplant operates using the principles of the Rankine cycle. Like the Brayton cycle, the ideal Rankine cycle operates on four internally reversible processes. Thermodynamic states of this cycle are depicted in Figure 2.3.

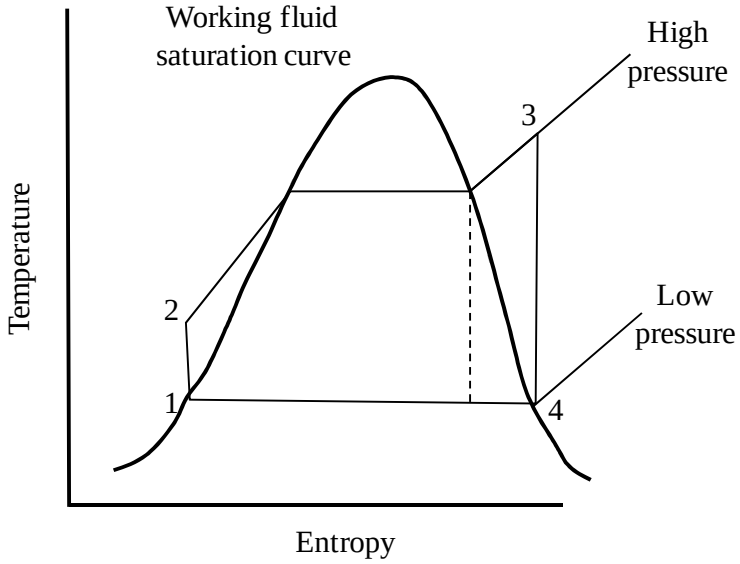

Figure 2.3. Thermodynamic states of the Rankine cycle (Stine & Geyer, 2004).

As depicted in Figure 2.3, the ideal Rankine cycle has four states. At the first state, the working fluid has certain thermodynamic properties; in particular, it must be a saturated liquid. From

point 1 to 2, a pump is used to increase the pressure in the liquid. In the ideal cycle, this is done isentropically. From point 2 to 3, heat is added to the fluid, while maintaining a constant pressure. From state 3 to 4, the now superheated vapor enters a turbine where it expands isentropically. The turbine rotates with this expansion, resulting in the production of shaft work. During this expansion, the pressure and temperature of the fluid decreases. At point 4, the fluid is a saturated liquid - vapor mixture. In order to return the fluid to state 1, a condenser is used to isobarically lower the temperature of the fluid until it is in a liquid state again, ready to repeat the cycle. Unlike the Brayton cycle, the Rankine cycle is usually operated in a closed cycle. The same fluid is reused continually.

The Rankine cycle also gives us a standard of comparison for the efficiencies of steam turbines. The conservation of energy relation for each component is represented by Equations 2.4-7.

$$w_{pump,in} = h_2 - h_1 \tag{2.4}$$

$$q_{boiler,in} = h_3 - h_2 \tag{2.5}$$

$$w_{turbine,out} = h_3 - h_4 \tag{2.6}$$

$$q_{condenser,out} = h_4 - h_1 \tag{2.7}$$

Equation 2.8 becomes the resulting equation for thermal efficiency of the Rankine cycle,

$$\eta_{th,Rankine} = \frac{w_{net}}{q_{in}} = 1 - \frac{q_{out}}{q_{in}} \tag{2.8}$$

where,

$$w_{net} = q_{in} - q_{out} = w_{turb,out} - w_{pump,in}$$

Reductions in steam turbine efficiencies in relation to the ideal Rankine cycle occur due to both, heat losses from the system during operation, as well as, pressure drops across the boiler, condenser, and other components.

2.3. Equipment / Operational Process

The specifics of design are very important in quantifying efficiency of components of combined cycle plants. In looking at the geometry and operation of the equipment in a combined cycle powerplant, we can see their importance.

The gas turbine for power production accomplishes three main tasks. These include the compressing of air, mixing it with fuel and burning, and finally getting work out of the system as the hot gases expand. These tasks are accomplished by the compressor, combustors, and the turbine. In all aspects of gas turbine design, system and material limitations have been pushed to extremes to improve efficiency. Figure 2.4 shows a diagram of the internal components of a modern gas turbine for power production.

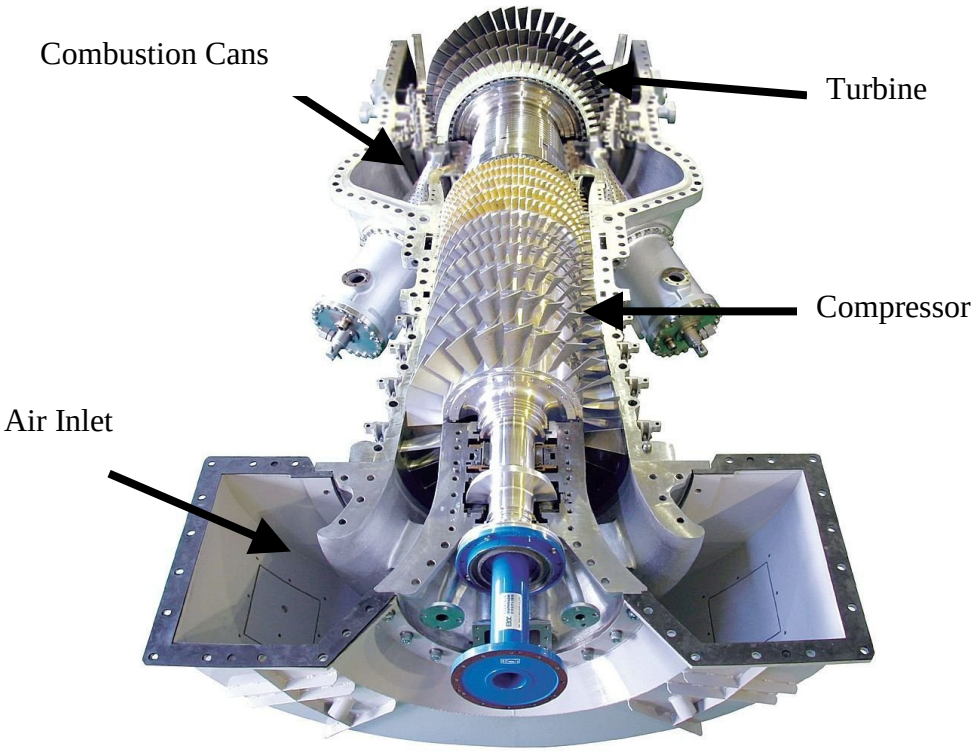

Figure 2.4. Internal components of a gas turbine (Kawasaki Gas Turbine, n.d.).

From Figure 2.4, the layout of an actual gas turbine can be seen. As described earlier, working fluid enters through the inlet. It is drawn in and compressed through the compressor portion of the turbine. Most compressors are axial flow types, with alternating rotating and stationary blades. Much consideration is given to the design of the compressor sections to optimize efficiency. Inter-stage cooling is often present for improved efficiency. Common compression ratios vary from mid-teens, in large stationary turbines, to upwards of 30 in smaller aircraft engines (National Fuel Cell, n.d.).

After being compressed, the warm working fluid enters the combustion portion of the gas turbine. Specialized fuel injection apparati have been developed to improve fuel mixing and encourage even combustion temperatures. Material limitations restrict the flame temperatures achievable by modern gas turbines. Current combustion temperatures can be as high as 2,600˚F (Chase & Kehoe, 2000).

Following combustion, the hot exhaust gases expand through the turbine section of the unit. The expansion of combustion gases impact the turbine blades in such a way that rotational work is created. In order to accommodate these extreme temperatures in the turbine section, many measures have been developed. These include coating turbine blades with ceramics, injecting cooling air into the turbine section, as well as injecting steam into the combustion and turbine sections. A portion of the shaft work created by the turbine is used to turn the compressor, keeping the cycle going. Exhaust gases exit the gas turbine at temperatures, ranging from 650˚F to 1,100˚F depending on design (Çengel & Boles, 2008). As dictated by the thermodynamic principles governing the cycle, larger temperature differences between the combustor to turbine exit result in higher thermodynamic efficiencies. Modern gas turbines have achieved thermal efficiencies of nearly 40% (Çengel & Boles, 2008).

In a combined cycle powerplant, the hot gases exiting from gas turbine are used to generate steam for the steam turbine. This is accomplished by passing the gas through a HRSG. These heat exchangers can vary greatly in size and capability, depending on desired applications. In the case of a combined cycle powerplant, they have three main components, an evaporator, superheater, and economizer. Figure 2.5 displays a typical layout of a HRSG.

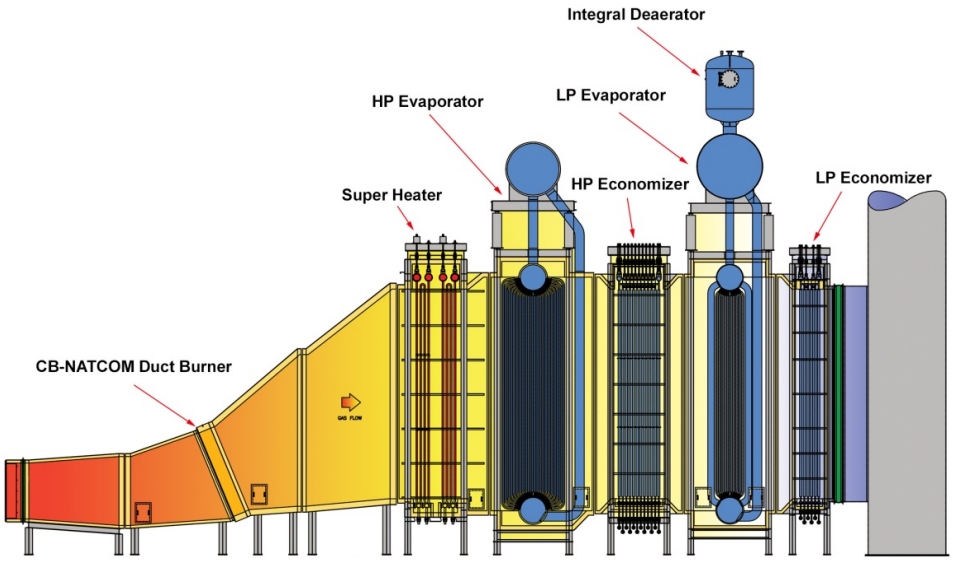

Figure 2.5. Layout of a typical HRSG (Cleaver Brooks, 2006).

Components in a HRSG can be arranged in various ways, depending on desired application. They can be arranged for vertical or horizontal flows of hot gases. Additionally, they can operate at multiple pressure stages. In Figure 2.5, the hot exhaust gas from the gas turbine pass from left to right horizontally through the various components. The economizer takes advantage of the lowest temperature heat to raise the desired working fluid to near its boiling point. The evaporator serves to convert a significant portion of the liquid into a low quality vapor. This steam is then condensed before passing to the superheater. The superheater takes the saturated vapor and further heats it until it becomes superheated steam, ready for entry into the steam turbine. While gas turbine exhaust temperatures entering the HRSG can range from 650˚F to

1,100˚F, they can exit the backside to the HRSG at temperatures ranging from 280˚F to 300˚F (Cleaver Brooks, 2006). On the steam turbine side of the HRSG, condensed feed water can enter units at temperatures ranging from 220˚F to 250˚F and exit as superheated steam at varying pressures and at temperatures around 1,000˚F (Ganapathy, 2001).

The thermodynamic fundamentals of heat transfer determine HRSG performance. Equation 2.9 is the driving equation for this steady flow process

$$Q = M * C_p * \Delta T \tag{2.9}$$

where, Q is the heat transfer, M is the gas turbine exhaust mass flow rate, C_p is the specific heat of the exhaust gas, and ΔT is the difference in turbine exhaust inlet and exit temperature. Special consideration has to be given to the stream inlet and outlet conditions. In HRSG design, the flow of the working fluids is countercurrent. Figure 2.6 shows the temperature profiles of both the gas turbine exhaust and steam turbine fluid through a single pressure HRSG.

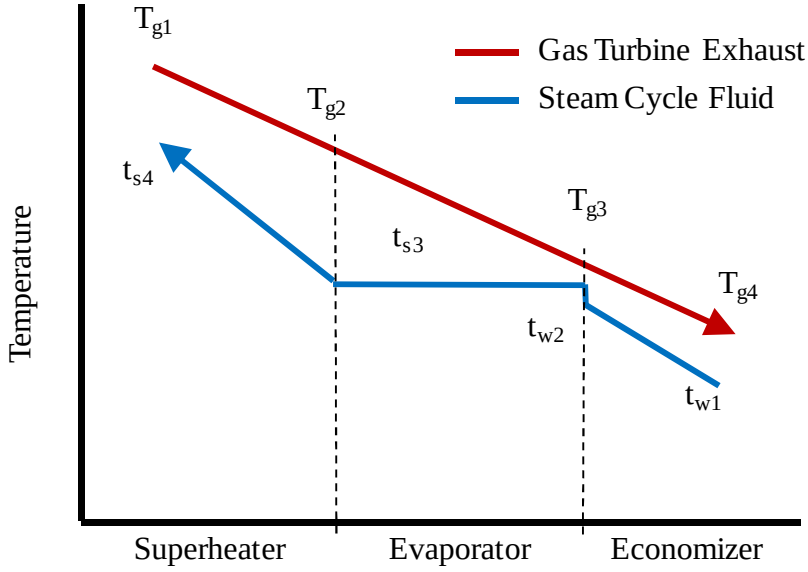

Figure 2.6. HRSG temperature profile.

The top line represents the decrease in temperature of the gas turbine exhaust as it passes through the HRSG from left to right. The bottom line represents the temperature of the water and steam

as it is heated. A critical design parameter is the difference in T_{g3} and t_{w2}. This point is referred to as the pinch point and constrains the minimum temperature difference that can be achieved between the water and exhaust gas.

Upon passing through the HRSG, the cooled gas turbine exhaust is vented into the atmosphere and the superheated steam enters the steam turbine. The steam turbine consists of several components. These include the multiple pressure turbine stages, condensate pumps, boiler feedwater pumps and a cooling system. Figure 2.7 displays a cross section of a Siemens steam turbine.

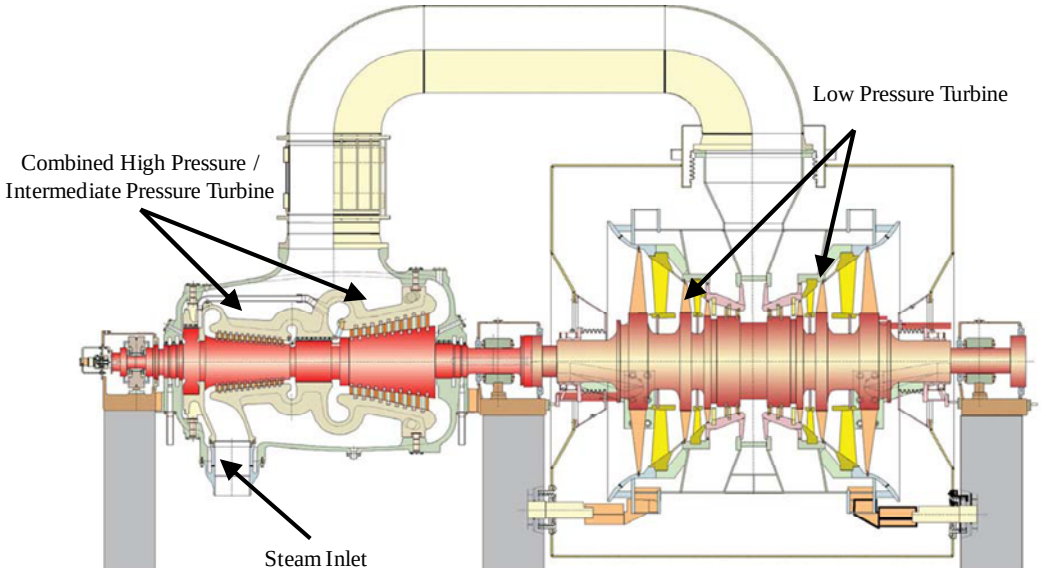

Figure 2.7. Siemens SST-5000 steam turbine (Siemens AG, 2008a).

As the superheated steam expands through the different turbine stages, it creates rotational movement of the shaft. This shaft is coupled to an electric generator for the conversion of shaft power to electricity. Upon exiting the final turbine stage, the steam has cooled and expanded greatly and is at pressures much less than atmospheric. It is a saturated liquid - vapor mixture. From here, the fluid passes through a condenser where further heat is removed, until it becomes a saturated liquid. Condensers can use air, dry type, or water, wet type, to remove the excess heat.

The fluid then proceeds to the boiler feedwater pumps, where the pressure is increased and the liquid returns to the HRSG to repeat the cycle. Many efforts have been made to increase the efficiency of the steam cycle, including lowering condenser pressure, increasing the temperature of the superheated steam, increasing the pressure of the steam, as well as reheating the steam between different turbine stages. These efforts have allowed modern steam turbines to reach thermal efficiencies of 40% (Çengel & Boles, 2008).

Configurations of combined cycle powerplants can differ greatly. Some arrangements include two gas turbines with their own HRSG's providing steam for one steam turbine. Additionally, they can include multiple electric generators. Figure 2.8 displays General Electric's single-shaft and multi-shaft configurations for combined cycle plants

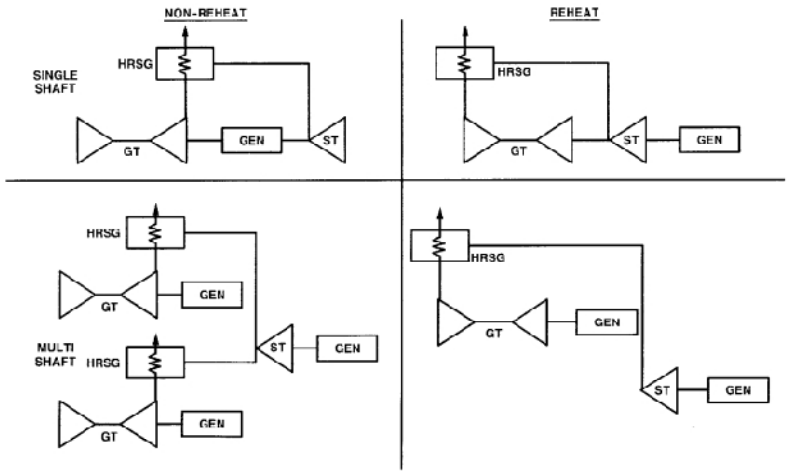

Figure 2.8. General Electric's available configurations for combined cycle powerplants (Chase & Kehoe, 2000).

In each case, the generators are attached to the shafts of the gas and steam turbines to convert rotational motion into electricity. Generators work by converting mechanical energy into electrical energy. Modern generators have efficiencies approaching 97% (Çengel & Boles, 2008).

With the multiple components of combined cycle powerplants, great flexibility in application and improved efficiencies can be achieved. In real world situations, this flexibility is very important. If desired, the gas turbine can be used without operation of the steam turbine. Additionally, portions of the steam generated from the HRSG can be used for power production in the steam turbine or for other processes. Further power generation can be achieved by burning additional natural gas in the HRSG during hours of peak demand. While individually, the gas and steam turbines have efficiencies approaching 40%, when operated in the combined cycle layout, thermal efficiencies can reach 60% LHV (Chase & Kehoe, 2000).

2.4. Combustion Fundamentals

The process of combustion has been a part of society since the discovery of fire. Modern combustion processes for energy production involve the consumption of hydrocarbon fossil fuels. Whether burning coal, natural gas, biofuels or refined petroleum products, the chemistry of combustion is similar. When a hydrocarbon based fuel is combined with O_2 and heat, exothermic chemical reactions occur. These reactions produce combustion products namely CO_2, heat, and water. Equation 2.10 represents a generic combustion equation for hydrocarbon fuel in air.

$$Fuel + Oxidizer \rightarrow Products \tag{2.10}$$

Several thermodynamic fundamentals govern the combustion process. These thermodynamic principles include the conservation of mass and conservation of energy. Conservation of mass allows us to balance a given chemical reaction equation. Given a specific fuel and oxidizer combination, the resulting products and quantities can be determined. This is critical in determining the necessary fuel and oxidizer feed rates in order to control a combustion process. The complete reaction during combustion of all fuel and oxidizer is called the stoichiometric reaction. If excess oxidizer is present in the products, the combustion process is

considered lean. If excess fuel is present, the reaction is considered rich. This principle can have drastic impacts on what flame temperatures are achieved, as well as reaction products. The term air - fuel ratio has been developed to describe the ratio of air to fuel on either a mass or mole basis, although the mass basis is much more commonly employed in combustion calculations. The equivalence ratio, Φ, is a way to compare the air - fuel ratio of an arbitrary air - fuel mixture to its stoichiometric ratio. The equation for equivalence ratio is given by Equation 2.11.

$$\Phi = \frac{\left(\frac{A}{F}\right)_{stoic}}{\left(\frac{A}{F}\right)} \tag{2.11}$$

Its usefulness can be seen in the effect that increasing and decreasing the equivalence ratio has on adiabatic flame temperatures of several fuels. Figure 2.9 displays the adiabatic flame temperature for varying equivalence ratios of various hydrocarbon fuels.

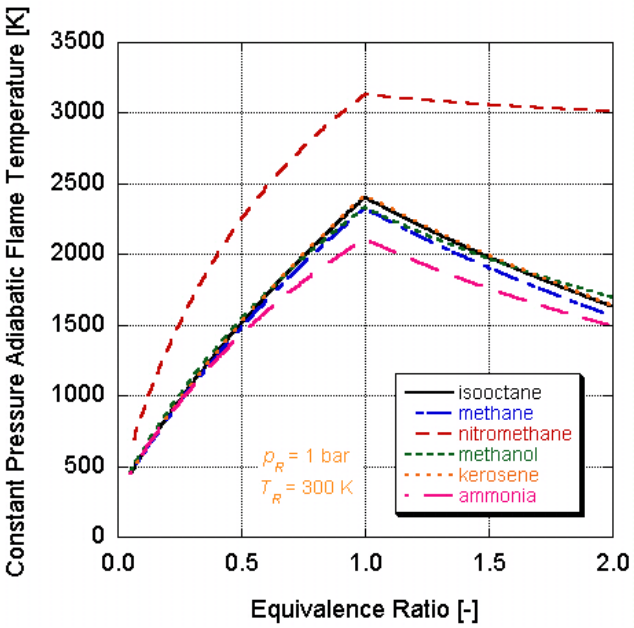

Figure 2.9. Adiabatic flame temperatures of various fuels through varying equivalence ratios (Flame temperatures, n.d.).

The conservation of energy principle allows us to determine the amount of heat that is released by a combustion reaction. From conditions prior to combustion, to post-combustion conditions, the amount of energy in a defined control volume must remain the same. This principle (the First Law) is represented by the Equation 2.12

$$ {}_1Q_2 - {}_1W_2 = \Delta E_{1-2} \tag{2.12} $$

where *Q* is the heat added to a system going from state 1 to 2, *W* is the work done by a system going from state 1 to 2, and *ΔE* is the change in total system energy from state 1 to 2. The *ΔE* term includes internal, kinetic, and potential energy. This principle becomes very useful in determining what temperatures a combustion process achieves. Neglecting changes in kinetic and potential energies, as well as, assuming that no work is done and the reaction occurs adiabatically, allows Equation 2.12 to be reduced to:

$$ \sum_{reac} n_i\left(\bar{h}_f^\circ + \Delta\bar{h}\right)_i = \sum_{prod} n_i\left(\bar{h}_f^\circ + \Delta\bar{h}\right)_i \tag{2.13} $$

where *n* is number of moles of the reactants and products, $\bar{h}_f^\circ$ is the enthalpy of formation at a reference temperature, and $\Delta\bar{h}$ is enthalpy of formation at the adiabatic flame temperature. From this equation, the flame temperature can be found using an average value of c_p, values of c_p varying with temperature change, or tabulated values for gas enthalpy.

While Equation 2.13 represents a very simplified method for calculating flame temperature, realities such as dissociation, incomplete combustion, and heat transfer all affect accuracy. Figure 2.10 displays the actual path of temperature rise compared to the percentage completion of a reaction.

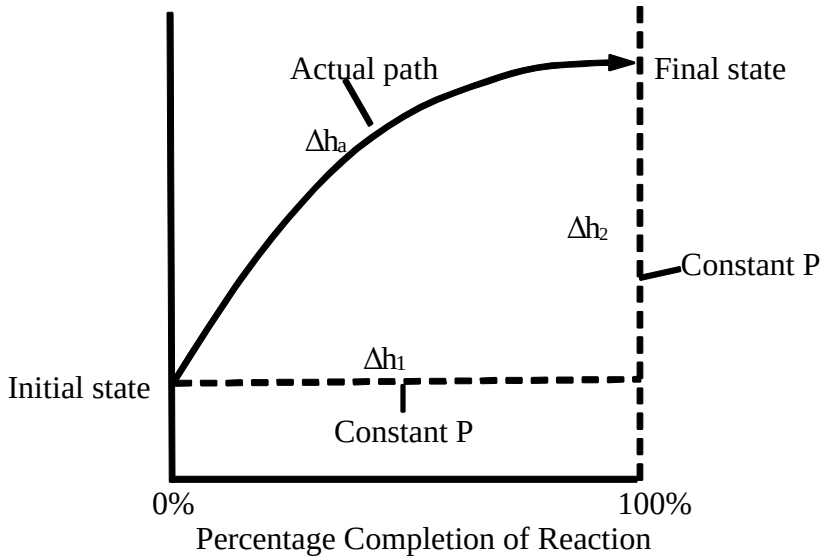

Figure 2.10. Increase in temperature as a function of reaction completion percentage (Adiabatic Flame Temperature, n.d.).

The method used to calculate the final temperature state follows the dotted line and assumes 100% complete combustion.

Combustion chemistry and thermodynamics in the gas turbine engine in a combined cycle powerplant are significant. As the goal of a power generating station is to generate electricity at the lowest cost possible, optimum fuel consumption is necessary. A constant flame temperature at the design limits of the gas turbine, coupled with complete fuel consumption is desired. As seen in Figure 2.9, adiabatic flame temperatures of hydrocarbons at stoichiometric conditions, or an equivalence ratio of 1, exceed the thermal limits of most materials. In order to reduce these temperatures to levels that can be tolerated by turbines, excess air is used. This reduces the equivalence ratio below 1 and gives operators, air control to achieve desired combustion temperatures. Using excess air, as opposed to excess fuel, where $\Phi > 1$, is nearly always implemented because of the expense involved with fuel vs. free air. Additionally, unburned hydrocarbons in exhaust are themselves regulated pollutants and serve as sources of particulate pollution.

An important part of combustion deals with the products. While the benefits of combustion include the heat and resulting work, the other products have implications as well. The majority of by-products from hydrocarbon combustion with ambient air include water, CO_2, and a significant amount of nitrogen. While the water, nitrogen, and CO_2 all occur naturally in our atmosphere, minor reactions, species and incomplete combustion can produce more harmful products. Several of these include sulfur dioxide, nitrogen oxides, particulate matter, as well as trace metals, depending on fuel source. Controlling aspects of combustion can help reduce the emission levels of these undesirable products.

An important unwanted byproduct of combustion are nitrogen oxides or NO_x. NO_x reacts in the atmosphere to contribute to acid rain and photochemical smog. The Environmental Protection Agency (EPA) has established National Ambient Air Quality Standards (NAAQS) for levels of NO_x in the ambient air at 53 ppb annual average (EPA, 2010b). Limitations such as this have led major emitters such as powerplants to take measures to reduce their emissions. NO_x can be created by three primary mechanisms. These include the N_2O, thermal, and prompt mechanisms. The N_2O mechanism occurs in three steps represented by Equations 2.14 – 16.

$$O + N_2 + M \leftrightarrow N_2O + M \tag{2.14}$$

$$H + N_2O \leftrightarrow NO + NH \tag{2.15}$$

$$NO + N_2O \leftrightarrow NO + NO \tag{2.16}$$

The N_2O mechanism is prevalent at equivalence ratios less than 0.8, very common in gas turbine engines (Turns, 2000). The thermal NO_x mechanism is prevalent at temperatures greater than 1,800 K, and is carried out in two reactions given by Equations 2.17 – 18.

$$O + N_2 \leftrightarrow NO + N \tag{2.17}$$

$$N + O_2 \leftrightarrow NO + O \tag{2.18}$$

The prompt NO_x mechanism occurs rapidly following the reactions represented by Equations 2.19 - 20.

$$CH + N_2 \leftrightarrow HCN + N \quad (2.19)$$

$$C + N_2 \leftrightarrow CN + N \quad (2.20)$$

The prompt NO_x mechanism is prevalent at equivalence ratios larger than 1.2. Figure 2.11 displays temperature zones in which different types of NO_x formation can occur for varying equivalence ratios.

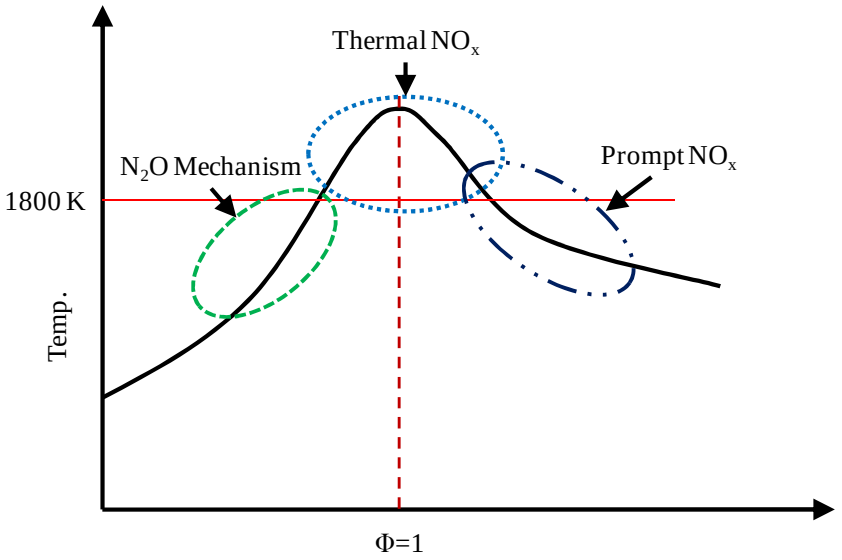

Figure 2.11. NO_x formation mechanisms for varying temperature and equivalence ratio realms.

The preceding three NO_x mechanisms form NO_x from nitrogen in the ambient air. Additional NO_x can be formed if it is contained in the supplied fuel. This is a concern when using coal as a fuel.

Methods to reduce NO_x formation in gas turbines include limiting the adiabatic flame temperature to less than 1,800 K. This is accomplished by increasing the air - fuel ratio. Additional methods include controlling the mixing of fuel and air. Theoretical calculations for flame temperature do not account for irregularities in mixing. If excess oxygen or fuel is present

in areas of the combustion chamber, hotspots occur and undesirable byproducts are formed. In order to ensure proper fuel air mixing, a number of measures are taken. One method is high pressure injection of liquid fuels. The high pressure injection better atomizes the fuel, improving mixing. Additionally, multiple combustors help ensure that temperatures are consistent throughout combustion chambers.

2.5. Carbon Dioxide

Another product of combustion that is of growing concern is CO_2. While CO_2 is naturally present in the atmosphere and is vital in plant photosynthesis, human emissions from combustion have greatly increased over the last 300 years. Figure 2.12 displays the increase in CO_2 emissions from human combustion sources.

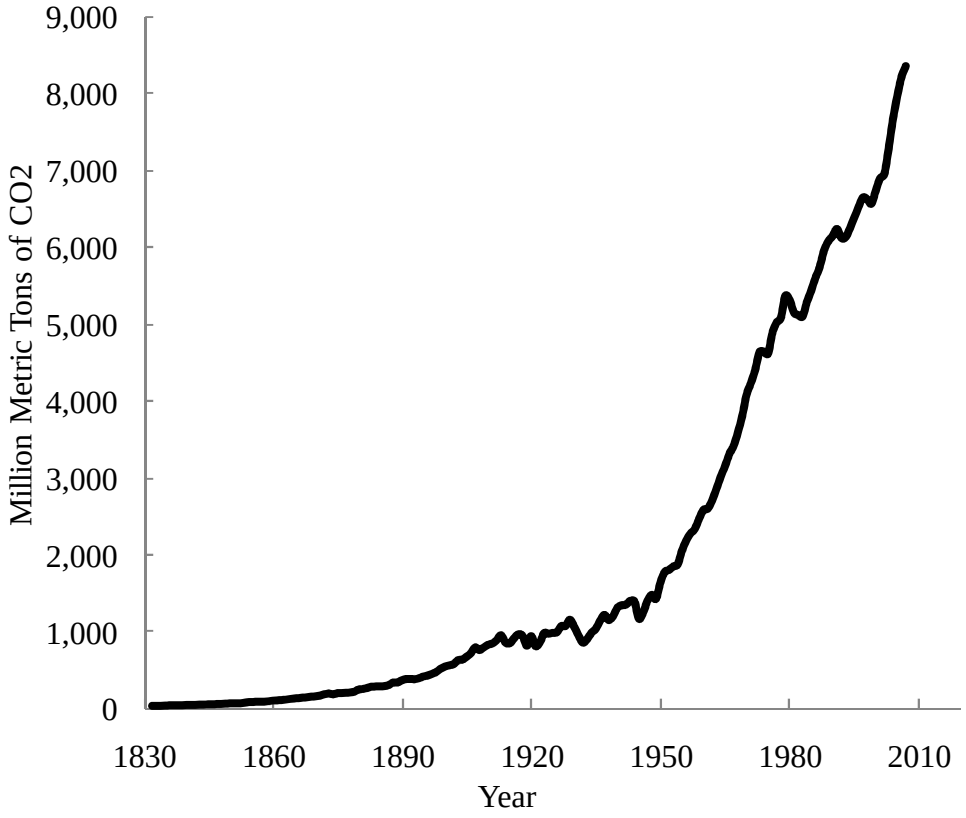

Figure 2.12. Historical global CO_2 emissions (Boden & Marland, 2010).

As seen in Figure 2.12, since the onset of the Industrial Revolution, the amount of CO_2 emissions from combustion sources has increased from 200 million tons in 1850 to over 29 billion tons in 2004 (Boden & Marland, 2010). Fossil fuels serve as a source of fuel for over 85% of the energy needs of the United States (Turns, 2000). In 2008, the United States emitted over 2.3 billion metric tons of CO_2 through the generation of electricity alone. (EPA, 2010a). This is a growing concern because of the impact these emissions are having on the ambient concentrations of CO_2 in the atmosphere. Figure 2.13 shows the increase on atmospheric CO_2 levels over the past 200 years.

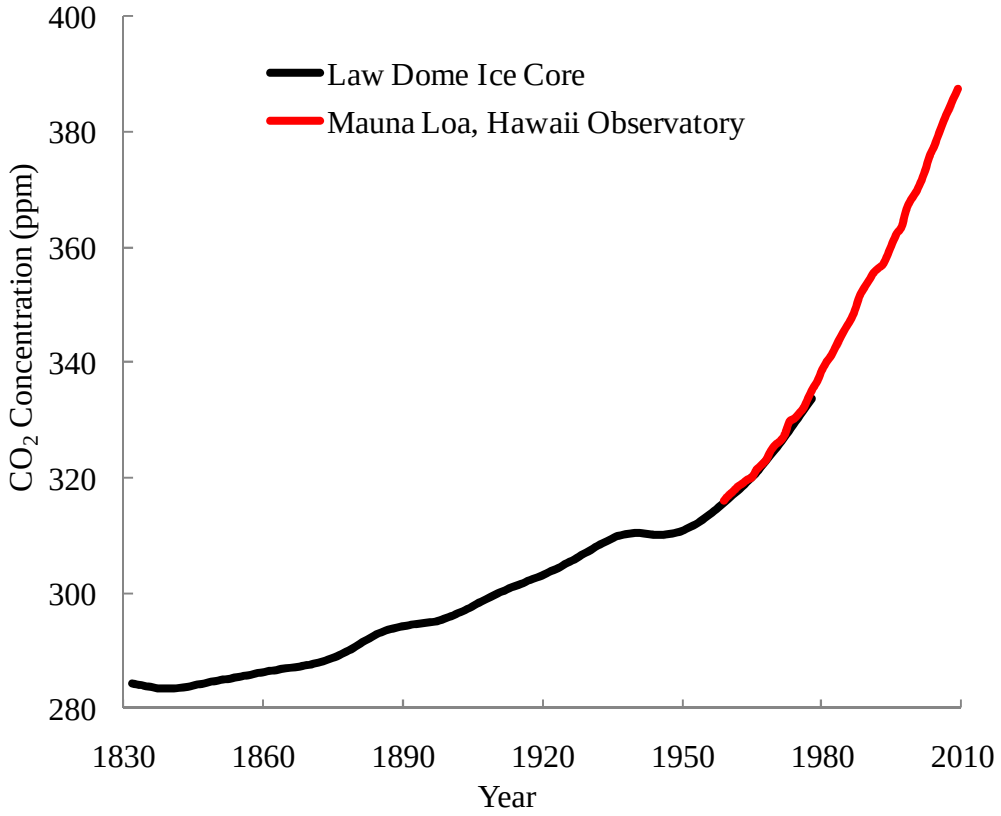

Figure 2.13. CO_2 concentrations from Law Dome, Antarctica Ice Core (Etheridge et al., 1998) and Mauna Loa, Hawaii Observatory (National Oceanic and Atmospheric Administration [NOAA], 2010).

Figure 2.13 was acquired from an ice core in Antarctica. CO_2 concentrations were taken from tiny air pockets trapped in the ice. Ambient levels have continued to increase from the year 2000 concentrations of 368.77 ppm shown in Figure 2.13, to 2010 levels of 389.22 ppm (NOAA, 2010). This is of significance because a correlation can be seen between CO_2 emissions from fossil fuel combustion, of which electricity generation plays a significant portion, and the increase in ambient concentrations of CO_2.

The natural change in ambient CO_2 concentration is part of a global carbon cycle. In this cycle, CO_2 is emitted, stored, and consumed by natural methods. Rates of each aspect are affected by various conditions. Figure 2.14 provides a simplified visual representation of the carbon cycle.

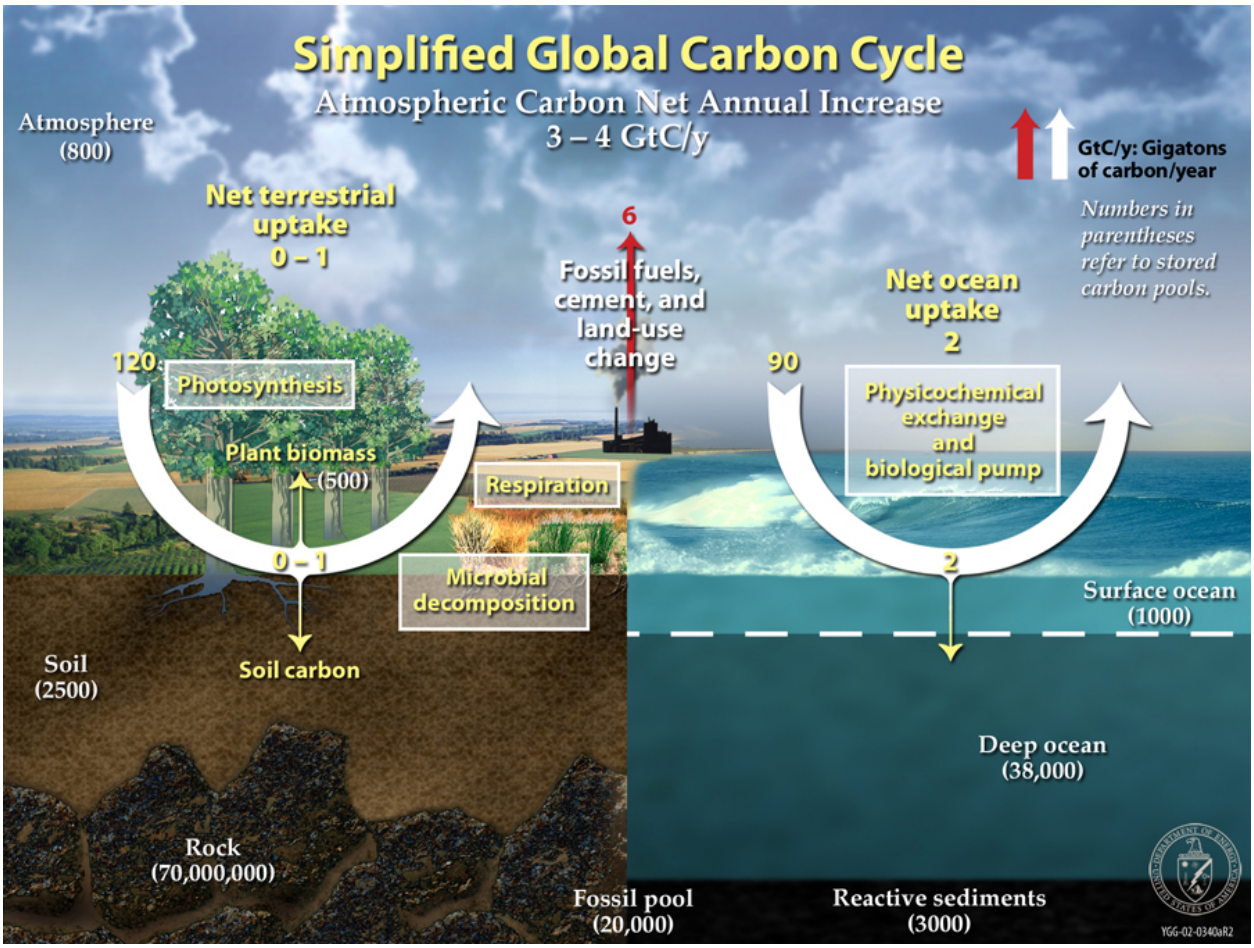

Figure 2.14. The naturally occurring carbon cycle (U.S. Department of Energy Genome Program, 1999).

As seen in Figure 2.14, carbon is naturally emitted through respiration, microbial decomposition, volcanic eruptions, as well as other sources. It is stored in rocks, plant biomass, fossil fuels, as well as the air and ocean. It is consumed through photosynthesis and physicochemical exchanges with the ocean. Concern arises with the emission of CO_2 from unnatural processes. Increased manmade emissions, with no corresponding increase in storage, has lead to the measurable increase in ambient concentrations. An estimated 3.2 billion metric tons of CO_2 is added to the atmosphere annually (Energy Information Administration [EIA], 2004). This is a problem because CO_2 is a greenhouse gas.

2.6. Greenhouse Gases

Greenhouse gases act to regulate the temperature of the earth. Naturally occurring greenhouse gases include CO_2, ozone, NO_x, and methane. These gases function in the stratosphere by allowing visible light from the sun to pass through to the earth, warming it. Infrared energy is then absorbed by the atmosphere. The gases absorb this infrared energy, serving to regulate the earth's temperature. As levels of CO_2 increase due to human consumption of fossil fuels, worries are arising that the earth's temperature will increase, leading to global climate change.

In recent years, worldwide political pressure has been mounting to curb and reduce the emission of CO_2. These efforts have been targeted at all emission sources. Vehicle manufacturers have been required to increase the fuel economies of their fleets. In the electricity generation sector, laws have been passed to reduce the consumption of fossil fuels and increase reliance on renewable and clean fuels. These renewable fuel sources, however, have larger costs per unit of electricity generated. Table 1 compares the costs of a megawatt hour of electricity for different generation sources.

Table 1

Estimated Levelized Cost of New Generation Resources (EIA, 2009)

Plant Type	Capacity Factor (%)	U.S. Average Levelized Costs ($ / MWh)				
		Levelized Capital Cost	Fixed O&M	Variable O&M	Transmission Investment	Total System Levelized Cost
Conventional Coal	85	69.2	3.8	23.9	3.6	100.4
Advanced Coal	85	81.2	5.3	20.4	3.6	110.5
Advanced Coal (CCS	85	92.6	6.3	26.4	3.9	129.3
Natural Gas-fired						
Convential CC	87	22.9	1.7	54.9	3.6	83.1
Advanced CC	87	22.4	1.6	51.7	3.6	79.3
Advanced Nuclear	90	94.9	11.7	9.4	3.0	119.0
Wind	34.4	130.5	10.4	0.0	8.4	149.3
Solar PV	21.7	376.8	6.4	0.0	13.0	396.1
Geothermal	90	88.0	22.9	0.0	4.8	115.7
Hydro	51.4	103.7	3.5	7.1	5.7	119.9

As seen in Table 1, natural gas and coal sources provide a highly competitive source of electricity. They have much lower capital costs as well as reduced operational and management costs. They do, however, have fuel related expenses. Despite this, the total levelized cost for the fossil fueled powerplants is less than that of the renewable sources. For this reason they will

continue to play a significant role in the power generation sector. A cap and tax system has been proposed to encourage the use of renewable fuels. A proposed tax on CO_2 emissions would greatly increase the costs of operations for fossil fuel consuming powerplants making renewable sources competitive. For this reason, efforts have been proposed to capture and store CO_2 emissions.

2.7. Carbon Capture and Sequestration

In order to capture and store the estimated 2.6 billion tons of CO_2 emitted annually by the United States, the most practical and efficient methods must be implemented. Two major challenges exist. Firstly, the CO_2 must be separated from the other components in combustion exhaust gas. Secondly, this CO_2 gas has to be stored or used in other processes that prevent it from entering the atmosphere.

There are five main techniques for the separation of CO_2 from a gas mixture. These include absorption, cryogenic cooling, gas separation membranes, gas absorption membranes, and adsorption. Existing CO_2 separation methods can function over a wide range of pressures, temperatures, and concentrations. Each of these five techniques, however, can be more practical for certain conditions than others.

Absorption is a bulk phase incorporate chemical phenomenon in which a substance in one state is chemically bonded to another substance in another state. In the case of CO_2 separation, it can occur through the use of either physical solvents or chemically reactive solvents. In the case of physical solvents, CO_2 is dissolved into another substance without altering its structure. This method follows Henry's Law given by Equation 2.21,

$$H = \frac{C_{solute}}{C_{solvent}} \tag{2.21}$$

where, C_{solute} is the partial pressure of the particular gas being absorbed, $C_{solvent}$ is the concentration of the particular gas in the solvent, and H is a constant which depends on the solvent, solute, and temperature. Physical solvents work best at high pressures, because the solubility of CO_2 is increased with higher pressures. The CO_2 is recovered by flashing off the CO_2 at lower pressures. Chemically reactive solvents first dissolve CO_2 and then react with it, forming other compounds. Their effectiveness is not altered by pressure changes. CO_2 is recovered from chemically reactive solvents by adding heat. For applications with low operational pressures and CO_2 concentrations this method is more effective.

The second method for CO_2 separation is carried out by cryogenic cooling. In this method, CO_2 is separated by liquefaction. Sufficient CO_2 concentrations must be present for this method to be effective. Figure 2.15 shows the phase diagram of CO_2.

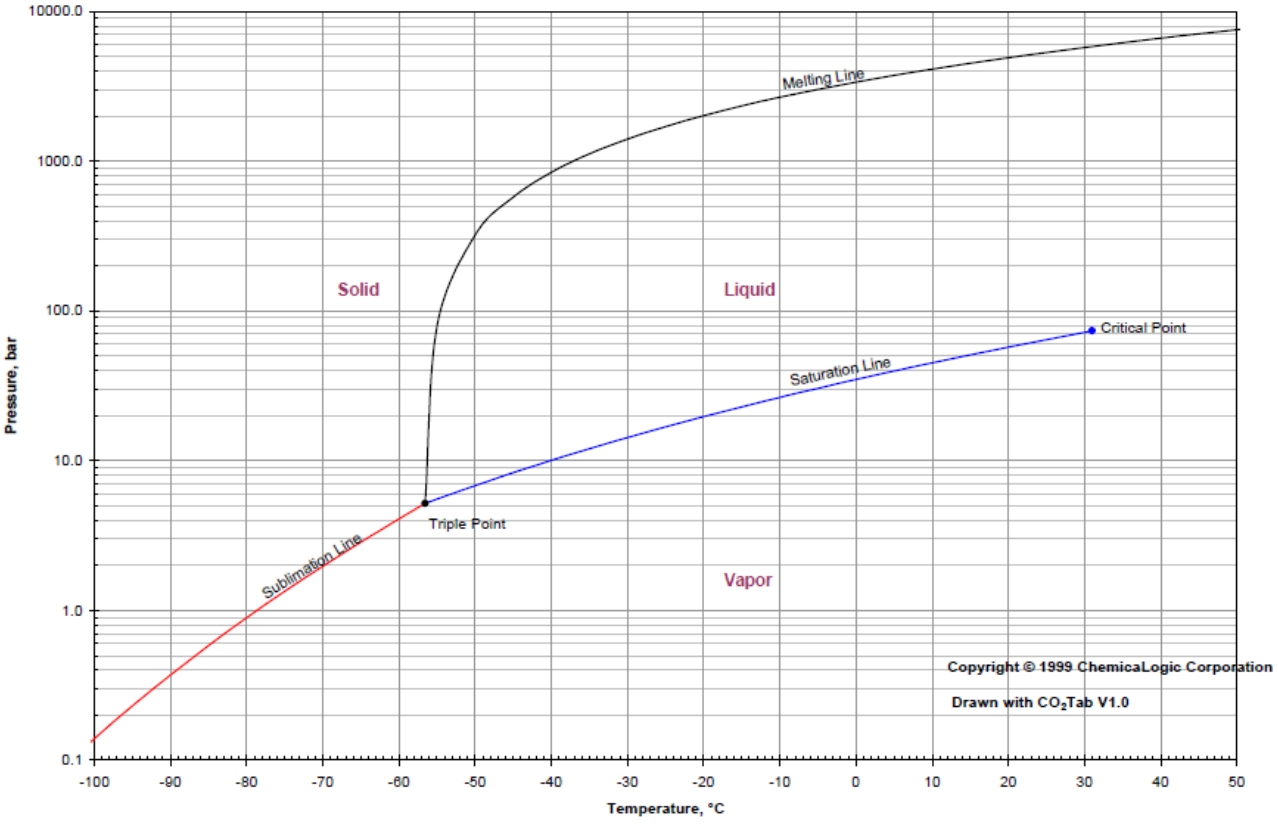

Figure 2.15. CO_2 phase diagram (Chemicalogic, 1999).

By taking advantage of the different sublimation, saturation, and melting lines of different gases, multi-gas streams can be separated into different phases. Three methods for cryogenic separation are used commercially. The first requires that the gas be compressed to 1,100 psi and then cooled with water to a temperature near its critical point. The second requires temperatures between 10˚F and 70˚F and pressures from 250 to 350 psi. To prevent freezing, water vapor must first be removed from the process gas. This method also requires the condensate to pass through a stripper column. The third method cools the process gas until the CO_2 condenses out of the gas phase.

Gas separation membranes use the varying partial pressures of different gases to facilitate separation. A membrane with particular characteristics interacts differently with different gases allowing them to pass through at different rates. Equipment is designed to separate the desired, permeate stream, from the undesired, retentate stream. This method of separation operates most effectively at high pressures and concentrations.

Gas absorption membranes work by serving as a medium for the contact between gases and an absorptive liquid. Unlike gas separation membranes, gas absorption membranes do not have to be selectively permeable. They merely serve as a contacting medium, while keeping flow of gas and liquid separate. The absorption liquid selectively removes a desired product from the gas stream. In the removal of CO_2 from flue gas, monoethanolamine (MEA) is most commonly used.

The fifth method for CO_2 removal is gas adsorption. Unlike absorption, in gas adsorption the CO_2 merely attaches to the surface of a particular compound. CO_2 gas adsorption is accomplished by compounds such as alumina, zeolite, or activated carbon. The gas mixture is passed through a bed of the compound, where CO_2 is selectively attached to the compounds.

Once the compounds become saturated, the CO_2 can be removed in several ways. This is referred to as regeneration. There are four methods for bed regeneration. The first of these is pressure-swing and vacuum pressure-swing adsorption. This involves increasing and decreasing the pressure inside the adsorption bed to capture and remove CO_2. Two or more beds would be in a system so that adsorption and regeneration could continually. The second method for regeneration is thermal swing. In this case changes in temperature encourage adsorption and regeneration of the CO_2. Regeneration can also be accomplished by washing. A clean fluid is passed through the bed removing the CO_2 for capture. A final method for regeneration of the adsorption bed is to use gas to drive off the CO_2. The gas displaces the CO_2 attached to the bed material, allowing it to be captured.

As seen above, there are many options for separating CO_2 from the exhaust gas of a combustion process. Depending on operational aspects, some methods are more effective than others. Even with best case designs, large expenses can be incurred in order to remove CO_2 from a combustion waste-stream.

Once separated, the storage of CO_2 raises many additional issues. Due to the large volume of CO_2 in gaseous form, it must be condensed into liquid state to handle practically. To accomplish this, the gas must be compressed into a liquid. Typical CO_2 transportation temperature and pressures are above 100 atm and below 30˚C.

Current research is being conducted into the feasibility of where to practically store the large volumes of CO_2. Potential storage options include direct injection into extreme depths of the ocean, depleted oil or gas reservoirs, unminable coal seams, as well as saline aquifers. At extreme ocean depths pressures are large enough that the CO_2 would remain in liquid form. CO_2 is also denser than water, allowing it to remain on the ocean floor. Several issues, however, exist.

There are concerns that the CO_2 would react with water to form H_2CO_3, carbonic acid, which could harm the aquatic ecosystem. Additionally, CO_2 reacts to form a solid CO_2, clathrate hydrate, which dissolves in water. Microorganism methanogens may also convert the CO_2 into methane, an even more powerful greenhouse gas. These and other concerns are being studied to better understand the implications of deep ocean sequestration.

Another option for storage is in saline aquifers. These aquifers are very common throughout the world and many are very large. This could be beneficial in minimizing large transportation distances and associated costs. This method has already been successfully demonstrated in the North Sea. The Norwegian company Statoil has been injecting 1 million tons of CO_2 a year into a saline aquifer since 1996 (Statoil, 2009). In the United States, studies are being conducted as to the feasibility for application on land.

Storing CO_2 in depleted oil and natural gas reservoirs is another proven technology. While not done to intentionally prevent CO_2 from entering the atmosphere, CO_2 has been pumped into depleted natural gas and oil reservoirs for the last 40 years. This procedure is referred to as enhanced oil recovery (EOR). The CO_2 displaces the oil and natural gas in a reservoir, allowing for 10 – 15% additional recovery (Biello, 2009). An additional benefit for oil recovery is the fact that CO_2 dissolves into oil, increasing its viscosity. This allows oil to be more easily extracted. Further development of this technology would not only allow for even greater EOR, but also serve as suitable storage for large amounts of CO_2.

Some other beneficial uses for captured CO_2 include injection into unminable coal seams. Coal is porous on its surface. Often, methane gas fills these spaces. When CO_2 is pumped into an unmined coal seam, it displaces this methane. This method of methane displacement was successful in displacing 23 million m^3 of 90% purity methane in the United States in 1996

(International Energy Agency [IEA], n.d.). Further implementation of this technique could provide additional storage capacity for CO_2 emissions. Storage of captured CO_2 in oil and gas reservoirs, or in economically unrecoverable coal seams provides additional benefits in that its side effects include a marketable resource to help offset the cost of implementation. Further studies are currently being undertaken to better understand how CO_2 moves once in these reservoirs, as well as evaluating the possibility for gases to escape.

In the industry, several technologies have been developed for capturing CO_2. These methods include removal of the CO_2 through a post-combustion, pre-combustion, or oxy-combustion process. Post-combustion CO_2 separation involves removing the CO_2 after it has been formed by the chemical reactions of combustion. Pre-combustion techniques involve altering the chemical composition of the fuel, such that CO_2 is removed before the combustion process occurs. Oxy-combustion involves burning the fuel with increased percentages of O_2 in order to produce a flue gas with a higher concentration of CO_2. Oxy-combustion has many implications for the combustion process and downstream conditions.

Post-combustion carbon capture technologies have been used in industrial processes for long periods of time. While gas adsorption, membranes, and solid sorbents can be used for separation, the primary method currently implemented is absorption by MEA scrubbing. This method is used to produce CO_2 for the food, petroleum, and chemical industries. Figure 2.16 represents a process flow diagram of post-combustion CO_2 removal using MEA scrubbing.

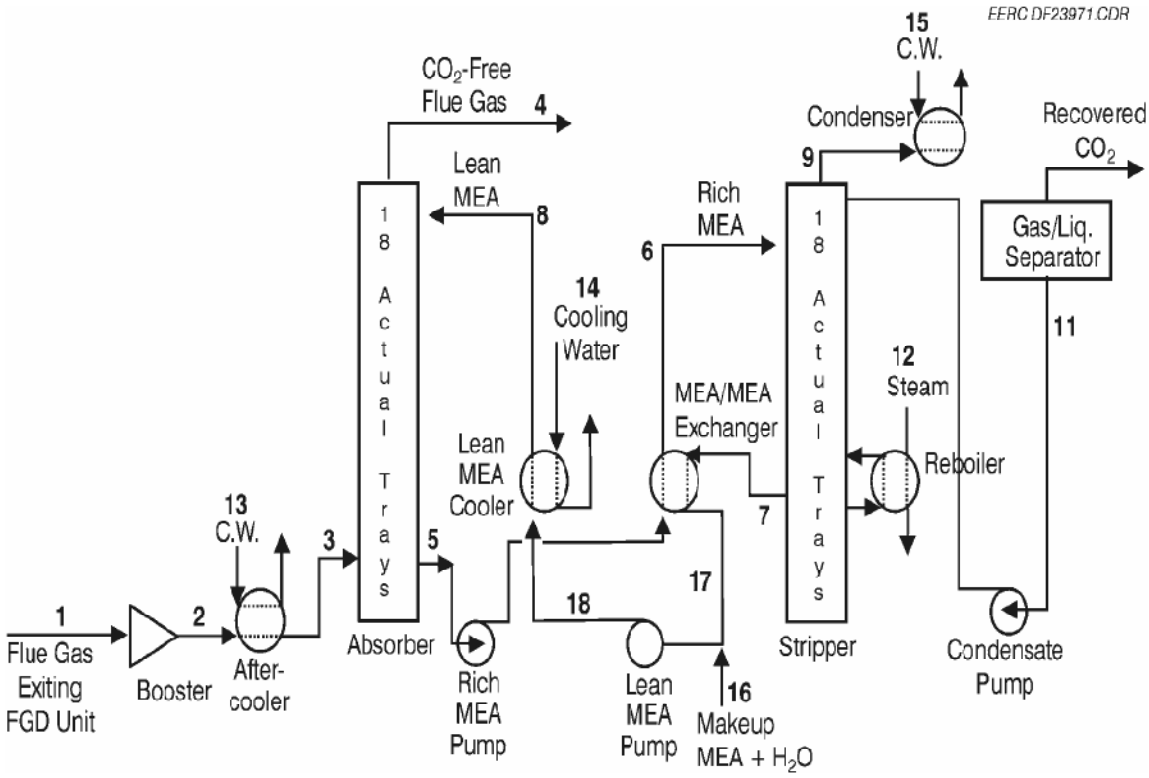

Figure 2.16. Process flow diagram of CO_2 removal by MEA scrubbing (Jensen et al., 2005).

As seen in Figure 2.16, this post-combustion separation method applies the gas absorption principle, coupled with gas wash regeneration. Flue gas enters at 1, in Figure 2.16, where desired operational pressure and temperature are established. The mixed gas then enters an absorption column, where it flows counter-current to a solution of MEA. The lean MEA absorbs the CO_2 from the gas stream as it flows downward. CO_2 free flue gas it vented from the top of the column. Between 85 - 95% of the CO_2 can be removed from the exhaust (Jensen et al., 2005). The now CO_2 rich MEA solution is taken from the bottom of the absorption column and pumped to the top of a stripper column. It then flows countercurrent to a stream of steam, at temperatures from 100 - 140˚C, where the CO_2 is removed from the MEA (Intergovernmental Panel on Climate Change [IPCC], 2005). The now lean MEA is cooled and returned to the absorption column, while the CO_2 and steam is condensed and separated. CO_2 purities of greater than 99%

are possible (Jensen et al., 2005). Equipment cost and operational expense are determined by several design parameters. These include flue gas flow rate, CO_2 content in the flue gas, desired CO_2 removal, solvent flow rate, heating requirements, and cooling requirements. Three commercially available post-combustion systems are currently available. They are the Kerr-McGee / ABB Lummus Crest Process, the Fluor Daniel ECANAMINE Process, and The Kanasai Electric Power Co., Mitsubishi Heavy Industries, Ltd. KEPCO/MHI Process (IPCC, 2005).

Issues with the MEA absorption technique include energy consumption, corrosion, solvent degradation, as well as current scale of implementation. Energy consumption is directly related to the heating and cooling requirements, as well as electrical equipment in the system. Heat requirements for leading amine absorption technologies range from 2.7 - 3.3 GJ / T CO_2. Electricity requirements range from 0.06 - 0.11 GJ / T CO_2 for coal and 0.21 - 0.33 GJ / T CO_2 for NGCC fueled plants (IPCC, 2005). Depending on fuel usage, many impurities may be present in the flue gas. Dissolved O_2, SO_2, SO_3, and NO_x all contribute to corrosion within the system and solvent degradation. Because of this, pre-treatment may be necessary in order to keep impurities at acceptable levels. This technology was implemented in 1996 in one of the first carbon capture and sequestration programs. The Statoil project in the North Sea's Sleipner gas field uses amine solvents to strip CO_2 from the natural gas it produces. Current equipment has only been implemented in the production scales ranging from 100 to 1,100 T CO_2 / day. Equipment for a 500 MW coal-fired plant would have to be able to process 5,500 T CO_2 / day (Jensen et al., 2005).

Pre-combustion methods for carbon separation and storage involve subjecting the fuel to several chemical reactions prior to combustion. This process consists of two main chemical

reactions. The first step is to take a hydrocarbon and break it into H_2 and CO. This can be accomplished through the addition of steam, steam reforming, represented by Equation 2.22.

$$C_xH_y + xH_2O \leftrightarrow xCO + \left(\frac{x+y}{2}\right)H_2 \quad (2.22)$$

It can also be accomplished by the addition of O_2. If added to a gaseous fuel it is referred to as partial oxidization. If added to a solid fuel it is referred to as gasification. Both partial oxidization and gasification processes can be represented by Equation 2.23.

$$C_xH_y + \frac{x}{2}O_2 \leftrightarrow xCO + \left(\frac{y}{2}\right)H_2 \quad (2.23)$$

Following this first step, additional steam is added in a process called the water gas shift reaction shown in Equation 2.24.

$$CO + H_2O \leftrightarrow CO_2 + H_2 \quad (2.24)$$

From this point, the CO_2 can be separated from the H_2 fuel.

Many different techniques are currently used to create desirable products from hydrocarbons, prior to combustion. These include many variations of the above chemical reactions. Methods exist to convert natural gas, coal, petroleum residues as well as biomass into desirable products. Usually, the CO_2 by-products are merely vented into the atmosphere. Opportunities exist, however, for easy capture from these processes. Figure 2.17 displays a simplified process for gasification with options for carbon capture, electricity generation, as well as other by-products.

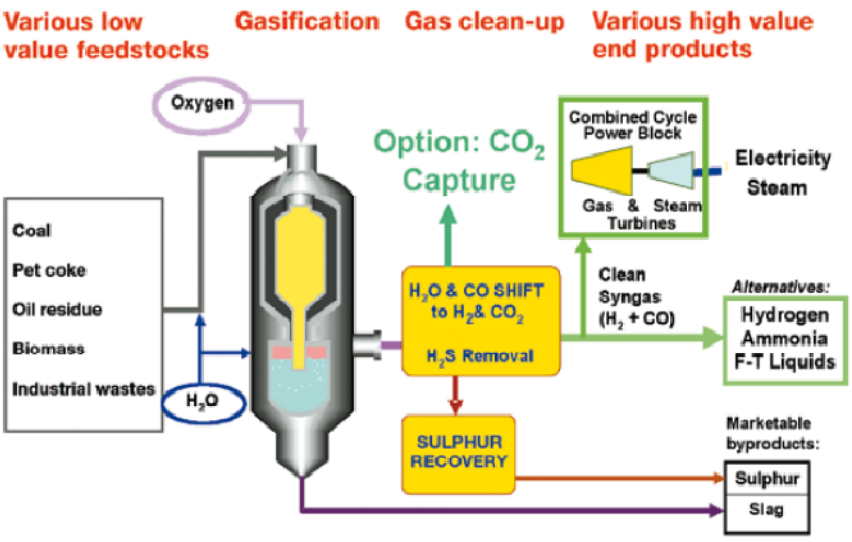

Figure 2.17. Simplified schematic of gasification process with optional CO_2 capture (IPCC, 2005).

This pre-combustion carbon capture technology was implemented in one of the world's largest carbon capture projects. The Weyburn - Midale CO_2 Project captures CO_2 from the Great Plains Synfuel plant in Beulah, ND. The CO_2 is then piped 205 miles to the Weyburn - Midale oilfield in Saskatchewan, Canada, where is used for EOR. An estimated 30 million tons of CO_2 can potentially be stored in that oil reservoir (National Energy Technology Laboratory [NETL], 2008).

The third technique for carbon sequestration, oxy-combustion, involves burning the working fuel with a high percentage of O_2. This increases the CO_2 concentration in flue gas, making separation less energy intensive. In nearly all fossil fired power generation facilities, ambient air is used as the source for the O_2 required for combustion. Ambient air consists of approximately 78% nitrogen, 21% oxygen, and 1% argon. An example of stoichiometric combustion of methane with ambient air resembles Equation 2.25.

$$CH_4 + 2(O_2 + 3.76N_2) \rightarrow CO_2 + 2H_2O + 7.52N_2 \quad (2.25)$$

As seen in Equation 2.25, a large fraction of the exhaust product is N_2. For every one mole of CO_2 captured, 7.52 moles of N_2 must be processed. Accommodating this volume of inert N_2 increases equipment sizes and resulting energy consumption, as seen in the post-combustion sequestration techniques. Methane oxy-combustion resembles Equation 2.26.

$$CH_4 + 2O_2 \rightarrow CO_2 + 2H_2O \quad (2.26)$$

In this idealized reaction, the only exhaust products are CO_2 and H_2O. Because no other gases are present, the CO_2 and H_2O can be separated through a condensation process. Condensation involves cooling the exhaust gas until the H_2O becomes a liquid and the CO_2 remains a gas. This is a very simplified overview of oxy-combustion. Many additional issues must be considered with this method.

Firstly, the adiabatic flame temperatures of combustion are altered greatly by removing the N_2. The adiabatic flame temperature of methane with air is approximately 1,950˚C, while the adiabatic flame temperature of methane and oxygen is 2,800˚C. Combustor material limitations prevent these high temperatures. When using ambient air, temperatures can be regulated by increasing the amount of air. In oxy-combustion, the high oxygen content oxidizer has to be produced. Because of its associated cost, flame temperatures are controlled by recirculating some of the exhaust gas. Oxy-combustion with exhaust gas recirculation (EGR) not only increases the concentration of CO_2 in the exhaust gas, but it reduces total exhaust gas volume as well. Depending on the purity of the O_2 and the desired flame temperatures, volumes of exhaust gas can be reduced from one-third to one-fifth (Jensen et al., 2005). An additional benefit of oxy-combustion is the fact that N_2 is removed from the combustion process. This reduces or eliminates the considerations for NO_x emissions assuming constant temperature.

In the NGCC application, special consideration would have to be given to how the change in working fluid would affect the performance of the gas and steam cycles. In the gas turbine, a change from a largely N_2 working fluid to a largely CO_2 and H_2O fluid would affect performance of current turbine designs because of the change in thermodynamic constants such as ratio of specific heats. Additionally, the reduction in volume of exhaust gas would affect the amount of steam created by the HRSG and resulting steam turbine.

The main limitation of the oxy-combustion method for carbon sequestration is the associated costs with O_2 production. O_2 production can be accomplished with either a cryogenic or non-cryogenic system. Cryogenic systems separate air based on their boiling points. Non-cryogenic systems rely on differences in molecular weight, size, or structure to facilitate separation. Some techniques for non-cryogenic separation include pressure swing adsorption, vacuum swing adsorption, and membrane separation. Cryogenic distillation of liquid air is the only presently known method that is practical on a scale for power production.

Cryogenic distillation is based on a process developed by Carl von Linde in 1902 (Linde AG, 2008). Table 2 displays the average composition of air and respective boiling points.

Table 2

Major Components of Air and Respective Boiling Points at 1 atm

	Volume (%)	Boiling Point (˚C)
Nitrogen	78.08	-195.8
Oxygen	20.95	-183.0
Argon	0.93	-185.9

As seen in Table 2, the different gases in air all have different boiling points. Separation involves cooling air to a point at which some gases turn into liquids, while others remain gases, allowing

separation. In order to accomplish this, air is first purified and moisture removed. The air is then compressed to 6 atm and cooled to -180˚C. Multi-stage compression and intercooling, as well as volumetric expansions provide cooling. The air then enters a separation tower where it continues to expand and cool. As this occurs, O_2 with the highest boiling point begins to turn into a liquid. Liquid O_2 droplets fall toward the bottom of the column interacting with rising vapors. This interaction encourages oxygen to condense and nitrogen to vaporize. The liquid O_2 at the bottom of the column and the gaseous N_2 are reboiled and condensed, respectively, until a desired purity is achieved. This process can be carried at multiple pressure levels, increasing efficiency and product purity. Figure 2.18 shows a typical diagram of an ASU.

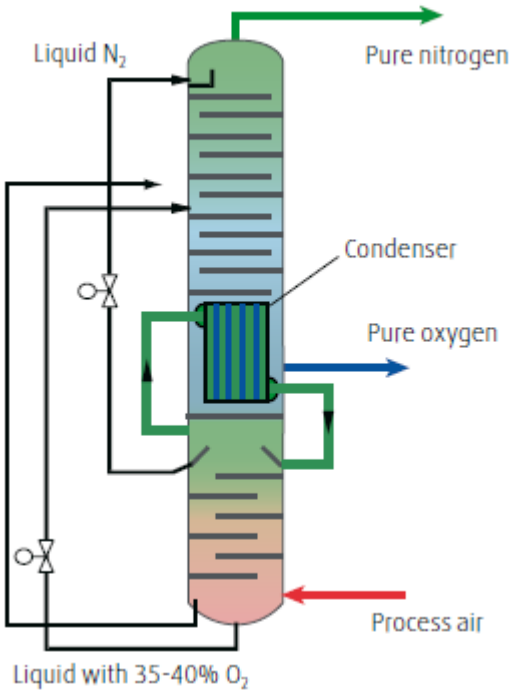

Figure 2.18. Diagram of Linde Double Column ASU (Linde AG, 2008).

Currently, the largest air separation plants can produce 3,500 T O_2 / day. Cryogenic separation requires large amounts of energy with compressors, reboilers, condensers and other equipment. Energy consumption for 95% purity 0.17 MPa O_2 can range from 200 to 240 kWh /

T O_2 (IPCC, 2005). As a mature technology, significant improvements to efficiency are not likely for the Linde process.

As seen above, several different techniques can be used to capture and store CO_2. Each method is best used in different applications. In considering that natural gas fueled powerplants had the capacity to produce 397,432 MW of power in the United States in 2008, many studies have been completed to determine the most efficient techniques for carbon capture (EIA, 2010).

2.8. First and Second Law Efficiency

Optimizing a system requires the quantitive analysis of operational parameters. This can be done in multiple ways, however, the First and Second Laws of thermodynamics provide some of the most valuable information regarding optimal operation. The First Law of thermodynamics quantifies the ratio of work exiting a system to the amount of heat supplied. Equation 2.27 represents the First Law or thermal efficiency.

$$\eta_{th} = \frac{Net\ Work\ Output}{Total\ Heat\ Imput} \tag{2.27}$$

The Second Law of thermodynamics provides a method of quantifying how a system is performing as compared to the best possible performance of that system. Calculating the Second Law efficiency involves several steps. An ambient “dead state” temperature and pressure must first be selected. Next, a control volume is selected around the system to be analyzed and streams entering and exiting are identified. The useful work potential, or exergy, of these streams is then quantified by comparing them to the ambient conditions. Equation 2.28 gives the exergy for a flowing system with neglected kinetic and potential energy.

$$\psi = (h - h_0) - T_0(s - s_0) \tag{2.28}$$

In Equation 2.28, *h* and *s* represent the enthalpy and entropy of a stream at its conditions and h_0 and s_0 represent the enthalpy and entropy at the ambient state. Finding the amount of exergy destroyed within the control volume is then calculated through Equation 2.29

$$X_{Destroyed} = \sum_{in} \psi \dot{m} - \sum_{out} \psi \dot{m} - \dot{W} \tag{2.29}$$

where *X* is exergy, *m* is the mass flow rate of the streams and $\dot{W}$ is the work added or removed from the system. Having the amount of exergy available as well as the amount destroyed by the system allows the Second Law efficiency calculation to be completed as shown in Equation 2.30.

$$\eta_{II} = 1 - \frac{X_{destroyed}}{X_{supplied}} \tag{2.30}$$

Using an exergy analysis and corresponding Second Law efficiency allows several important observations to be made. Primarily, minimum exergy destruction translates into maximum Second Law efficiency. Identifying operations with large exergy destruction indicates where improvements in efficiency are possible.

CHAPTER 3

METHODOLOGY AND VALIDATION

CHEMCAD is a chemical and physical process analysis software developed by Chemstations Inc. It provides great flexibility in design and optimization of chemical, physical, and operational processes. It contains a vast library of chemical components, thermodynamic methods, and unit operations that allow both steady-state and dynamic processes to be modeled (CHEMCAD, 2010). User interface with CHEMCAD is provided by a palette of various chemical and physical process simulators displayed in Figure 3.1.

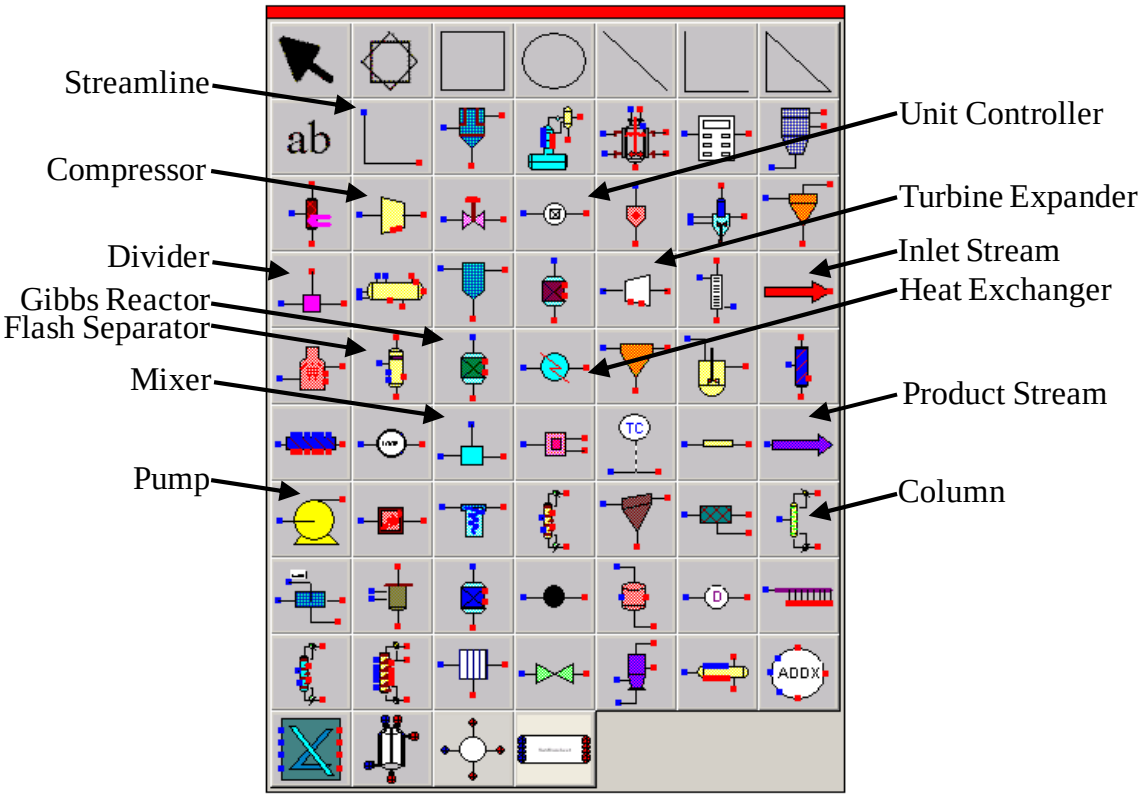

Figure 3.1. CHEMCAD chemical and physical unit operator palette (Chemstations Inc.,2010).

Each component can serve as a building block to simulate a process when linked with streamlines. Each of the various building blocks has dependent and independent variables that can be specified.

In the modeling of a combined cycle powerplant for carbon sequestration, several building blocks were used in this study to simulate existing processes. In Figure 3.1, the necessary components have been labeled. The first step in creating a model is to use the inlet stream unit. With this unit, components, conditions, and feed-rates entering a system can be specified. Likewise, the product steam unit will output characteristics of the stream exiting the system. The streamline operator is used to transfer all properties exiting one unit to the entrance of the next unit. The compressor and turbine expander serve to represent either an isentropic or polytropic compression or expansion respectively. Either the outlet pressure or pressure ratio, and efficiency must be specified. These units will produce a stream with the specified properties, as well as calculate power, temperature or pressure changes, and other thermodynamic properties. The divider and mixer units allow a stream to be either divided or mixed by specified parameters. The output streams will contain components and properties calculated by the program. The pump unit is used in increase the pressure of a liquid. The efficiency as well as the pressure increase, pressure ratio, or outlet pressure must be specified. The unit will calculate several properties including power required. The heat exchanger unit carries out the transfer of heat from one stream to another. If only one stream is present, the unit acts as a heater or cooler. If multiple streams are present, the unit can be operated in multiple operational modes. The unit controller can be used in two modes, feed-forward and feed-backward. In feed-forward mode, the controller takes a value from a previous unit and applies it to a unit that has not run yet. In feed-backward mode, the controller can be used to adjust a variable until certain downstream

conditions are met. The Gibbs reactor can be used to carry out thermal or material balances, by minimizing the Gibbs free energy from the overall mass balance. Input conditions are specified by the feed streams and resulting products and conditions are calculated. The flash separator unit allows for different components to be separated based on several different thermodynamic principles. The column unit allows for the modeling of a distillation column. Multiple operational specifications can be made and the software will calculate necessary parameters.

3.1. Modeling Overview and Objectives

In order to optimize a system for carbon sequestration for a natural gas fired combined cycle powerplant, several steps were followed. A specific, pre-designed NGCC powerplant was selected. While maintaining operational constants for the specified powerplant, a combination of oxy-combustion and post-combustion carbon capture equipment were specified to facilitate carbon capture. Additionally, CO_2 must be brought to specified pressure and temperature, as well as purity, per transportation and sequestration requirements. CHEMCAD software was used to model each component in this system. In order to determine the optimum operating condition for the system, the oxidizer O_2 purity was increased from 21-100% on a mole basis. Resulting power consumption from the ASU and post-combustion carbon capture were analyzed. Figure 3.2 displays a simplified layout of the proposed system.

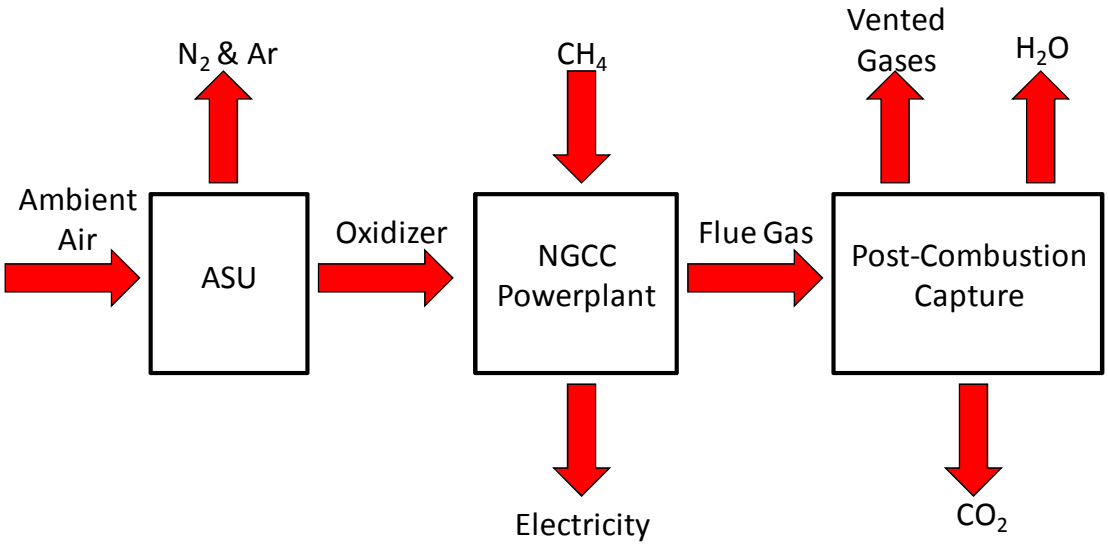

Figure 3.2. Simplified layout of NGCC powerplant with sequestration equipment.

The main parameters of investigation were the energy needed for the ASU and the post-combustion equipment. At ambient conditions, 21% O_2, there will be no energy consumption from the ASU, however, significant energy will be required to operate the amine scrubber / stripper. As the O_2 purity is increased, energy consumption from the ASU will increase. Correspondingly, power consumption from the post-combustion treatment will decline. As O_2 purity approaches 100%, ASU power will continue to increase, while amine scrubbing will become unnecessary resulting in zero energy consumption. Figure 3.3 represents the hypothetical energy consumption trends as O_2 purity increases.

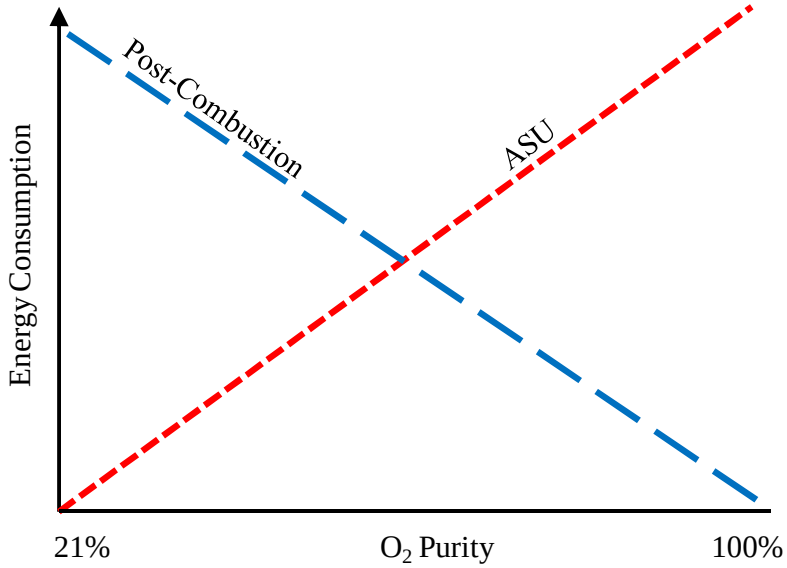

Figure 3.3 Energy consumption trends varying with O_2 purity.

Of interest is the O_2 percentage at which parasitic energy consumption related to carbon sequestration is minimized.

3.2. NGCC Powerplant Model

The first component necessary for the analysis of energy consumption for carbon capture is the combined cycle powerplant. A commonly used Siemens SCC6 - 5000F combined cycle plant was selected for modeling. This unit includes two gas turbines and HRSG's providing steam for a single steam turbine. This combined cycle plant includes state of the art technologies for increased efficiencies. Depending on firing conditions, with natural gas fuel, the combined cycle plant is capable of generating 580 - 598 MW with a maximum net efficiency of 57.2% (Siemens AG, 2008b).

The initial steps in accurately modeling the SCC6 – 5000F NGCC powerplant include recreating the major operational components. These include the two gas turbines with their respective compressor, combustion, and turbine sections, the HRSG, and finally, the steam

turbine. Figure 3.4 represents the CHEMCAD model of the simplified Siemens SCC6 - 5000F combined cycle plant.

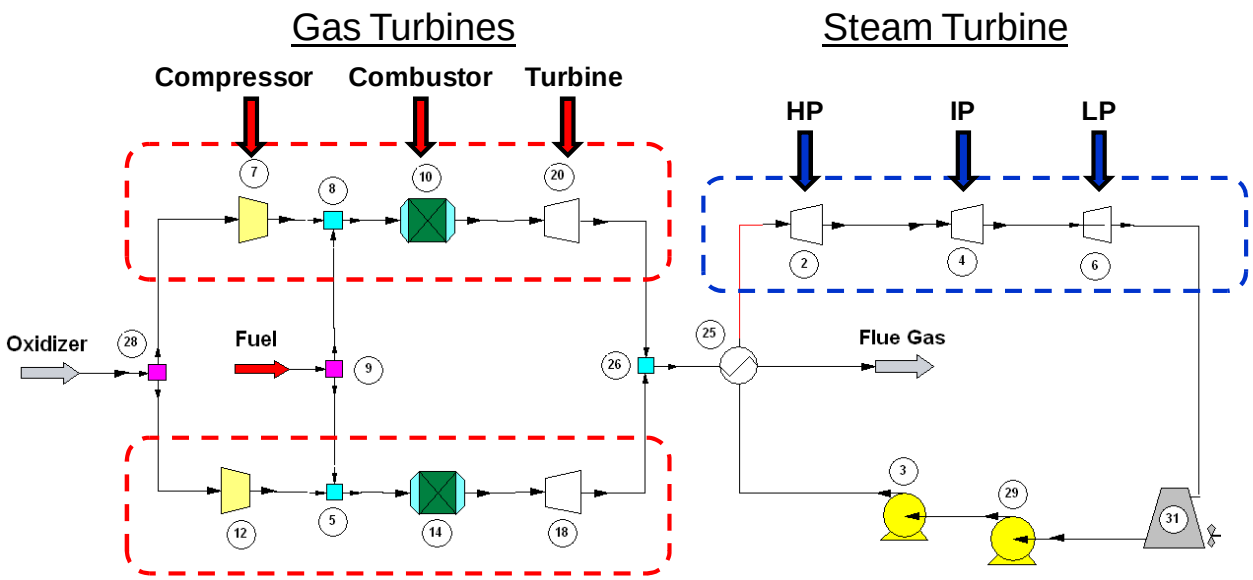

Figure 3.4. CHEMCAD model of simplified SCC6 - 5000F combined cycle powerplant.

In Figure 3.4, components are identified by numbers. Components 7 and 12 represent the compressor portion of the gas turbine. Components 10 and 14 are Gibb's combustion reactors, simulating the combustion of the fuel and oxidizer. Components 20 and 18 represent the turbine portion of a gas turbine. The HRSG is modeled by a simple heat exchanger, component 25. The steam turbine is portrayed with a three-stage turbine section, components 2, 4, and 6. The cooling tower, 31, and twin pumps, 3 and 29, return the working fluid to the HRSG. Operational parameters of each component were then specified in order to as accurately as possible recreate the Siemens unit. Table 9 in the Appendix provides the specific input values for each component of the CHEMCAD powerplant. An additional consideration in the modeling process included eliminating the reheater present in the Siemens model. This was necessary to ensure that convergence of the model could be achieved across all operational parameters.

When increasing the O_2 purity in the oxidizer stream, some components of the CHEMCAD powerplant model had to change from the validation case. Primarily, the increase in O_2 concentration resulted in an increased flame temperature in the Gibb's combustion reactors. In order to limit the combustion temperature, an EGR stream was added. The exhaust gas was returned to the oxidizer stream at a rate necessary to maintain a temperature 2,600˚F. Figure 3.5 displays the CHEMCAD powerplant model modified for EGR.

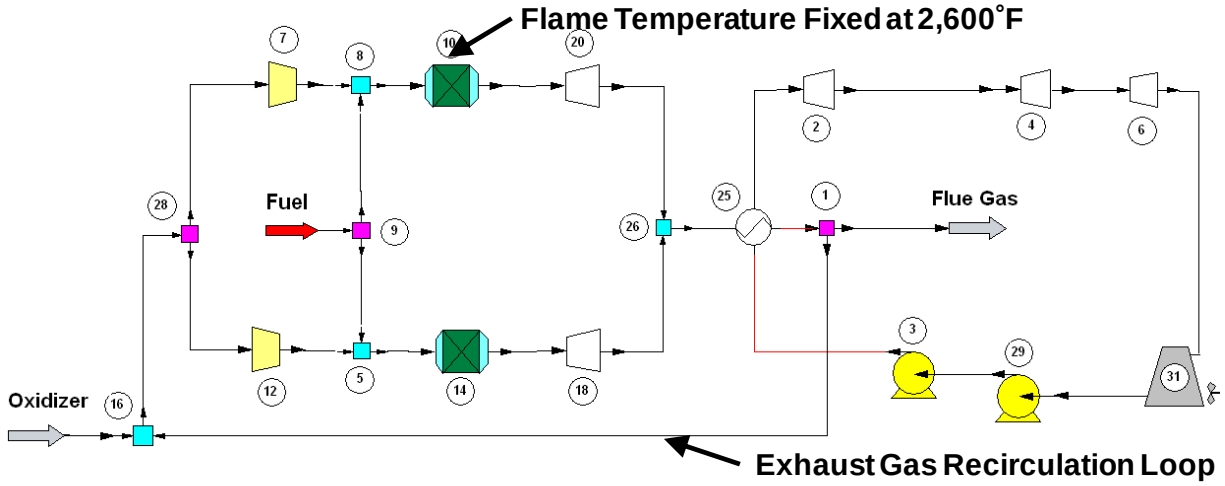

Figure 3.5. CHEMCAD model of a powerplant modified for EGR.

As seen in Figure 3.5, a divider, Unit 1, allows for a specified fraction of the exhaust flue gas to be recirculated and mixed with the incoming oxidizer stream.

In considering operational parameters of the SCC6 - 5000F powerplant, the methane consumption rate of 21.3 kg/s is held constant for all cases. In order for stoichiometric combustion to occur, the oxygen feed rate must be 84.96 kg/s. As per the operational specifications of the actual powerplant 63% excess O_2 is supplied. In a real world situation, there is no associated cost for this oxygen. However, when considering higher purity O_2, there are associated costs at the ASU. For this reason, while not realistic in real world operational

conditions, O_2 feed rates were maintained at 85.5 kg/s. This is less than a 1% excess O_2 rate. This is possible because the Gibb's combustion reactors simulate idealized combustion.

3.3. NGCC Powerplant Validation

The second component of the model that must be validated for accuracy is the powerplant. Initially, the powerplant model was given operating specifications comparable to the manufacturer's operational data from the Siemens SCC6 - 5000F product catalogue. These input values are summarized in Table 3.

Table 3

Operational Specifications for Siemens SCC6 - 5000F and CHEMCAD Powerplant Model (Siemens AG, 2008b)

Specification	Siemens SCC6 - 5000F	CHEMCAD Model
Number of Gas Turbines	2	2
Number of Steam Turbines	1	1
Number of HRSGs	2	1
Fuel	Natural Gas	CH_4
Fuel Flow Rate (kg/s)	21.3	21.3
Air Flow Rate (kg/s)	492.8	492.8
Compressor Pressure Ratio	17:1	17:1
Steam Turbine Stages	3	3
HRSG Exhaust Temperature (˚F)	340	340

Upon running the CHEMCAD model simulating real life operational specifications, several key results have been compared to ensure accuracy. These results are displayed in Table 4.

Table 4

Operational Results for Siemens SCC6 - 5000F and CHEMCAD Powerplant Model (Siemens AG, 2008b)

Specification	Siemens SCC6-5000F	CHEMCAD Model
Exhaust Gas Flow Rate (kg/s)	1,007	1,007
Gas Turbine Outlet Temp (˚F)	1,088	1,145
Steam Turbine Throttle Temperature (˚F)	1,050	1,100
Steam Turbine Throttle Pressure (atm)	125	174
Steam Turbine Back Pressure (atm)	0.0527	0.0425
Net Power Output (MW)	580 - 598	582
Net Plant Efficiency LHV (%)	54.4 - 56.1	54.6

Inspection of Table 3 and Table 4 allows a comparison between the CHEMCAD model and the actual Siemens powerplant to be performed. Major simplifications in the model include the use of pure methane as the specified fuel as well as the use of only one HRSG instead of the two specified by the manufacturer. In inspecting the results, it can be seen that the gas turbine outlet temperatures differ by 57˚F. This is due to the Gibb's combustion reactor. It simulates an ideal combustion processes, resulting in higher combustion temperatures. Because the composition of "natural gas" is not quoted by Siemens, it is likely that the heating value of pure methane is higher than that of the natural gas used, thus resulting in higher combustion temperatures. This higher combustion temperature results in higher exhaust gas temperatures. In order to account for the removal of the steam turbine reheater, the steam turbine throttle pressure was increased from 125 atm to 174 atm. The CHEMCAD model's net power output of 582 MW falls within the net power output of the actual powerplant. While operational conditions will vary greatly in the

analysis, this validation confirms that the model can accurately represent a real world powerplant.

3.4. ASU Model

Operationally, the ASU unit is needed to provide O_2 at purities from 22% to 99.6% on a mole basis. The O_2 stream must also supply the 85.5 kg/s O_2 for complete combustion in the powerplant. A Linde Double Column ASU was selected for producing the O_2 at varying purities. The process of separating air was carried out using the model shown in Figure 3.6.

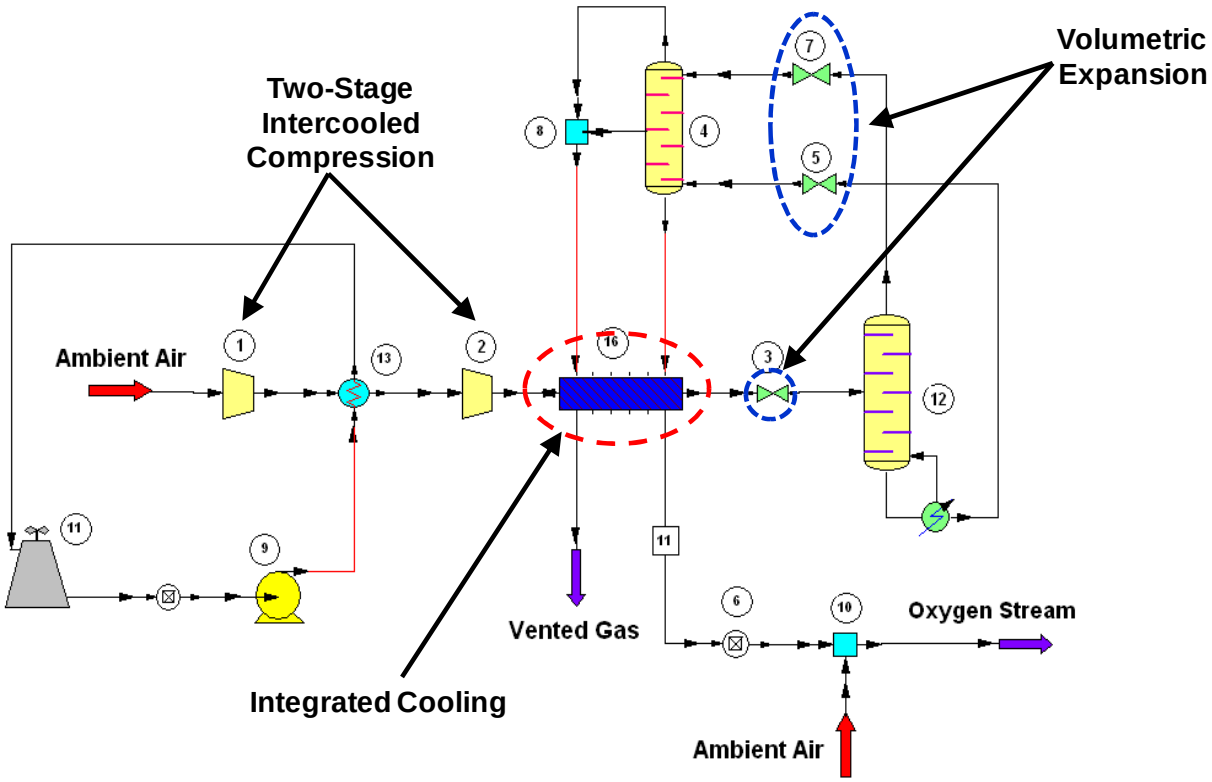

Figure 3.6. CHEMCAD model of a Linde Double Column ASU.

The ASU model has been designed to produce a 99.6% pure stream of O_2. The stream is then diluted with ambient air to create any lower purity O_2 stream desired. Ambient air is taken to be at 298 K and 1 atm, with a molar concentration of 78% nitrogen, 21% oxygen, and 1% argon. This air enters the process diagram and is compressed, in two stages, with intercooling. The first

compressor, Unit 1, increases the pressure of the air to 3 atm. Inter-stage cooling is provided by water, in a recirculation loop. Water enters the heat exchanger, Unit 13, at 298 K and 3 atm, it cools the compressed air stream to a temperature of 300 K. The now heated water then flows to a cooling tower, Unit 11, where it is returned to ambient conditions. The cooling water then enters a pump, Unit 9, where it is returned to 3 atm. As the volume of air entering the ASU varies, the flow rate of water in the recirculation cooling loop changes as necessary to maintain the air's intercooling temperature at 300 K. The cooled intermediate pressure air is then compressed again by Unit 2, where it reaches 9 atm. An integrated heat exchanger, Unit 16, further cools the air stream. The cooling is provided by the vented gas product from the top of Unit 4 as well as the liquid bottom from Unit 4. This cooling brings the air stream to a temperature of nearly 105 K. At this temperature some components of the air stream have entered the liquid state. An expansion valve, Unit 3, lowers the air stream's pressure to 5 atm. This volumetric expansion allows for further cooling of the air. At this point the partial liquid partial vapor, air stream enters the high pressure column, Unit 12. This distillation column separates the liquid components, exiting the bottom of the column, from the vapors, exiting the top. The top stream contains a high purity nitrogen, and argon stream, while the bottom stream contains an increased purity O_2 stream. Both streams then pass through another set of expansion valves, Units 5 and 7, reducing the streams pressure to 1 atm. Again, this volumetric expansion reduces the temperatures of both streams. The streams then enter the low pressure column, Unit 4, where further distillation occurs. Oxygen, at 99.6% purity and a temperature of 89.8 K, exits from the bottom of Unit 4. The top stream contains nitrogen, at nearly 98% purity and a temperature of 77.6 K. A side draw on the low pressure distillation column removes a large part of the argon. Because the only desired product is the O_2 enriched stream, the top and side product streams are passed through

Unit 16, and vented into the environment at ambient conditions. As stated above, the O_2 enriched stream passes through Unit 16, providing cooling to the entering air stream. It is returned to 300 K. Unit 10 mixes a stream of ambient air with the 99.6% purity product. The resulting O_2 enriched stream can be varied in purity as desired, and fed to the powerplant. Table 10 in the Appendix provides a complete overview of the CHEMCAD ASU model specifications.

3.5. ASU Validation

Upon completion of each model component, a comparison of output data with previous modeling studies was conducted to insure model accuracy. The ASU model has been compared with data from several previous modeling works. Specifically, the power consumption per ton of O_2 at various O_2 purities is compared. Figure 3.7 displays the specific power consumption for the modeled ASU compared to results from previous modeling studies of 85% and greater O_2 purities.

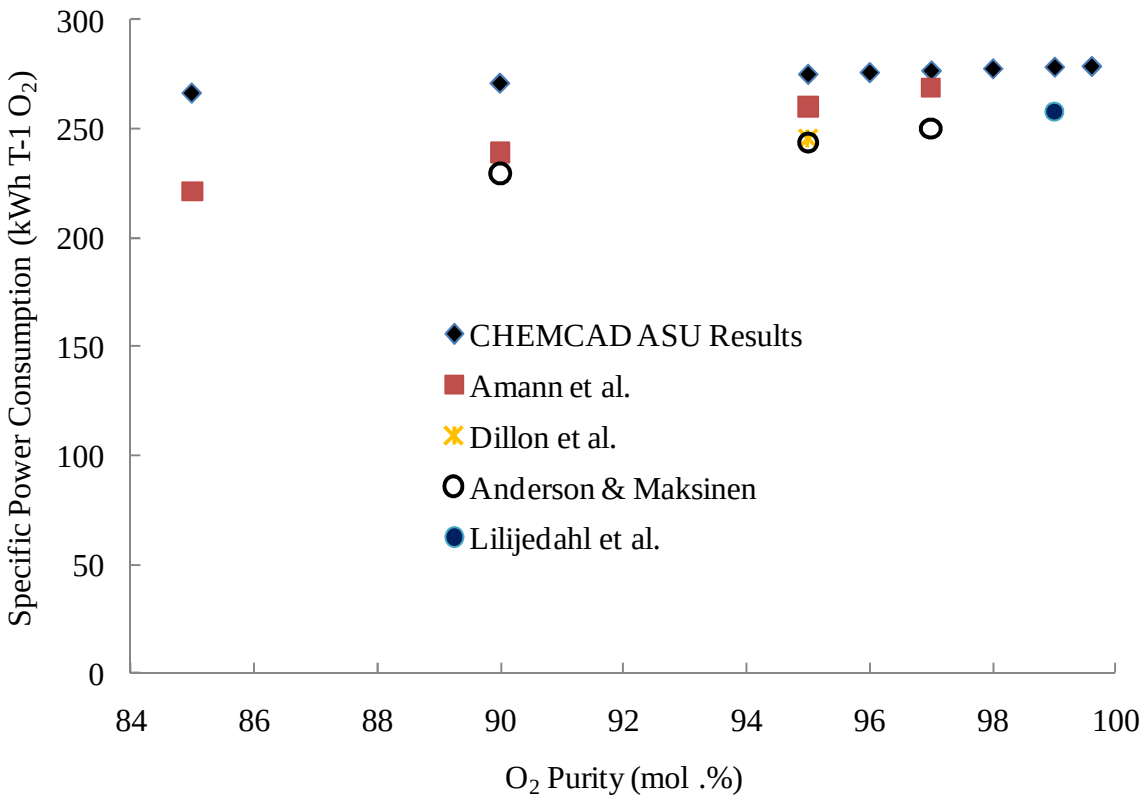

Figure 3.7. Specific power consumption of the CHEMCAD ASU model with varying O_2 purity.

Figure 3.7 presents the results from previous works. Results from Anderson & Maksinen, Dillon et al., and Lilijedahl et al. were accumulated and compared with additional data by Amann, Kanniche, & Bouallou (2009). Table 5 compares Amann et al.'s data concerning power consumption per varying O_2 purity to results from the current modeling effort.

Table 5

Comparison of Results from Previous Models Investigating ASU Performance

O_2 purity mol. %	Author	Specific consumption kWh T^{-1} O_2	Current results kWh T^{-1} O_2	% Difference
85	J.-M. Amann et al.	221.3	266.6	18.6
90	J.-M. Amann et al.	239.2	270.9	12.5
90	Anderson & Maksinen	229.6	270.9	16.5
95	Dillon et al.	245.6	274.9	11.3
95	J.-M. Amann et al.	260.2	274.9	5.5
95	Anderson & Maksinen	243.8	274.9	12.0
97	Anderson & Maksinen	250.1	276.5	10.0
97	J.-M. Amann et al.	268.7	276.5	2.8
99	Lilijedahl et al.	257.6	278.1	7.6

It can be seen from both Figure 4.1 and Table 5 that as the purity of O_2 is increased the specific power consumption increases as well. The percent difference in comparing the results varies from 18.6% at a purity of 85%, to as small as 2.8% at a purity of 97%. The increase in discrepancy corresponding to a decrease in purity can be described by a difference in modeling methods. In the previous modeling cases performed by other researchers, O_2 purity was varied by changes in the inlet pressure prior to the high pressure distillation column. Thus, a decrease in O_2 purity resulted in a decrease in compressor power consumption. In the current modeling effort, only a unit producing 99.6% purity O_2 was created. Regardless of the change in desired purity, the inlet air had to be compressed to a consistent 9 atm. Despite the differences, the current

model does a reasonably accurate job portraying the trends in energy consumption with O_2 purities varying over the complete range.

3.6. CO_2 Amine Scrubber Model

In order to produce a high purity CO_2 stream from the powerplant's exhaust gas, post combustion gas processing is required. The amine MEA has been determined to be the most applicable for this application. Figure 3.8 displays the CHEMCAD model developed for carbon dioxide capture using MEA.

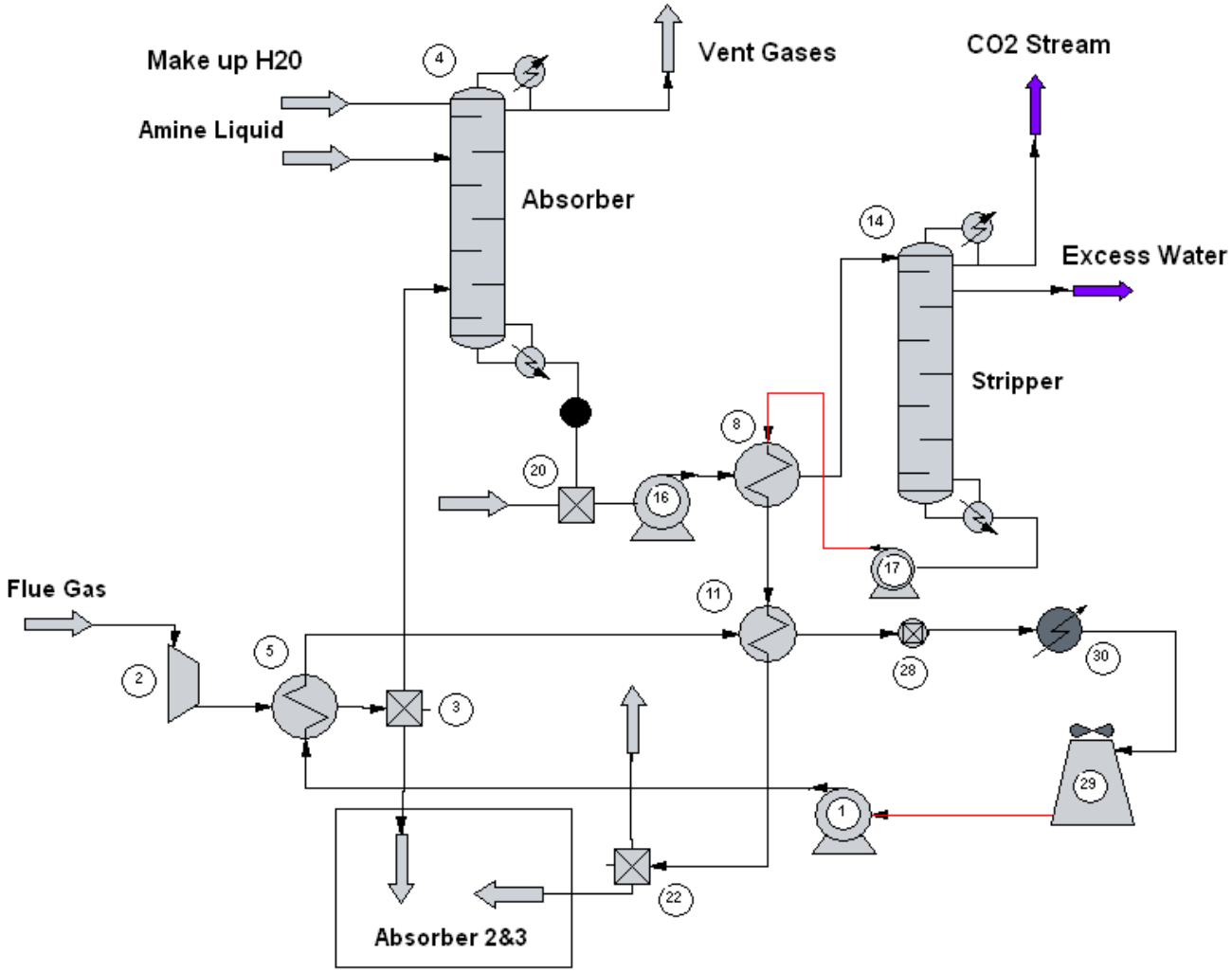

Figure 3.8. CHEMCAD model of an amine scrubber for CO_2 removal from flue gas.

This model represents the processes that are necessary for CO_2 to be removed from a stream of flue gas. The gas is washed by a solution of MEA in the absorption column. High temperature steam is then used to remove the CO_2 from the amine resulting in a stream of CO_2 ready for dehydration and compression.

Upon entry into the system, the flue gas passes through a blower, Unit 2. This blower raises the pressure of the gas to 1.01 atm. As the composition and volume of the flue gas varies with varying percentages of O_2 purity, the amount of power consumed by the blower will vary. Additionally, the temperature of the gas will vary as it exits the blower. This variance in temperature will affect absorption rates in the absorption column. In order to prevent this temperature variance, a heat exchanger, Unit 5, has been incorporated. It uses a water cooling loop to bring the exhaust temperatures to a constant 329 K. Because of the large volume of flue gas, the absorption takes place in three parallel columns. Unit 3 divides the flow stream such that one-third of the exhaust gas passes to each column. For modeling processes, only one column is displayed. The gas enters the bottom of the absorption column, Unit 4, and rises toward the top. A stream of amine liquid and make up water enter the top of the column. As the gas rises and liquid falls, the CO_2 binds with the MEA. The flow rate and composition of the amine liquid are determined by the amount of CO_2 being processed, as well as the desired recovery rate. Corrosion is an issue with MEA, thus the concentration has been limited to 30% on a mass basis. The rest of the amine stream is composed of water. The ratio of moles of CO_2 to moles of MEA is critical in determining the recovery rate of the system. Existing scrubbing units have ratios varying from 0.2 – 0.5 moles CO_2 per mole amine (Edwards & MacDonald, n.d.). A ratio of 0.2 was specified for this model. This ratio allows for a successful capture rate of approximately 90% of the inlet CO_2. The gases, minus the CO_2 removed by the amine solution are vented from

the system at a temperature of 352 K and 1 atm. The amine solution, now rich with CO_2, exits the bottom of the absorption column. At this point, Unit 20 simulates the recombination of the fluids from the three absorption columns into one stream. The pump, Unit 16, raises the pressure of the CO_2 rich amine solution to 3.6 atm. The temperature is then increased by the heat exchanger, Unit 8, to 378.15 K. Heating is provided by the bottom stream of the stripping column, Unit 14. The warmed, higher pressure, CO_2 rich amine solution enters the stripping column where the CO_2 bond with MEA is broken by steam. The stripping column contains a condenser and reboiler. The condenser removes heat from the gases reaching the top of the column until they return to liquid. The reboiler adds heat to the liquids reaching the bottom of the column, returning them to vapors. This condensing and reboiling continues until specified products at the top and bottom of the column are reached. The reboiler specification is defined such that 90% of the CO_2 in the flue gas exits the top of the column. An intermediate stream on the stripping column, removes excess water from the CO_2 product stream. The now lean MEA solution exits the bottom of Unit 14 and is pumped, by Unit 17, through the heat exchanger warming the rich stream. An additional, heat exchanger, Unit 11, returns the solution to 323 K. this solution is returned to the absorption column, to undergo the CO_2 loading and unloading process again.

The heating and cooling requirements for the stripping column are accounted for in two ways. The cooling requirements are provided for by the cooling loop incorporated with the lean MEA return. In this loop, water, at 298 K and 1 atm is pumped, by Unit 1, through the heat exchanger, Unit 5, removing heat from the inlet flue gas as mentioned above. The water then passes through another heat exchanger, Unit 11, where it returns the lean MEA solution to inlet conditions. The cooling loop then passes through a controller, Unit 28. The unit controller takes

the cooling requirements of the condenser in Unit 14 and specifies that as the heat added requirement in the heat exchanger, Unit 30. The water then passes to a cooling tower, Unit 29, where it is returned to ambient conditions. Unit 1 increases the pressure to 3 atm, and the loop is continued. As seen, this cooling loop provides for all of the cooling requirements of the scrubbing system. The heating requirements for the stripping column are accounted for by the removal of heat from the steam cycle in the powerplant. Figure 3.9 shows a heat exchanger, Unit 11, incorporated into the steam cycle of the powerplant. The heating requirements for the stripping columns' reboiler are transferred to the heat removal rate of Unit 11.

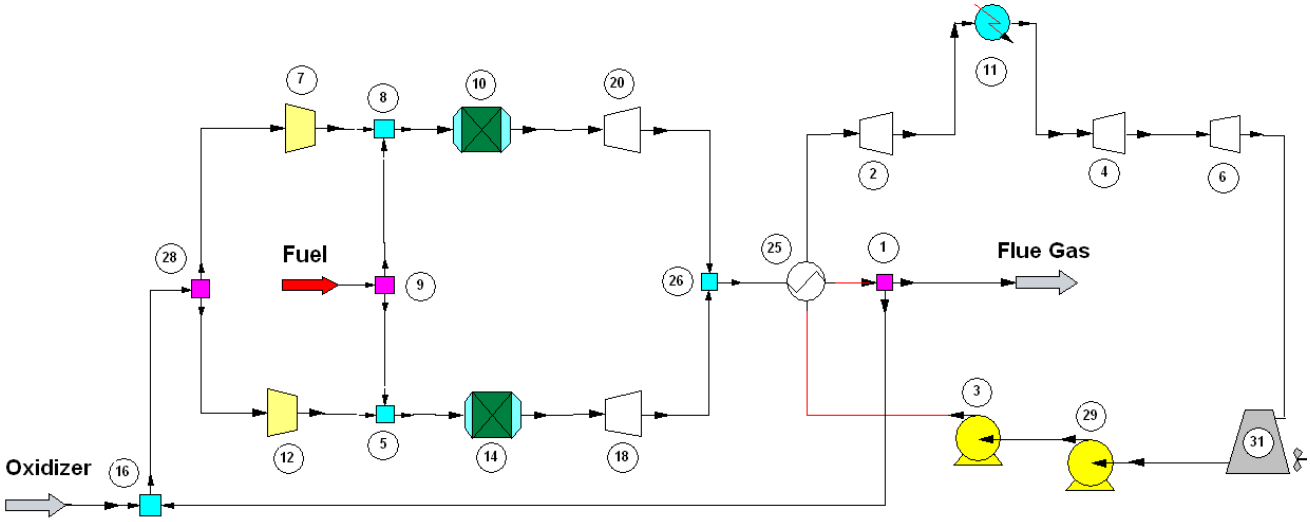

Figure 3.9. CHEMCAD model of a powerplant with heat removal from steam cycle for stripping column heat requirements.

Table 11 in the Appendix provides a complete overview of the CHEMCAD amine scrubber model specifications.

3.7. CO_2 Amine Scrubber Validation

In order to validate the results from the amine scrubber model, two previous modeling studies were compared with the current study. The primary energy consuming portions of the amine scrubber include the blower fan, the condenser in the stripping column, and the reboiler in

the stripping column. The blower electric consumption is directly related to the volume of gas being compressed as well as the desired outlet pressure. Amann et al. has investigated the energy requirements of an amine carbon dioxide removal unit operating with ambient air. As Amann et al. discusses, the specific electric consumption for the blower fan is 5 kWh / T flue gas with a specified outlet pressure of 1.13 atm (2009). The CHEMCAD model's blower has an outlet pressure of 1.01 atm and a corresponding specific energy consumption of 2.7 kWh / T flue gas. This difference is explained by the difference in specified outlet pressures. Additionally, for a CO_2 recovery rate of 85%, the stripping column requires between 2.56 and 5.44 MJ / kg CO_2 corresponding with MEA loading rates of 0.25 and 0.16 mol. CO_2 / mol. MEA respectively (Amann et al., 2009). With a MEA loading rate of 0.2 mol. CO_2 / mol. MEA, the model achieves a 90% CO_2 removal rate with a specific energy consumption of 7.2 MJ / kg CO_2. An additional study by Singh, Croiset, P. Douglas, & M. Douglas, investigates the operational parameters of flue gas scrubbing with MEA. Singh et al.'s results for the re-boiling and cooling duty requirements are 351 MW and 430 MW respectively (2003). This correlates with the CHEMCAD model that requires 380 MW re-boiling duty and 448 MW cooling duty. It appears that the current model provides reasonable results.

3.8. CO_2 Dehydration & Compression Model

Upon exit from the amine CO_2 removal unit, the exhaust gas must be brought to conditions suitable for transport and sequestration. This final treatment of the flue gas is accomplished with a dehydration and compression unit. Flash separation at multiple stages allows water to be removed from the waste stream, while progressively increasing the pressure, until the CO_2 meets specified criteria for pipeline transport. Figure 3.10 depicts the CHEMCAD model for the drying and compression of a CO_2 stream.

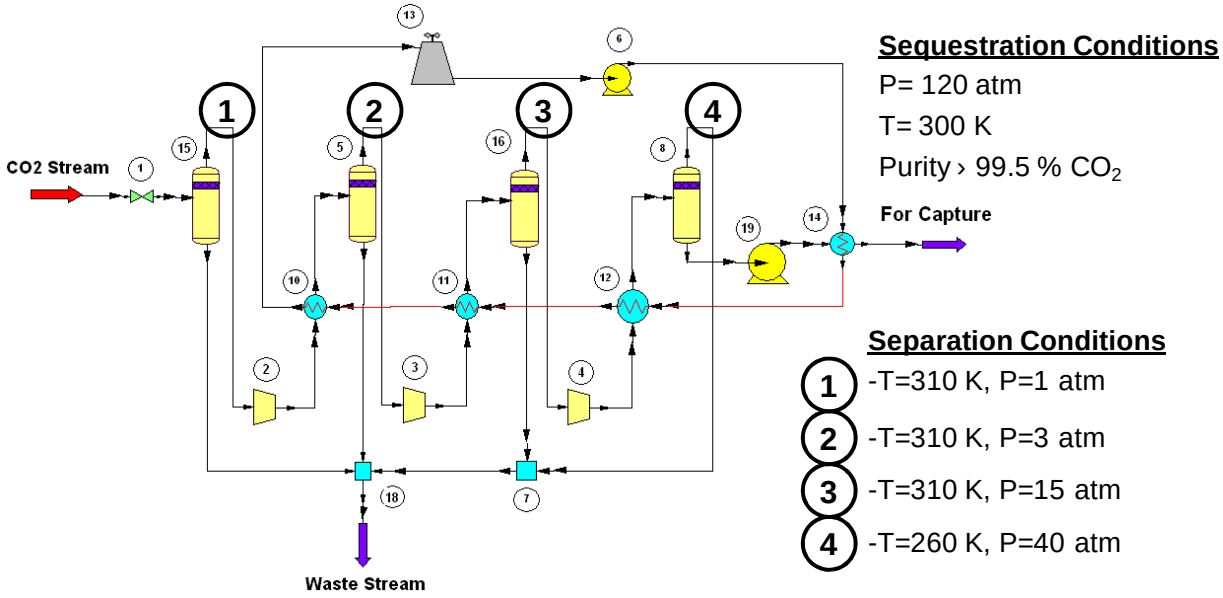

Figure 3.10. CHEMCAD model of a flue gas dehydration and compression unit.

The specifications desired for pipeline transport of CO_2 for this study were liquid CO_2 at 120 atm, 300 K, and purity no less than 99.5% on a mole basis. In order to obtain this specification, the CO_2 stream exiting the amine scrubbing column undergoes several processing steps. Separation is achieved by bringing the fluid to conditions where the H_2O becomes a liquid and the CO_2 remains a gas. This is done at four evolving points specified in Figure 3.10. Unit 1 is a valve that first reduces the pressure of the stream to 1 atm. It then enters a separation column, Unit 15, where liquid exits the bottom, while gas exits the top. The gas is then compressed by Unit 2 to pressure of 3 atm. Cooling is provided by a heat exchanger, Unit 10. A large water cooling loop, consisting of four heat exchangers, a pump and a cooling tower, provide all necessary cooling requirements for the dehydration and compression system. Unit 10 reduces the temperature to 310 K, and again, a separation column, Unit 5 removes liquid from the stream. This process is repeated two more times at temperatures and pressures of 15 atm and 310 K and 40 atm and 300 K, respectively. The resulting high purity liquid CO_2 stream is pumped by Unit 19 to a pressure of 120 atm. The heat exchanger, Unit 14, brings the final stream to the specified

temperature of 300 K. This stream is now suitable for transport and ultimate end use. Table 12 in the Appendix provides the complete specifications for the CHEMCAD CO_2 drying and compression model.

3.9. CO_2 Drying & Compression Validation

The CO_2 drying and compression model is compared with various sources for specific power consumption in order to insure model accuracy as well. Table 6 displays the specific electrical power consumption per ton of CO_2 sequestered for several previous studies.

Table 6

Parameters and Results from Models Comparing Drying and Compression of CO_2

	Gottlicher & Pruschek. (1997)	Cormos et al. (2010)	Singh et al. (2003)	CHEMCAD Model
Sequestration pressure (atm)	108.6	118.6	-	120
Sequestration purity (%)	-	-	99.6	99.7
Specific power consumption (kWh T^{-1} CO_2)	108.9	96.8	88.7	100.9

As seen in Table 6, the CHEMCAD model closely recreates the results from several other modeling studies into power consumption related to CO_2 drying and compression.

3.10. Complete Model Configurations

With each component individually compared to previous works, the models can be combined with the assurance of accuracy. Different operational parameters in each of the four

models will vary as the O_2 purity is changed. Investigation into these changes is to be the purpose of this study. As the variance of the oxygen concentration is the primary variable being adjusted, the different percentages investigated are of importance. The O_2 purity will be increased from 21% to 25% by intervals of 1%. From 25% to 95%, the purity will be increased by intervals of 5%. Finally, from 95% to 99.6% the purity will be increased by 1% intervals, again. At ambient air conditions, 21%, two cases will be investigated. These include limiting the combustor flame temperature with excess air, as well as limiting the temperature with EGR.

As mentioned previously, the necessary equipment for different oxygen purities will differ. At ambient conditions, the ASU is not necessary. For the two ambient cases the model will contain the powerplant, amine scrubber, and compression and dehydration units as displayed in Figure 3.11.

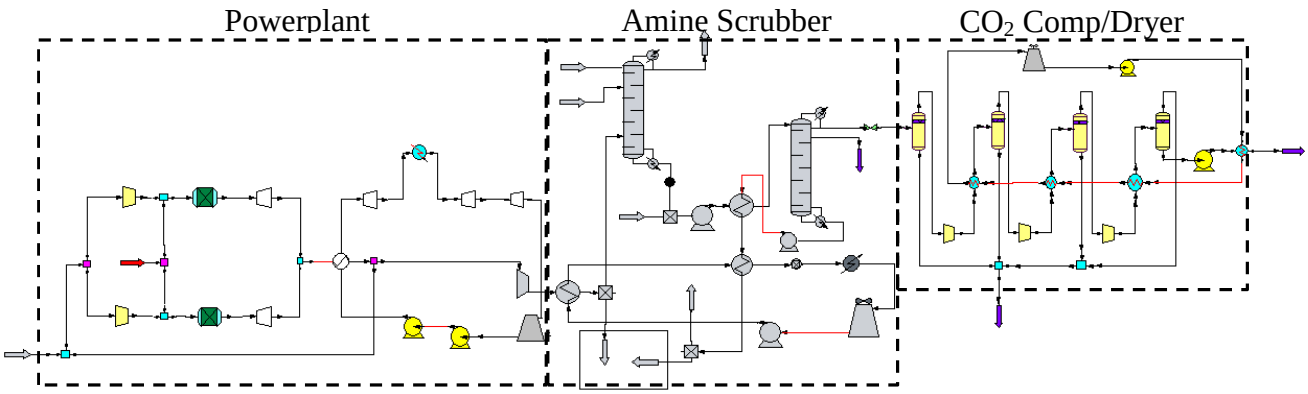

Figure 3.11. CHEMCAD model layout for 21% O_2 purity cases.

For the cases with O_2 purities varying from 22% to 99%, the model will include the same components as the ambient condition, as well as the ASU. Figure 3.12 displays a complete model for O_2 purities varying from 22% to 99%.

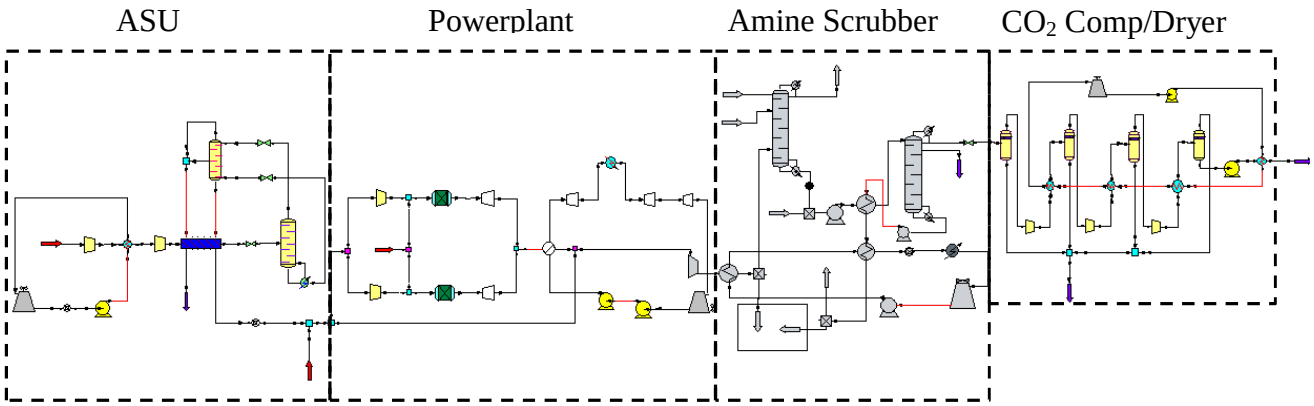

Figure 3.12. CHEMCAD model layout for O_2 purities from 22% to 99%.

For an O_2 purity of 99.6%, there is no longer a need for the amine scrubber. In this case, the complete CHEMCAD model will resemble that of Figure 3.13.

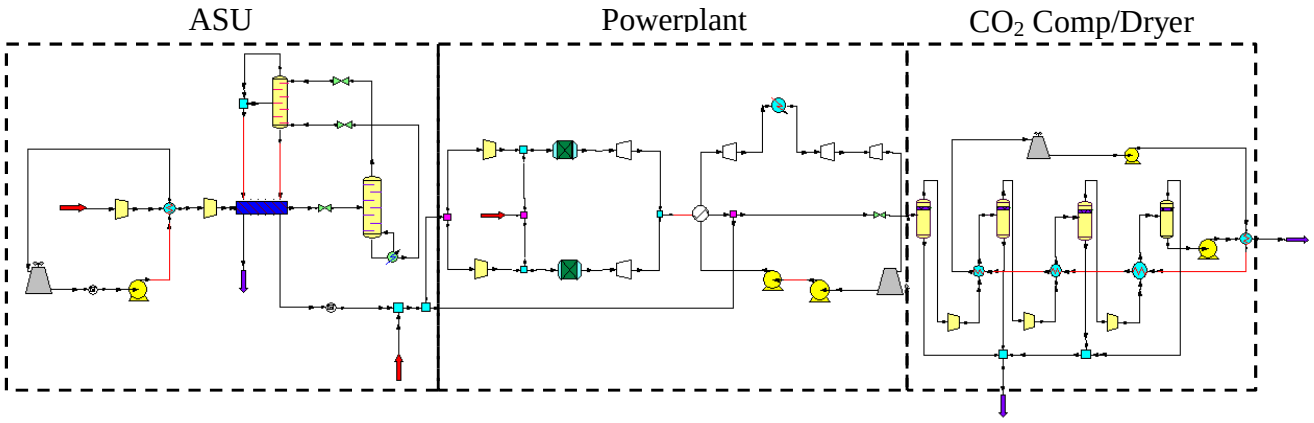

Figure 3.13. CHEMCAD model layout for O_2 purity of 99.6%.

CHAPTER 4

RESULTS

The motivation for this study is to investigate the operational parameters of a combined cycle powerplant modeled for carbon capture with varying O_2 purity combustion. In investigating the results of the study, several key items will be discussed. These include the parasitic power consumption of components, how stream flow rates and compositions vary, the affects of oxy-combustion with EGR on powerplant operations, as well as specified overall efficiencies.

4.1. ASU Results

The first unit under consideration is the ASU. Its purpose is to provide a fixed amount of oxygen to the powerplant while increasing O_2 purity. Primary energy consumption occurs with the compression of ambient air. As the purity increases, the volume of air compressed increases. Figure 4.1 displays the power consumption of the ASU with increasing O_2 purity.

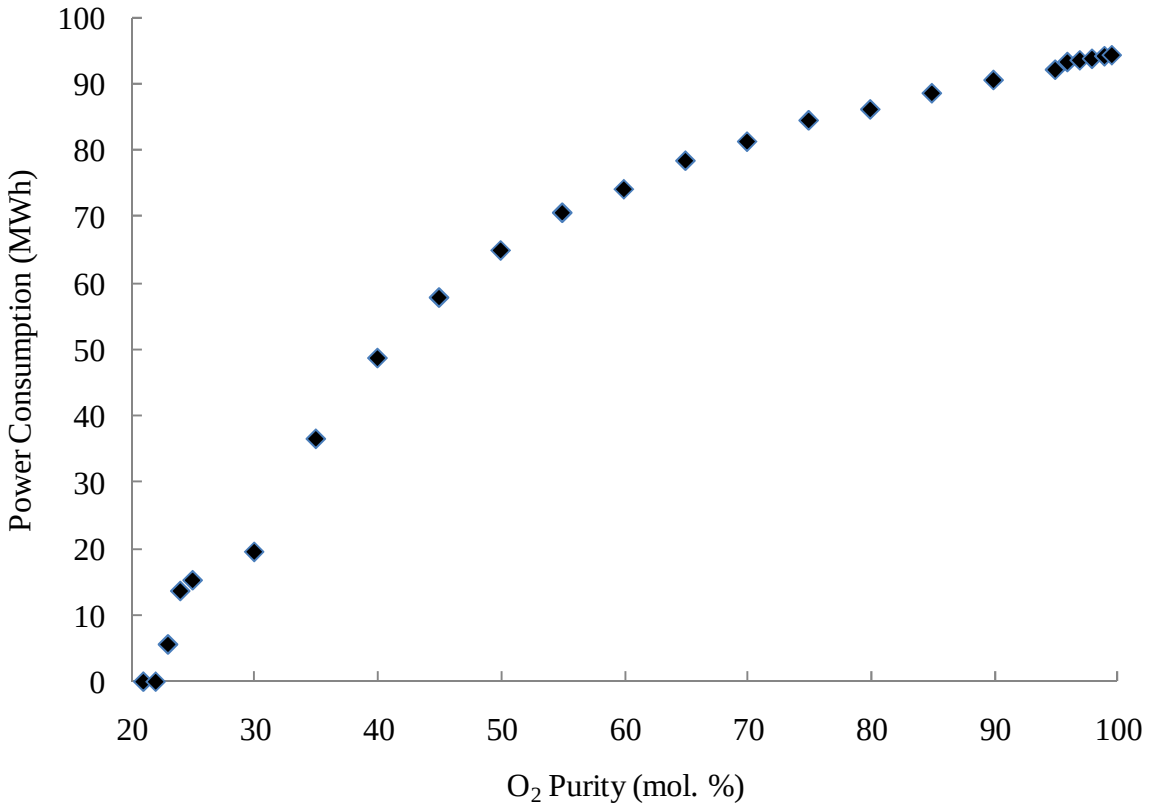

Figure 4.1. ASU power consumption with increasing O_2 purity.

As seen in Figure 4.1, power consumption ranges from zero, when ambient air is supplied, to 94.5 MW corresponding to 99.6% O_2 purity. The power consumption increases in a logarithmic manner. Of additional interest is the composition of the fluid sent to the powerplant. Figure 4.2 displays the mole fractions of the various elements as O_2 purity increases.

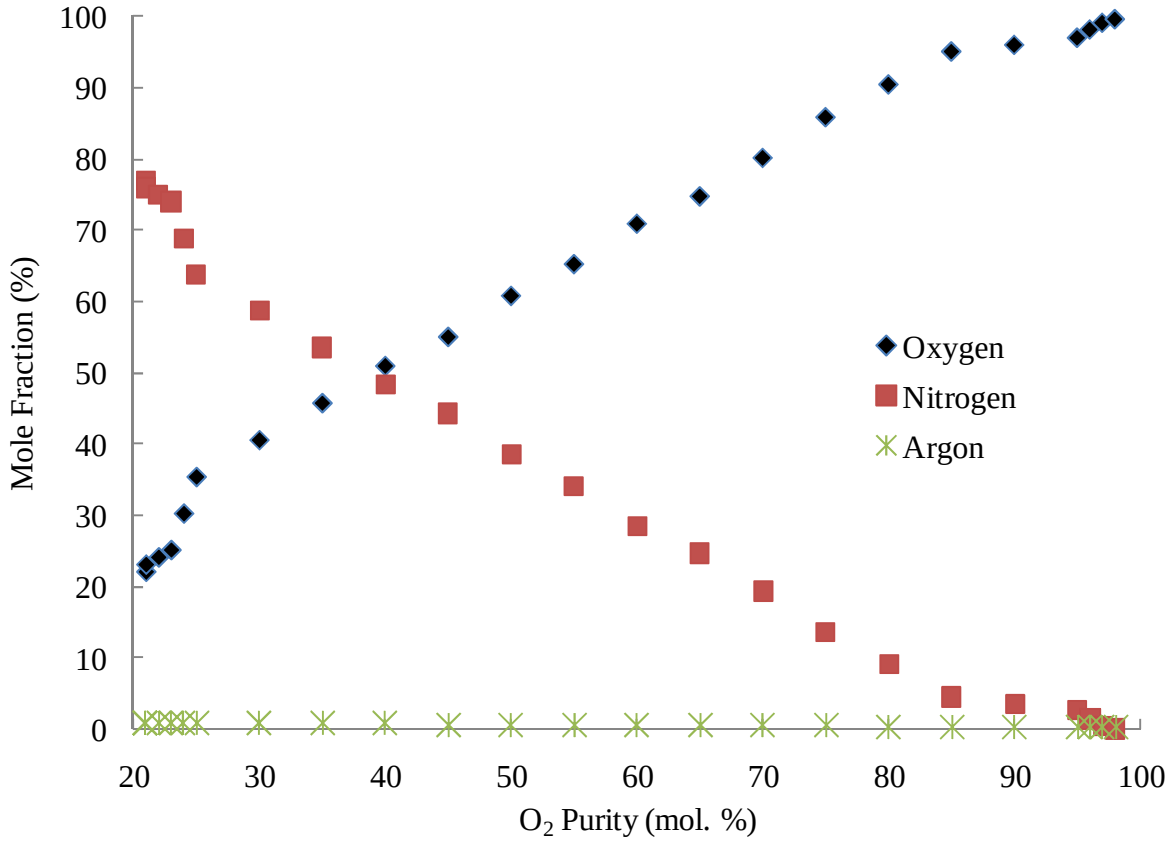

Figure 4.2. Mole fraction of components exiting the ASU.

Nitrogen makes up approximately 78% of ambient air on a mole basis. As seen in Figure 4.2, the mole fraction of nitrogen is reduced greatly. While maintaining the specified 85.5 kg / s of O_2 required for the powerplant, the volume of fluid decreases significantly. Figure 5.3 shows the mass flow rate of the stream entering the powerplant.

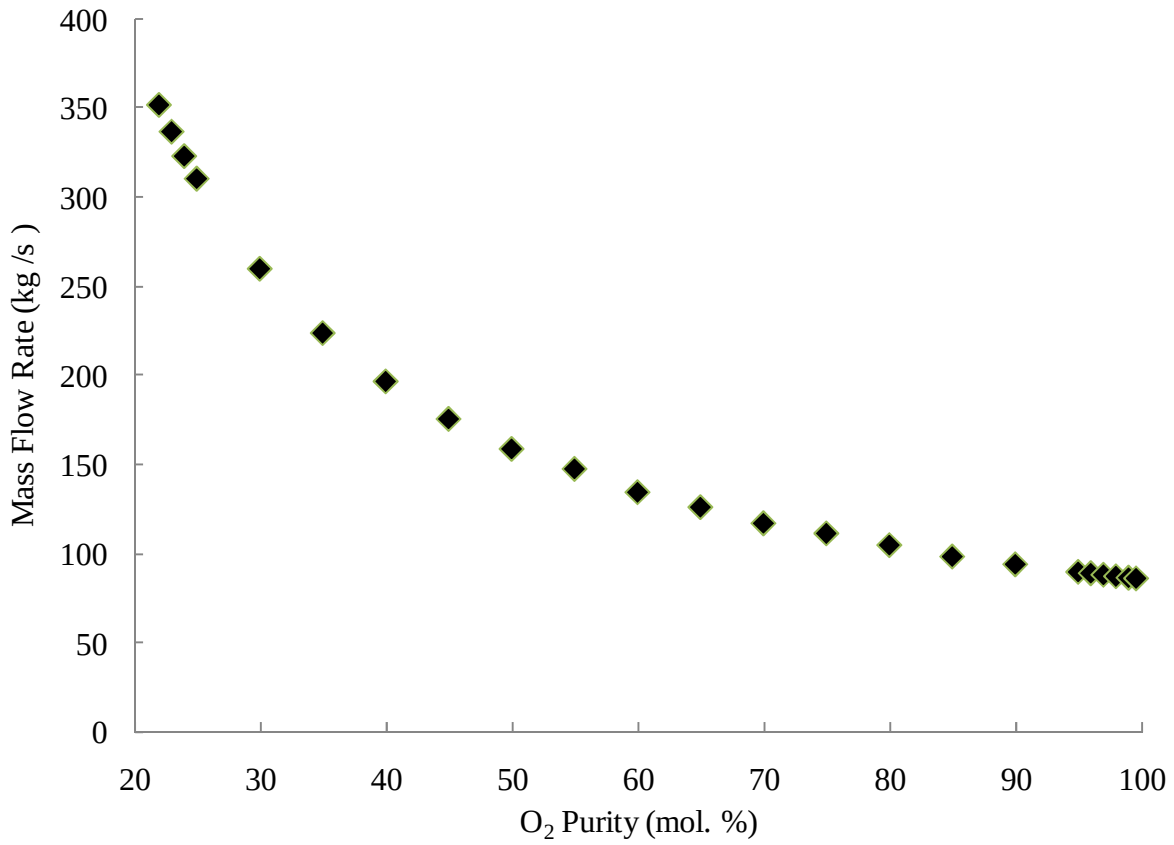

Figure 4.3. Mass flow rate of stream exiting the ASU as O_2 purity increases.

As Figure 4.3 depicts, the mass flow rate exiting the ASU and entering the powerplant decreases by 75.6% across the ASU operational range. If considering the ambient case where no ASU is required and excess air is used for combustion temperature control, this figure is even larger, at 89.6% mass flow reduction.

4.2. Powerplant Results

Upon entry into the powerplant the volume and composition of the oxidizer stream will have impacts on multiple components. At 21% purity two cases are investigated, excess air and EGR temperature control. With excess air, an 825 kg / s stream of ambient air flows into the system. With recirculation, a 369 kg / s stream of ambient air is required. The EGR rate of 57.5% maintains a consistent combustion temperature. This EGR rate increases to nearly 84% at an O_2

purity of 99.6%. As can be expected, the working fluid of the gas turbine portion changes with the variance in EGR. This will impact the amount of compressor work required, as well as the output work created by the turbines due to the variation in thermodynamic properties of the working fluid. Figure 4.4 displays the changes in compressor and turbine performance as O_2 purity and corresponding EGR rates change in a single gas turbine.

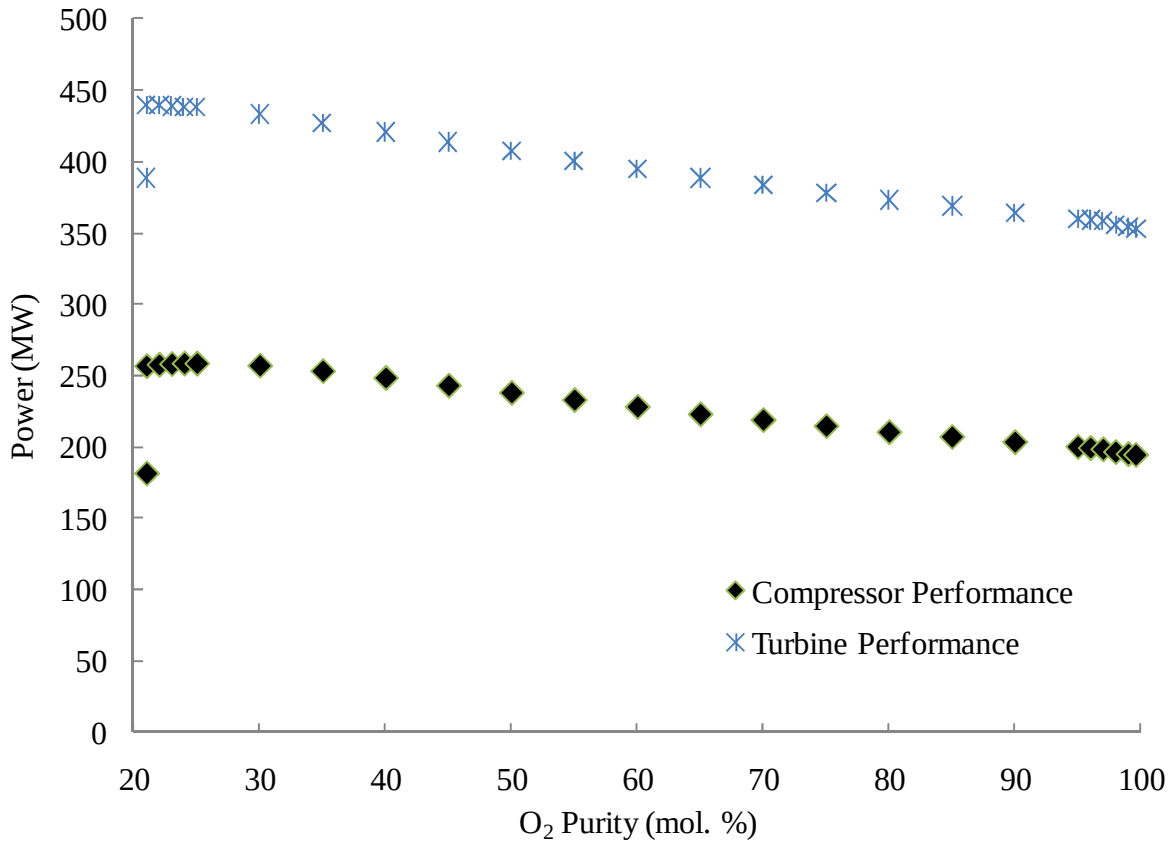

Figure 4.4. Gas turbine compressor and turbine performance with varying O_2 purities.

As visualized in Figure 4.4, at ambient air inlet conditions, EGR for temperature control requires 29% more compressor work than corresponding excess air temperature control. Additionally, the turbine puts out 11.6% more power with EGR. As the O_2 purity increases, resulting increased EGR rates reduce the compressor and turbine power specifications. Overall, the net electricity produced by the two gas turbines decreases as seen in Figure 4.5.

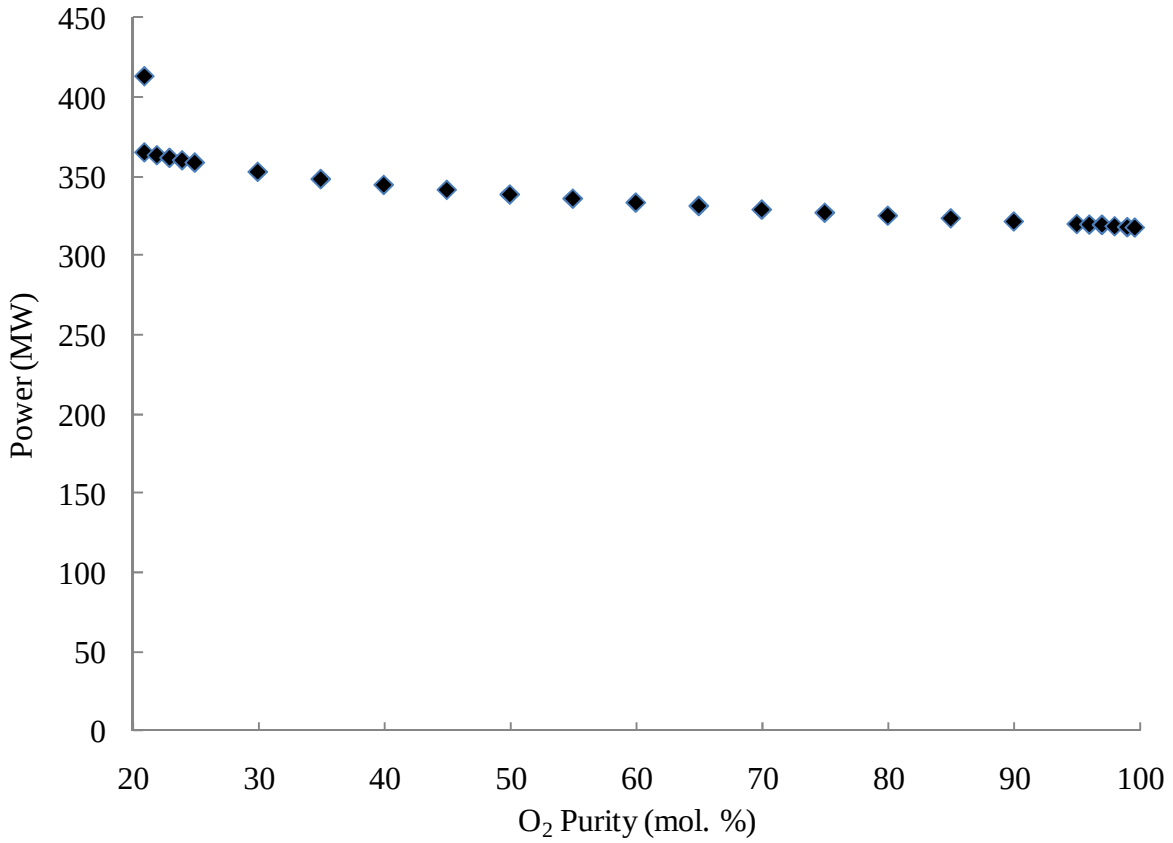

Figure 4.5. Power production by gas turbines as O_2 purity increases.

If considering all cases, this decrease represents a 23.2% reduction in power output. However, neglecting the excess air case reduces the power loss to 13.1%.

While isolated from the combustion process, the steam cycle is still affected by variations in gas turbine working fluid and related performance. As the recirculation rates increase, the flow rate of exhaust gas exiting the gas turbine decreases. Intuitively, one would think that, because of the reduced flow rate, the HRSG would produce less steam. However, because of the altered composition of the exhaust gas, more heat can be transferred to the steam cycle, increasing its performance. Figure 4.6 displays the performance of the steam turbines. This figure does not include the parasitic load required for reboiler duties in the amine scrubber.

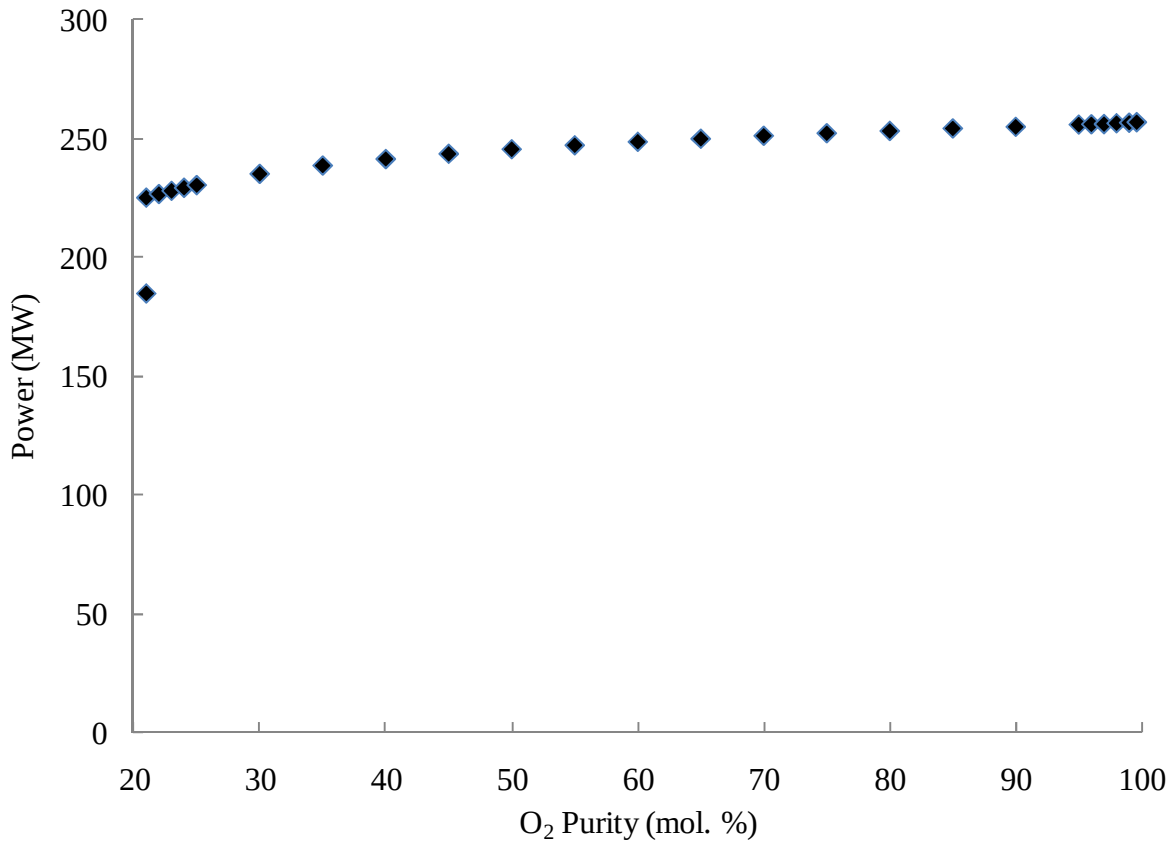

Figure 4.6. Power output from the steam cycle as O_2 purity varies.

As seen in Figure 4.5 and Figure 4.6, increasing O_2 purity decreases performance of the gas turbines while increasing the performance of the steam turbines. Accounting strictly for the powerplant's parasitic load, Figure 4.7 displays the overall power output as the working fluid changes with O_2 purity.

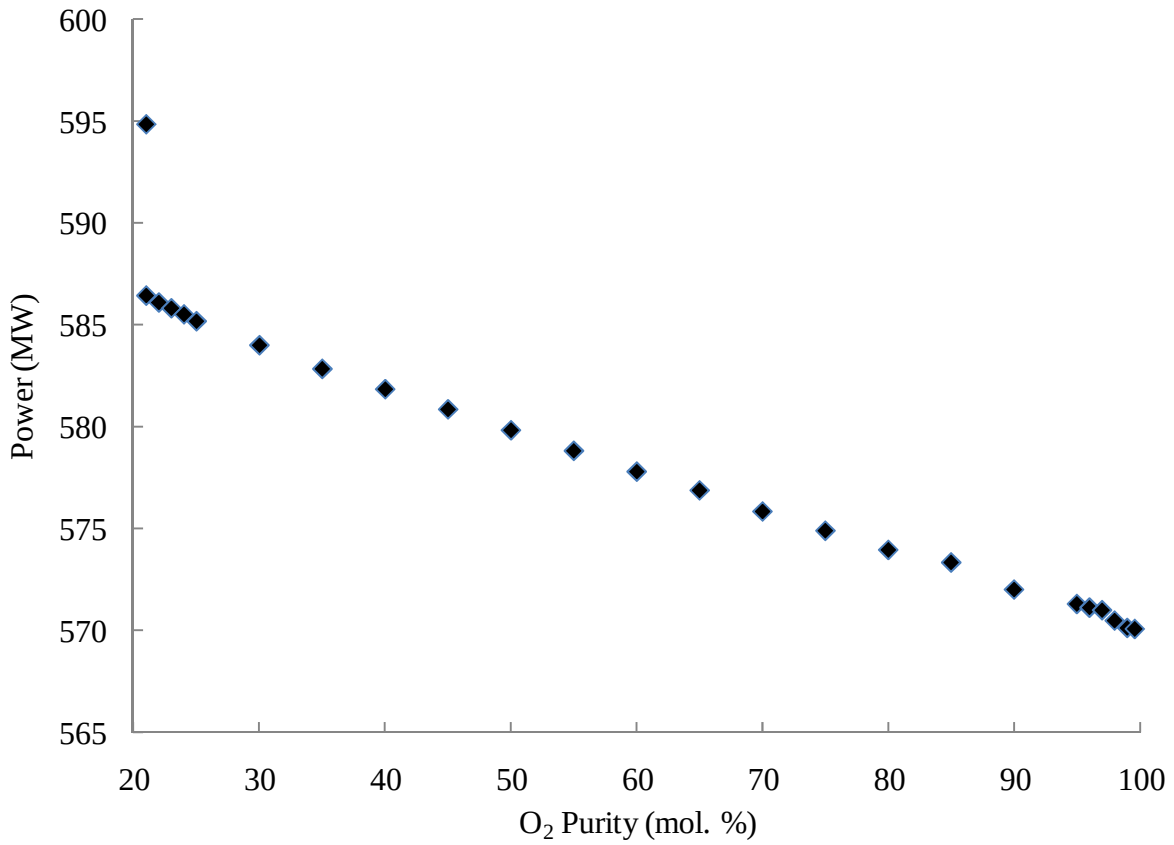

Figure 4.7. Gross power production from NGCC powerplant as O_2 purity varies.

It can be noted from Figure 4.7 that, despite the increase in steam cycle power production, losses in the gas turbine portion lead to an overall decrease in gross power production. The highest net power production is 595 MW and occurs when excess air is used to control flame temperature. In real world applications, a specific gas turbine would be designed for unique operating fluids. Optimization of the gas turbine design could lead to a reduction or elimination of generation losses. Also note that the drop off in power shown in Figure 4.7 appears exaggerated because of the smaller range of y-axis values compared to other figures shown.

Upon exit of the HRSG, the flue gas corresponding to all O_2 purities except 99.6% enters the post combustion amine scrubbing equipment. It is important to recognize that as the EGR

rates increase, the volume of gas exiting the HRSG decrease. Figure 4.8 displays the mass flow rate of exhaust gas entering the amine scrubber as well as corresponding EGR rates.

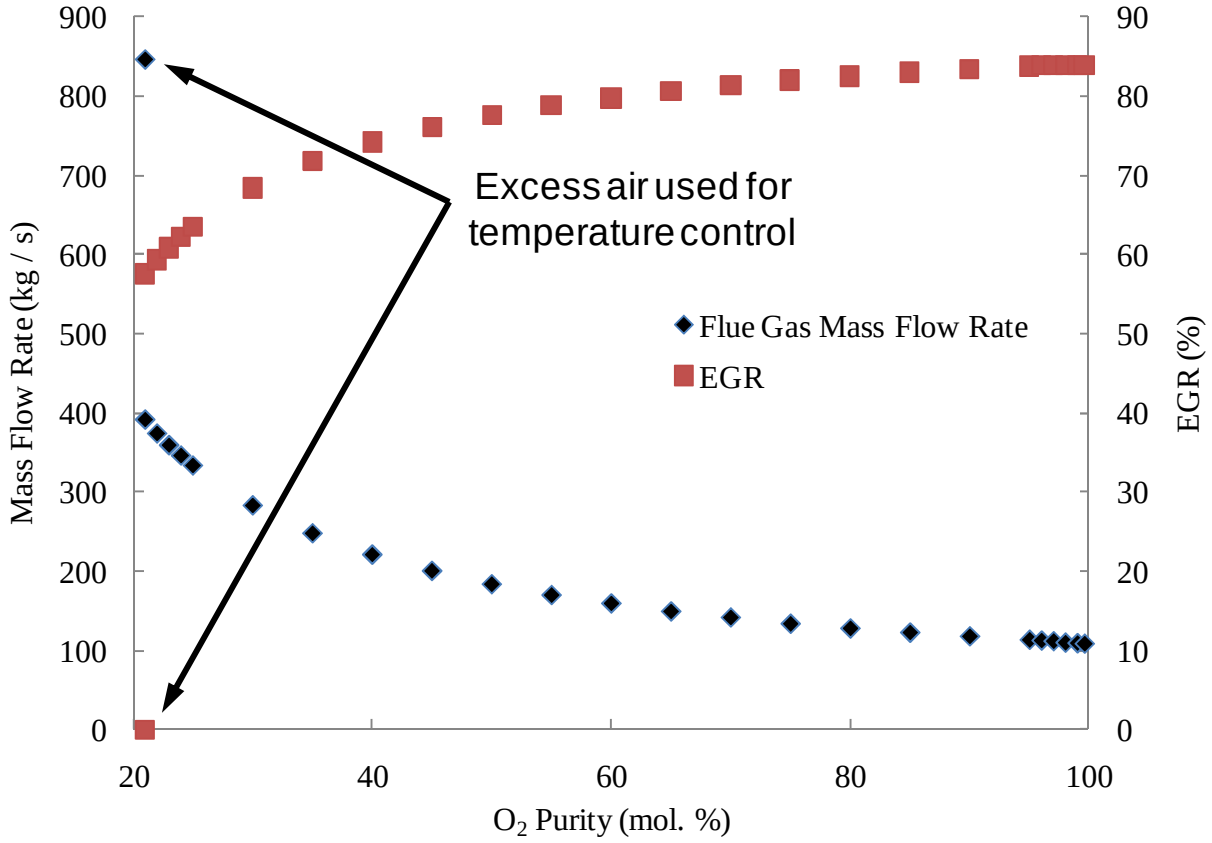

Figure 4.8. Mass flow rate of exhaust gas and corresponding EGR rates as O_2 purity varies.

It is also interesting to note that, as the O_2 purity increases, the resulting concentration of CO_2 in the exhaust gas for amine processing increases. Figure 4.9 gives a component breakdown of the flue gas exiting the HRSG on a mass basis.

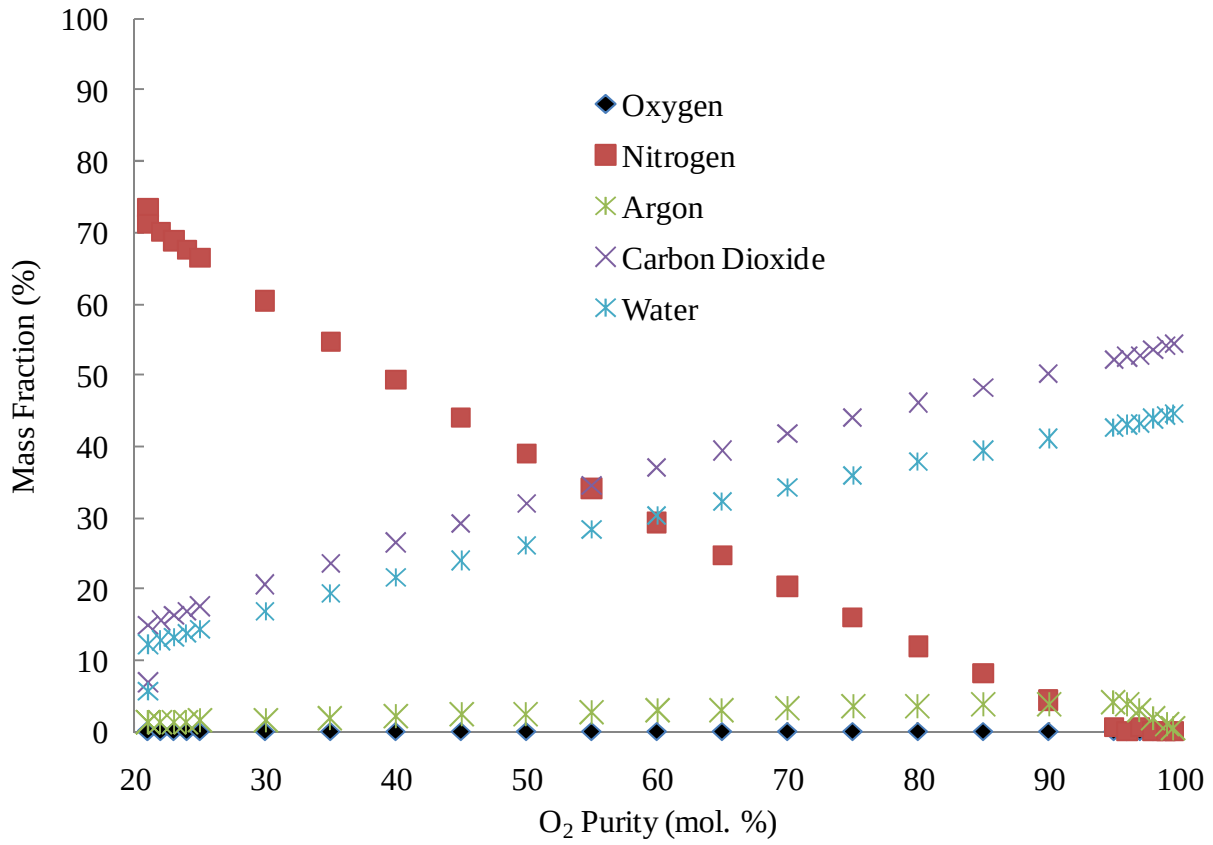

Figure 4.9. Mass composition of flue gas with varying O_2 combustion purities.

As evident in Figure 4.9, the increasing O_2 purity oxidizer supplied to the powerplant for combustion directly corresponds to a decrease in nitrogen in the exhaust gas. Additionally, as O_2 purities increase over 95%, argon is reduced in flue gas. This results from an increasing amount of argon being removed by the ASU. A constant fuel and O_2 feed rate translates into a fixed amount of CO_2 and water in the exhaust gas. Correspondingly, the reduction of nitrogen and argon increase the water and CO_2 concentration. This is the case when 99.6% purity O_2 oxygen is provided. The exhaust is 99.1% CO_2 and water. Subsequently, with dehydration and compression, a CO_2 stream with necessary purity can be achieved without amine processing. In all cases except that of excess ambient air, O_2 in the exhaust gas is practically negligible because combustion is carried out with minimal excess “air”.

4.3. CO_2 Amine Scrubber Results

Investigating the operational characteristics of the amine scrubbing system provide several interesting results. As the volume of flue gas decreases, depicted in Figure 4.8, the power consumption of the blower fan decreases, in a similar manner, from 11.1 MW to 0 MW. A consistent 58.4 kg / s of CO_2 entering the absorption column translates into a consistent feed rate of amine solution and make up water as well. Only the CO_2 is washed out of the flue gas, thus, the rest of the amine scrubbing equipment operates in a consistent manner. The cleaned gas is vented from the top of the absorption column. Its composition varies with the inlet gas composition minus the majority of the CO_2 and H_2O. The consistent nature of the process fluid exiting the absorption column renders the operational characteristics of varying O_2 purity unchanging. Consideration for necessary operational requirements is still important to the overall processes efficiency. In the stripping column, steam is required for the removal of CO_2 from the amine solution. This steam is supplied by a heat exchanger integrated into the powerplant's steam cycle. The quantitive requirement for this heating duty is 380 MW. The condenser's cooling duty in all cases is 187.5 MW. The amine scrubbing unit's cooling loop provides the necessary cooling requirements for the condenser. The cooling loop also brings the lean amine solution and inlet flue gas to the appropriate temperatures for absorption. The total cooling requirements of the loop vary from 448.6 to 523 MW. Like the entire system, the only variable affecting necessary cooling requirements is the volume of flue gas entering the unit. Across the O_2 purity ranges from 21% to 99% the CO_2 stream leaving the top of the stripper column is consistently 96% CO_2, 3.9% H_2O, and 0.1% trace gases.

4.4. CO_2 Dehydration and Compression Results

The CO_2 drying and compression unit was designed to handle both the gas stream from the amine scrubbing unit as well as the stream directly from the powerplant operating at 99.6% O_2 purity. Table 7 provides an overview of operational parameters and results for the cases presented in this study.

Table 7

CO_2 Drying and Compression Operational Parameters and Results

		21% - 99%	99.6%
Inlet Stream (kg / s)	CO_2	52.5592	58.4248
	H_2O	0.88	47.8311
	N_2	0.0086	0.0001
	Ar	0.0016	0.4276
	O_2	0	0.5149
Inlet Stream Temperature (K)		100	340
Inlet Stream Pressure (atm)		1.64	0.9412
Sequestration Stream (kg / s)	CO_2	52.5489	56.7486
	H_2O	0.0884	0.1002
	N_2	0.0086	0
	Ar	0.0016	0.0218
	O_2	0	0.0247
Sequestration Stream Temperature (˚F)		80.3	80.3
Sequestration Stream Pressure (atm)		120	120
Sequestration Stream CO_2 Purity (mol.%)		99.6	99.5
Power (MW)		17.2	22.7
Specific Power (kWh T^{-1} CO_2)		82.4	100.9

As seen in Table 7, the 99.6% O_2 purity case has a large increase in specific power consumption. This is due to the increased water content in the inlet stream. Despite a large difference in inlet

pressure, temperature, and water content, the unit produces a CO_2 stream at specified temperature and pressure with consistent 99.5% or greater CO_2 purity.

4.5. Combined Model Results

As seen in the previous results, the ASU, powerplant, amine scrubber, and drying and compression all play vital roles in carbon capture. By increasing the O_2 purity from ambient conditions to 99.6% purity and investigating the operational changes of each component, we can gain a better understanding of the overall system. The powerplant is a net electricity producer, while the other three components are consumers. In this model, the electrical requirements of the three sequestration units are provided for by the powerplant. Minimizing this parasitic loss is essential in determining the optimum operational point. Figure 4.10 depicts the electrical energy requirements for each component as O_2 purity changes.

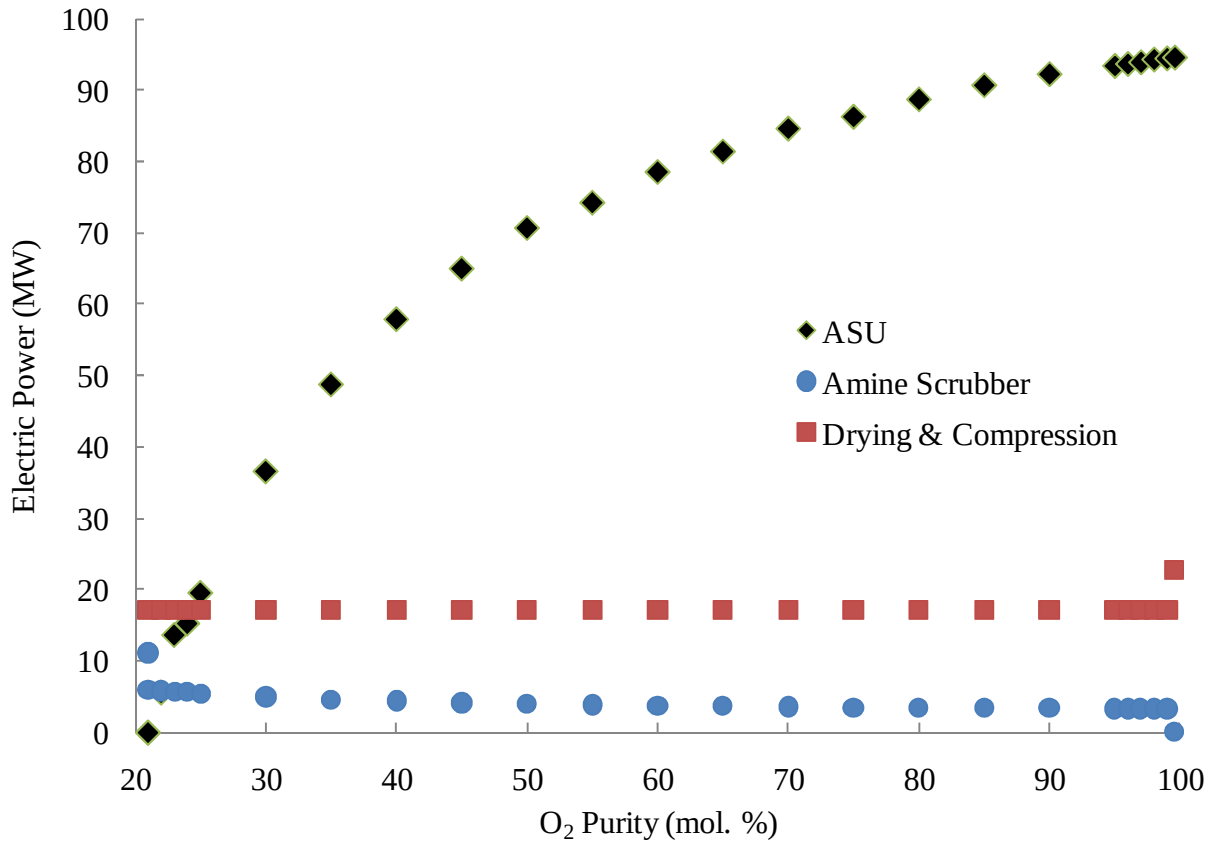

Figure 4.10. Electrical requirements for each component as O_2 purity changes.

As seen in Figure 4.10, the ASU electrical requirements increase with purity. As stated earlier, the amine scrubber's electrical requirements decrease with increasing purity. Keep in mind, however, that the amine scrubber consumes some of the steam from the steam cycle for amine desorption. This contributes additional parasitic losses at the steam turbine, not represented in Figure 4.10.

Combining the electrical production of the powerplant, with all requirements and parasitic losses will begin to reveal more about the cost of carbon capture. Figure 4.11 shows the net electrical power available for sale accounting for all losses.

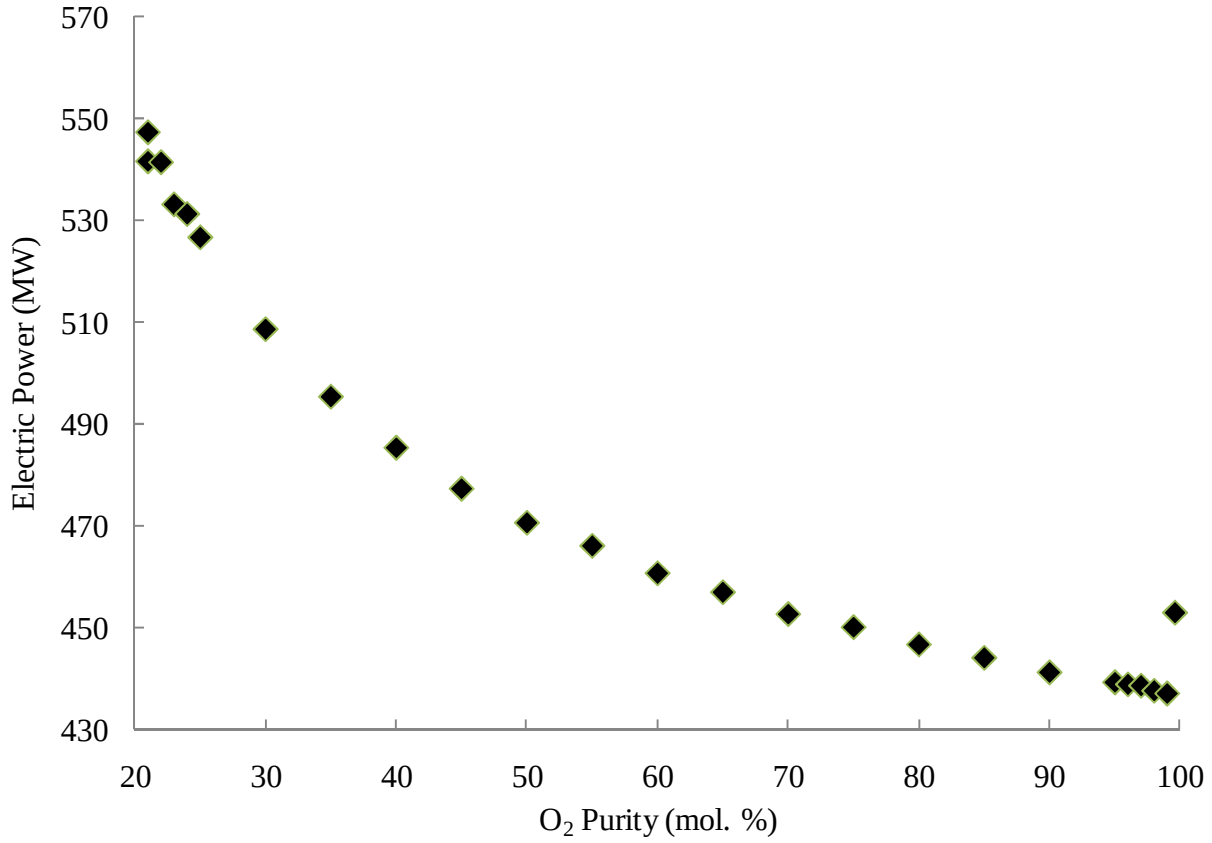

Figure 4.11. Net electrical production as O_2 purity varies.

Figure 4.11 displays a clear reduction in net power production as O_2 purity increases. Note that at the ambient condition, excess air temperature control yields 541.4 MW, while EGR temperature control yields 547.1 MW. With these net power outputs, a thermal efficiency based on the higher heating value of the fuel can be calculated. Figure 4.12 displays the net thermal efficiency of the systems as O_2 purity varies.

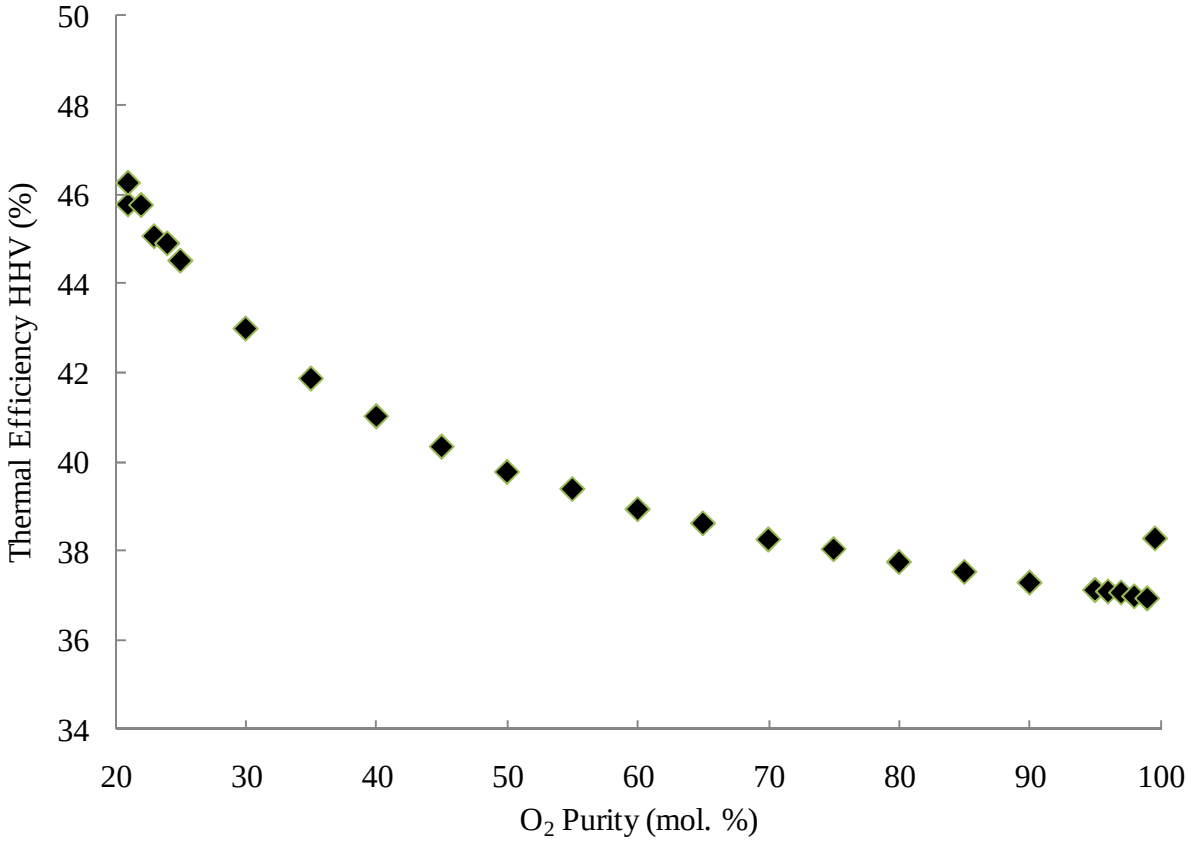

Figure 4.12. Thermal efficiency of system as O_2 purity varies.

The thermal efficiency for the unit operating without carbon capture is 54.7%. At the most efficient operating conditions, the thermal efficiency is 51.4%. This is a 3.3% reduction in efficiency. While multiple factors contribute to the reduction in net power production, the ASU plays the most significant role in the trend of the losses. At an O_2 purity of 99.6%, there is a

discontinuous 15.8 MW increase in net power production. This is due to the fact that the amine scrubbing equipment is not necessary.

Noting that without carbon capture, the powerplant is capable of producing 582 MW, we can assign a specific energy cost per mass of CO_2 avoided. Figure 4.13 depicts the specific energy cost per ton of CO_2 avoided.

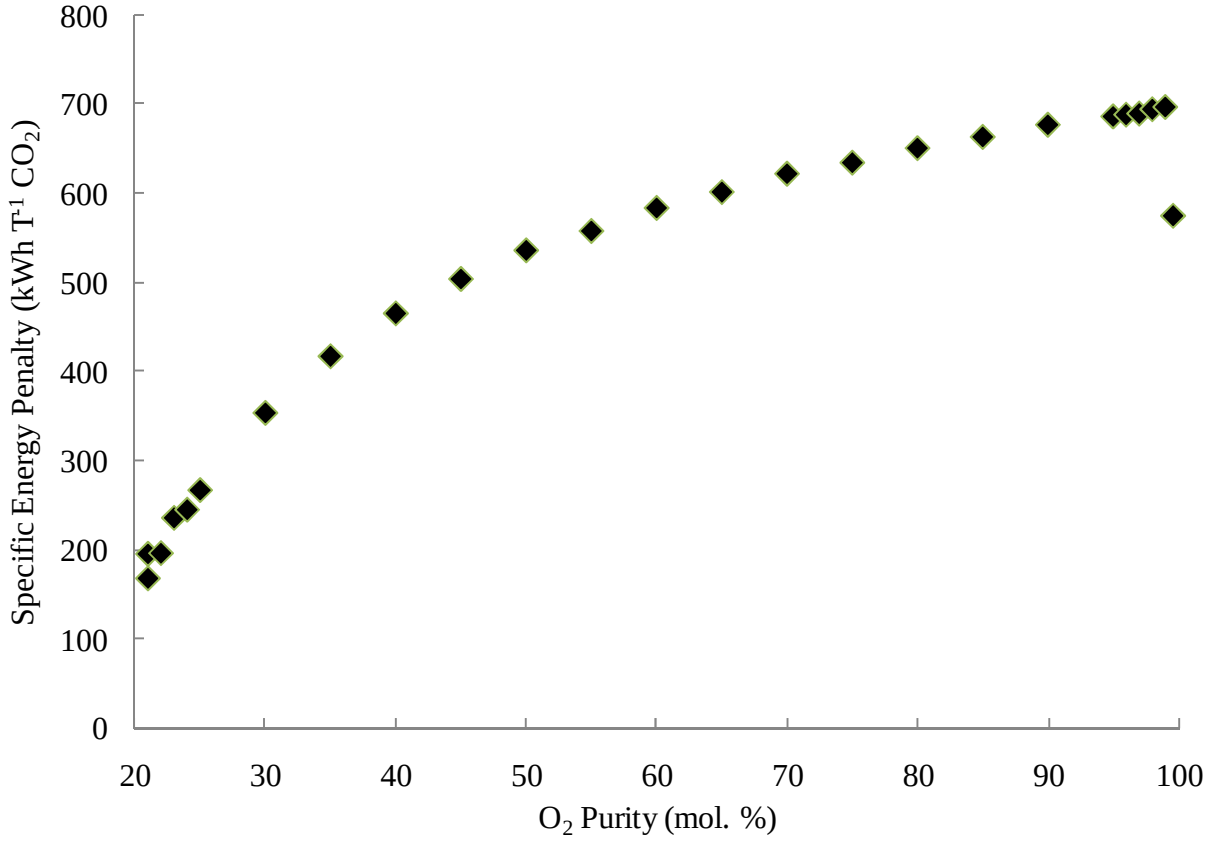

Figure 4.13. Specific energy penalty of CO_2 sequestered as O_2 purity varies.

As confirmed by Figure 4.13, the operational condition at which the specific energy penalty is minimized occurs when ambient air is used with EGR. This specific cost is 168.3 kWh T^{-1} CO_2 avoided. Taking the cost of electricity to be 0.10 $ / kWh, a cost for associated CO_2 avoided can be calculated (EIA, 2010). Figure 5.14 displays the cost variance per ton of CO_2 avoided.

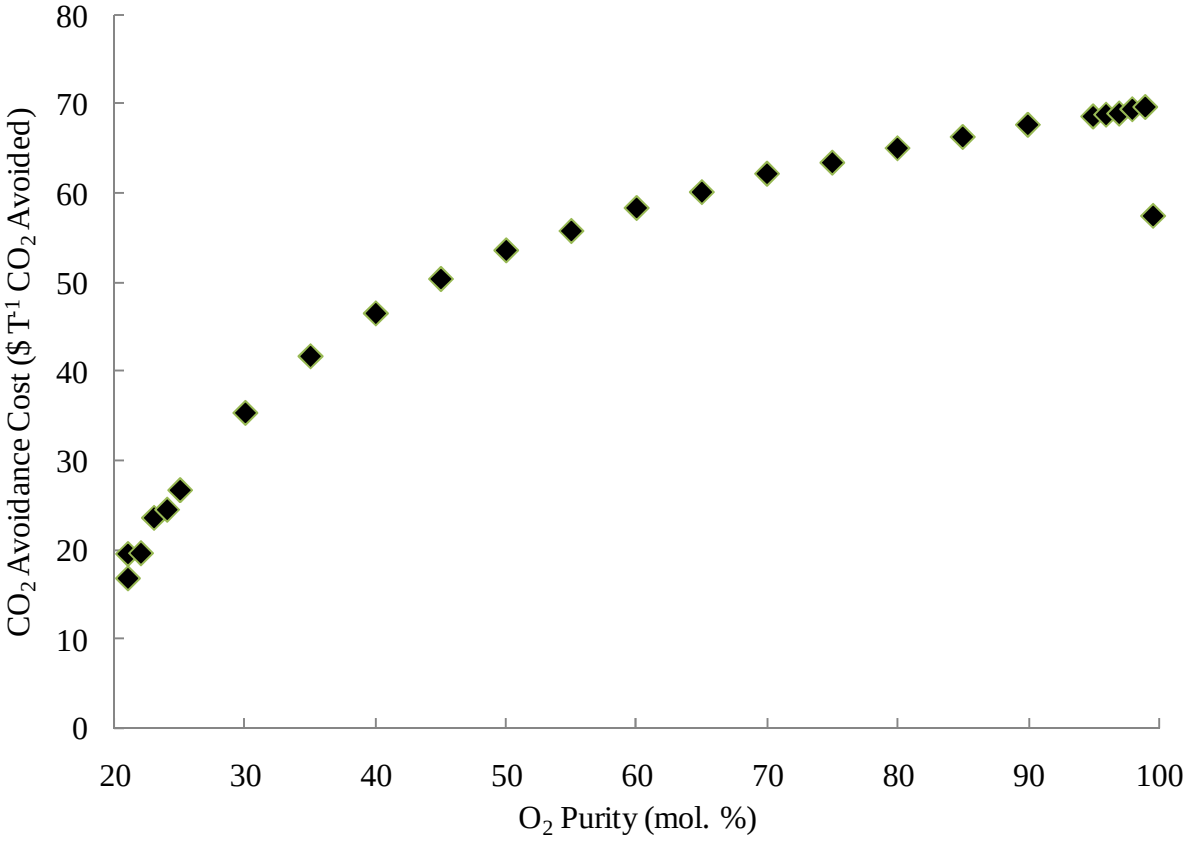

Figure 4.14. CO_2 avoidance costs with varying O_2 purity.

The costs vary from 16.8 – 69.7 \$ T^{-1} CO_2 avoided. Keep in mind that these costs are strictly reflective of the operational penalty. Capitol costs, as well as, associated maintenance expenses are not considered in this study because of the difficulty of obtaining good cost data. These additional costs would have a large impact on any real world application.

4.6. Overall Exergy & Second Law Analysis

An exergy analysis of the entire system, as well as each individual component, provides another tool for optimization consideration. Exergy is defined as the availability of energy that could be converted completely to useful work. In carrying out an exergy analysis, the ambient conditions, referred to as the "dead state" in exergy analyses, were taken as T_o = 298.15 K and P_o = 1 atm. All operational equipment was enclosed in the control volume and consideration was

given only to streams entering and exiting the control volume. Considering the entire system, the inlet streams include the ASU inlet and make up air, the powerplant's fuel stream, the amine scrubber's solution and make up water. Outlet streams include the ASU's N_2 vent, the scrubber's absorption column vent, water take off, amine recycle stream, and finally, the drying and compression CO_2 sequestration stream and waste stream. The net electrical power production was also considered as pure exergy leaving the system. Summing the exergy streams and calculating the exergy destruction allows the Second Law efficiency to be calculated for the entire system, as displayed in Figure 4.15.

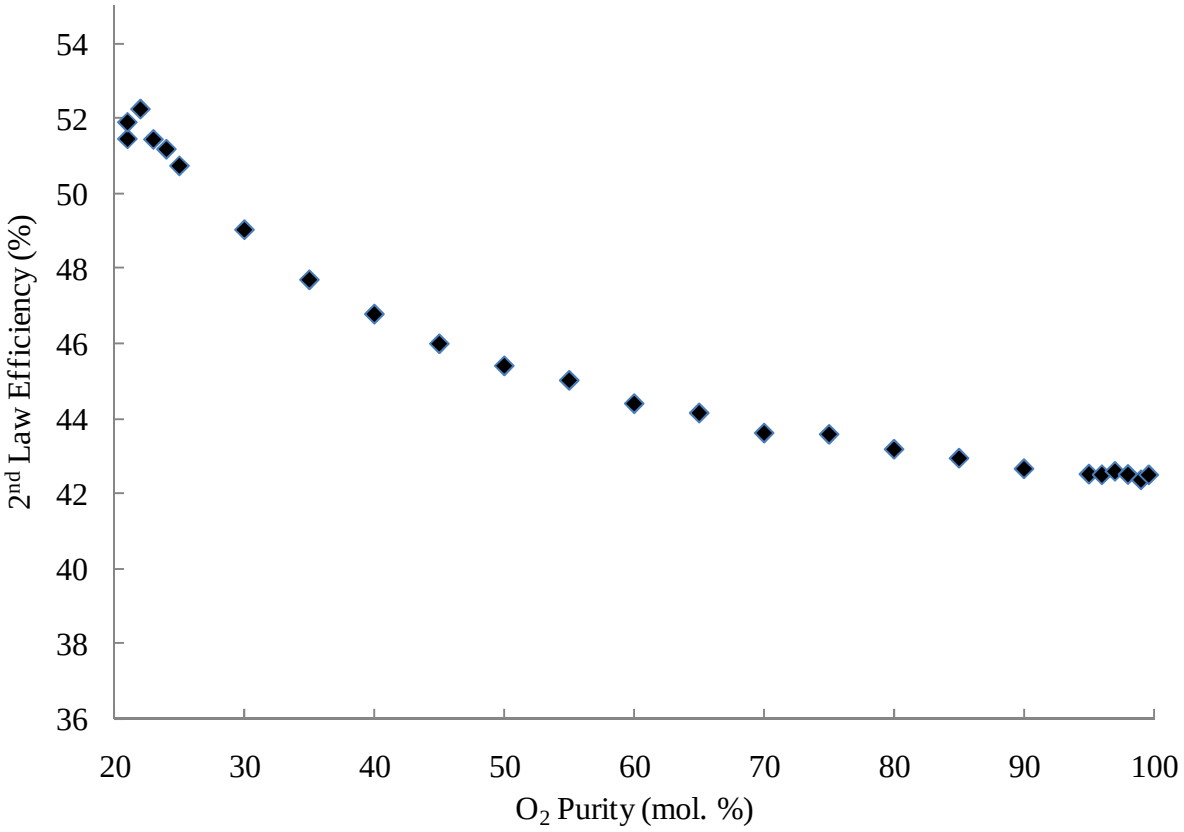

Figure 4.15. Second Law efficiency of entire system as O_2 purity changes.

As noted in Figure 4.15, the highest Second law efficiency does not occur at ambient conditions such as with the thermal efficiency. Instead, the maximum Second Law efficiency occurs at 22%

O_2 purity, with a corresponding 52.2% efficiency. The processes associated with air separation, CO_2 scrubbing, and preparation for sequestration clearly destroy exergy.

4.7. ASU Exergy & Second Law Analysis

When considering each of the four components individually, an analysis of the exergy destruction and corresponding Second law efficiency can help identify where the greatest possibility for improvement exists. The ASU consists of two inlet streams, two exit streams, as well as electrical input. Its exergy destruction and corresponding Second Law efficiency is shown in Figure 4.16.

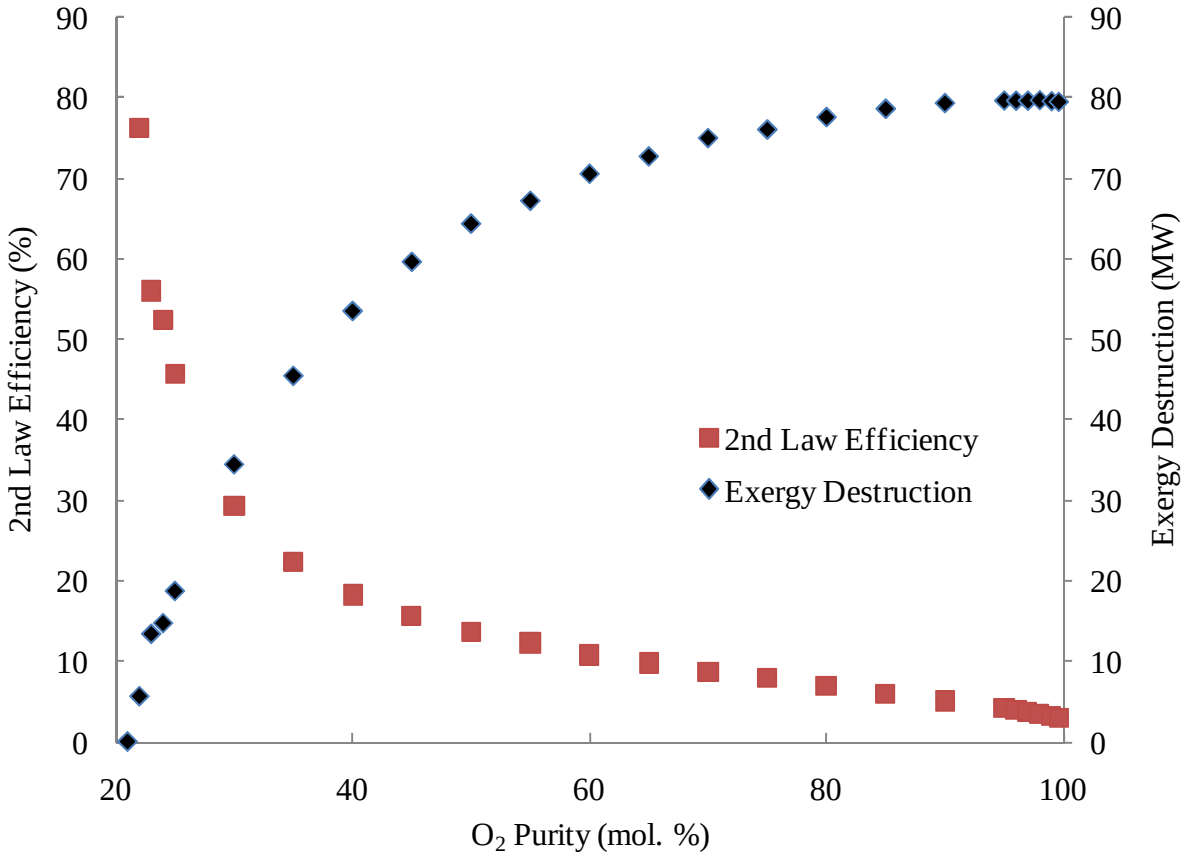

Figure 4.16. ASU's exergy destruction and Second law efficiency as O_2 purity varies.

As visualized in Figure 4.16, when O_2 purity is very low, the exergy destruction is minimized and corresponding Second Law efficiency is nearly 77%. As O_2 purity is increased, not only is

more power required, equating to more exergy destruction, but less exergy is recovered from the stream exiting the ASU. Figure 4.16 identifies that the most improvement in ASU effectiveness can be achieved at high O_2 purities.

4.8. Powerplant Exergy & Second Law Analysis

The powerplant contains two inlet streams, one exit stream, as well as electrical power output. In this component exergy analysis, the parasitic loads from the carbon capture components are not subtracted from the electrical output. Since a fixed fuel feed rate is used through all cases, a fixed fuel stream exergy inlet value exists. The oxidizer inlet stream has a decreasing exergy value corresponding to an increase in O_2 purity. Composition of the exiting exhaust gas has a decreasing exergy composition with increasing purity. Figure 4.17 displays the total exergy destruction of the powerplant and corresponding Second Law efficiency.

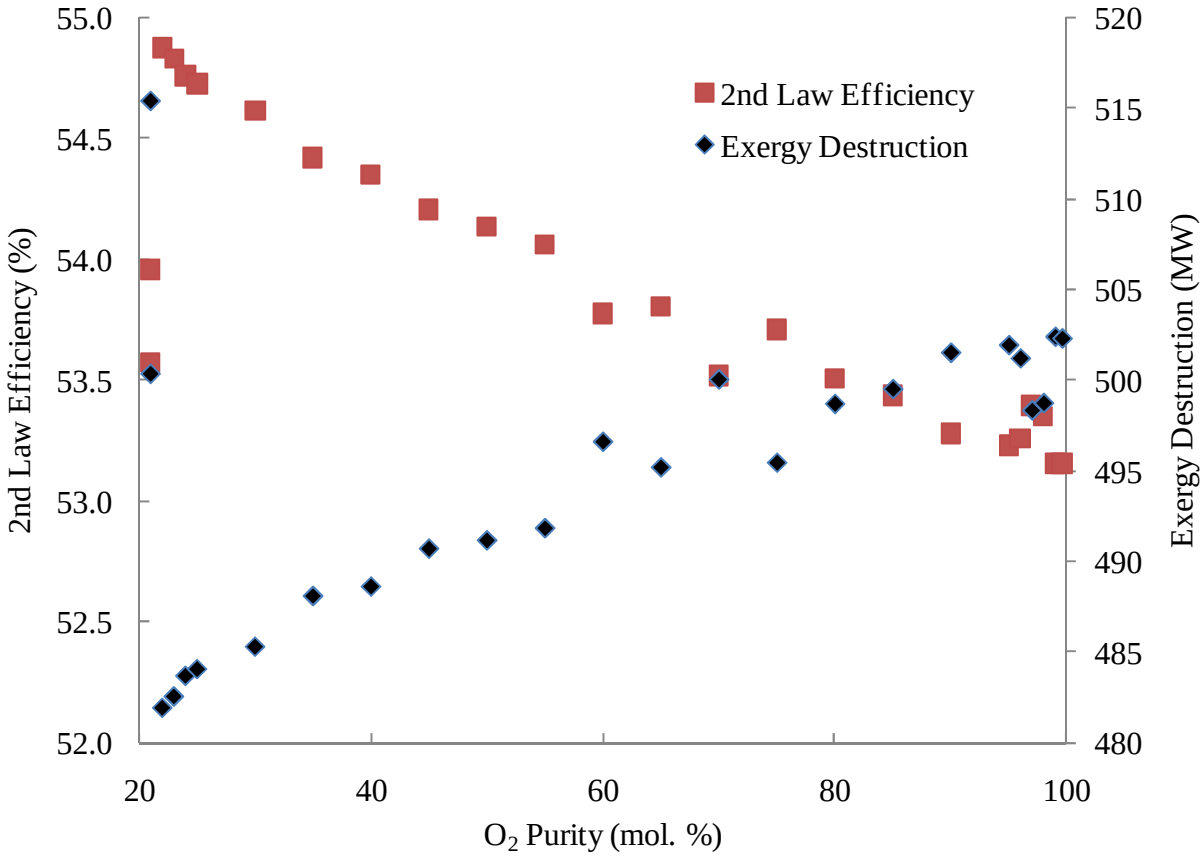

Figure 4.17. Second Law efficiency and exergy destruction of the powerplant.

Figure 4.17 indicates that operations with excess ambient air result in the largest exergy destruction. Additionally, the optimum Second Law efficiency is 54.9%, corresponding to a 22% O_2 purity.

4.9. CO_2 Amine Scrubber Exergy & Second Law Analysis

The amine scrubber contains three input streams, including the powerplant exhaust, the amine solution and the make-up water. Output streams include the absorption column vent, excess water take-off, the lean amine recirculation fluid, as well as the CO_2 stream for sequestration. The primary variance in flow exergy occurs in the absorption column vent. As the O_2 purity increases the volume of gas exiting the column decreases resulting in a decrease in exergy displayed in Figure 4.18.

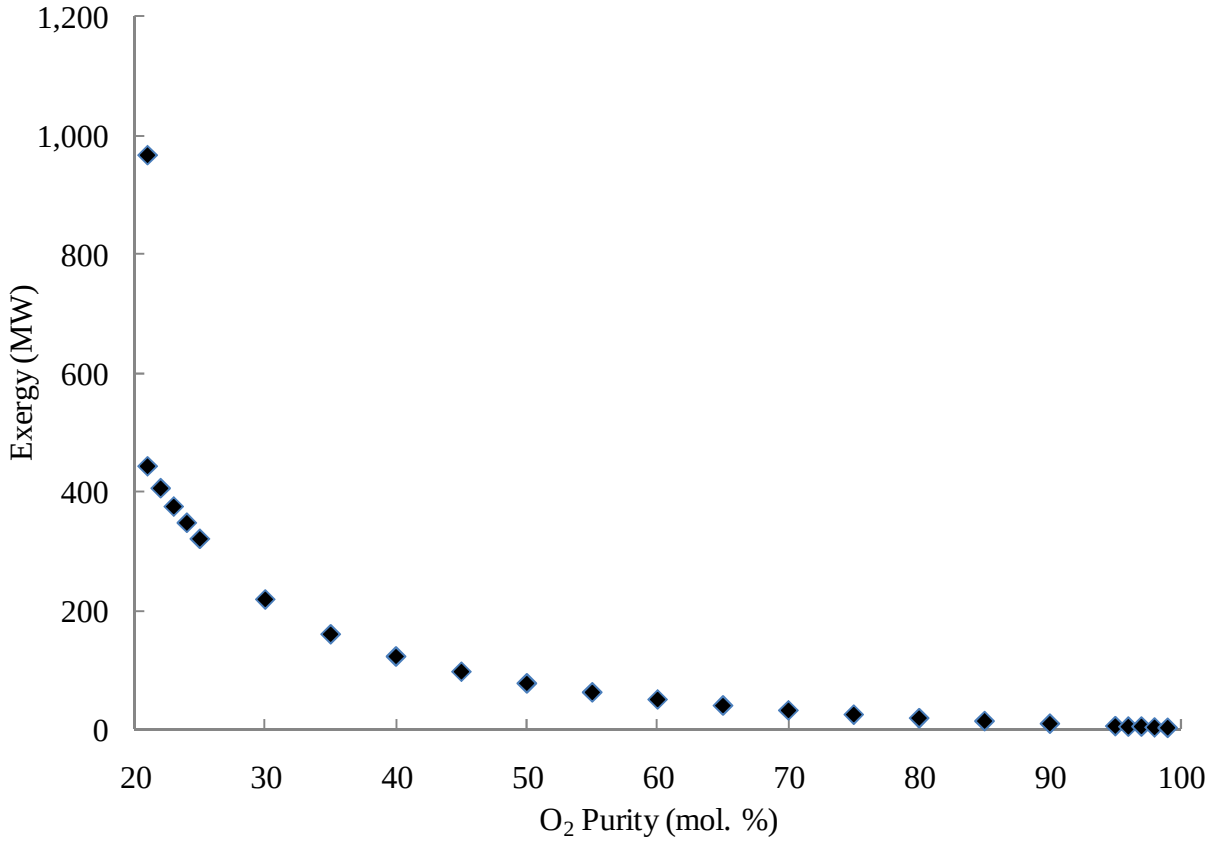

Figure 4.18. Amine scrubber absorption column vent gas exergy as O_2 purity varies.

As seen in Figure 4.18, the exergy exiting the absorption column vent decreases nearly exponentially with the increase in O_2 purity. The amine streams, make-up water, take-off water, and CO_2 sequestration stream maintain nearly constant composition and flow rates across all O_2 purities. Figure 4.19 displays the amine scrubber's overall exergy destruction.

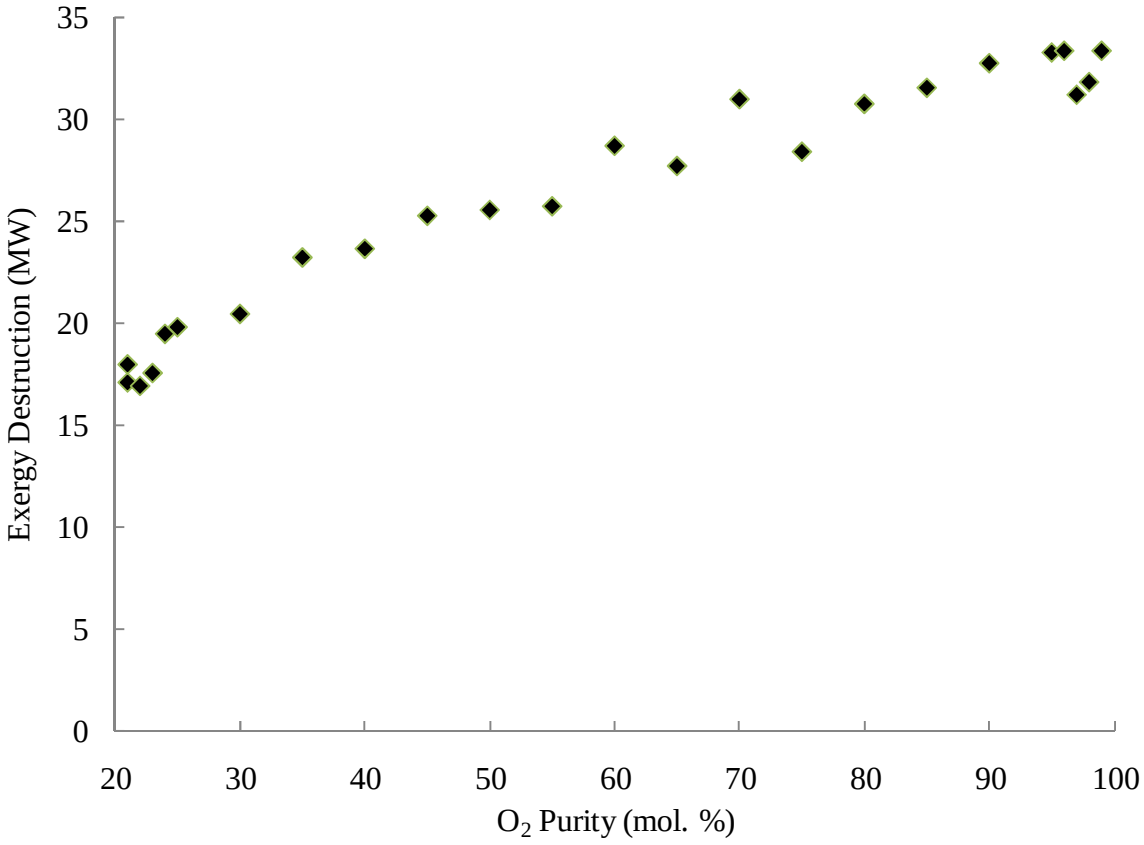

Figure 4.19. Amine scrubber overall exergy destruction with varying O_2 purity.

As seen in Figure 4.19, a minimum exergy destruction of 18.65 MW occurs at an O_2 purity of 22%. The exergy destruction ranges from 18.65 – 33.29 MW, while the exergy entering and exiting from the amine solution and make-up water are nearly 14,200 MW. This vast difference in scale renders exergy destruction's effect on Second Law efficiency nearly negligible. Because of this, the Second Law efficiency calculation yields essentially 100% for all cases.

4.10. CO_2 Dehydration & Compression Exergy & Second Law Analysis

The final component for consideration is the CO_2 drying and compression unit. This component operates under only two different circumstances. The single inlet stream is the output from either the amine scrubber when O_2 purities vary from ambient to 99%, or the powerplant exhaust when the O_2 purity is 99.6%. The outlet streams include the final CO_2 stream and the waste stream. Table 8 provides a summary of the exergy considerations for this unit.

Table 8

Exergy Analysis of CO_2 Drying and Compression Unit

	Work In (MW)	Exergy Flow In (MW)	Exergy Flow Out (MW)	Exergy Destroyed (MW)	Efficiency (%)
21 – 99%	-17.2	-481.7	-469.3	4.75	94
99.6%	-22.7	-1,131.1	-1,138.9	30.56	98

Table 8 shows the difference in exergy that is contained in the inlet and exit streams of the two cases. Again, the removal of gases by the amine stripping column allows for the similarity in streams for 21 – 99% O_2 purities.

CHAPTER 5

CONCLUSIONS AND RECOMMENDATIONS

Using the computer software CHEMCAD, models of components necessary for carbon capture from a NGCC powerplant have been created. From the validation of models presented in Chapter 4 and the results presented in Chapter 5, multiple conclusions can be drawn. As O_2 purities are increased from ambient levels to 99.6% purity, the efficiency losses associated with carbon capture range from 3.3 – 13.6%. Based on a First Law thermodynamic efficiency analysis, the optimum O_2 purity point for operation with carbon capture occurs when ambient air is used with EGR for temperature control. At this condition, the powerplant is operating at an efficiency of 51.4%. Additionally, the operational CO_2 avoidance cost is 16.8 \$ T^{-1} CO_2.

In performing an exergy analysis of the entire system, it can be noted that another point of interest exists. The exergy destruction is minimized at an O_2 purity of 22%. This corresponds with the highest Second Law operational efficiency of 52.2%. This is a 2.28% reduction in Second Law efficiency from the powerplant modeled without carbon capture. Overall, the operational point with the most room for improvement occurs when the plant is consuming 99% O_2 purity. At this point there is an exergy destruction rate of 619 MW corresponding to a Second Law efficiency of 42.4%.

The exergy analysis of each component provides information for further conclusions. The ASU, powerplant, and amine scrubber individually have minimum exergy destructions at an O_2 purity of 22%. Second Law efficiencies of the amine scrubber and CO_2 drying and compression systems are very high, at approximately 100% and mid to upper 90%, respectively. This leaves

little room for improvement. The powerplant has Second Law efficiencies varying from 53.2 – 54.9%. The combustion process, however, contributes greatly to the exergy destruction and significant improvement is not feasible. The ASU's Second Law efficiency varies from as high as 76% to as low as 3%. Air separation is highly irreversible, thus exergy destruction is going to vary in this manner. However, optimized designs for each purity case could improve these values. It should be noted that some of the streams exiting the process, such as the mostly nitrogen stream from the ASU, may have commercial value but this was not included in this analysis.

5.1. Recommendations

While the modeling of this NGCC powerplant has provided insight into operational penalties associated with carbon capture, many generalizations have been made. It is important to remember that these penalties are strictly related to operational losses. Further investigation into the associated capitol cost of necessary equipment would provide valuable costs figures. Furthermore, investigation could be conducted into the use of alternative O_2 production methods. At low purities, it may be viable to use selectively permeable membranes to produce the necessary oxygen. Finally, a better understanding of how the gas turbine operates with high concentrations of CO_2 as a working fluid would be beneficial. It may be possible to reduce the losses associated with EGR.

REFERENCES

Adiabatic Flame Temperature [Schematic]. Retrieved June 17, 2010, from http://web.mit.edu/16.unified/www/FALL/thermodynamics/notes/node111.html

Amann, J. –M., Kanniche, M., & Bouallou, C. (2009). Natural gas combined cycle powerplant modified into an O_2/CO_2 cycle for CO_2 capture. *Energy Conservation and Management, 50, 510-521.* doi. 10.1016/j.enconman.2008.11.012

Biello, D. (April 2009). Enhanced oil recovery: How to make money from carbon capture and storage today. *Scientific American,* 09. Retrieved June 22, 2010, from http://www.scientificamerican.com/article.cfm?id=enhanced-oil-recovery

Boden, T., & Marland, G. (June 8, 2010). *Global CO_2 emissions from fossil-fuel burning, cement manufacture, and gas flaring: 1751-2007*. Retrieved September 21, 2010, from http://cdiac.ornl.gov/ftp/ndp030/global.1751_2007.ems

Brayton Energy (Creator). Thermodynamic states of the Brayton cycle. [Graphic]. Retrieved September 21, 2010, from http://www.braytonenergy.net/about/

Çengel, Y. A., & Boles, B. A. (2008). *Thermodynamics: An engineering approach* (6th ed.). New York, NY: McGraw Hill.

Chase, D. L., & Kehoe, P. T., (2000). *GE combined-cycle product line and performance* (GER-3374G). Schenectady, NY: GE Power Systems. Retrieved June 21, 2010, from http://www.gepower.com/prod_serv/products/ tech_docs/ en/downloads/ger3574g.pdf

Chemicalogic. (Creator). (1999). CO_2 phase diagram [Schematic]. Retrieved June 18, 2010, from http://www.chemicalogic.com/download/co2_phase_diagram.pdf

Chemstations Inc. (2010). CHEMCAD (Version 6.3.0) [Computer software]. Houston, TX: Chemstations Inc.

Cleaver Brooks. (2006). CB energy recovery: HRSG fundamentals. Retrieved June 17, 2010, from http://www.hrsg.com/heat_exchangers.htm

Cormos, A. M., Gaspar, J., Padurean, A., Cormos, C. C., & Agachi, S. (2010). *Techno-economical analysis of carbon dioxide adsorption in mono-ethanolamine by mathematical modeling and simulation.* 20th European Symposium on Computer Aided Process Engineering. Retrieved June 25, 2010, from http://www.undeerc.org/PCOR/ default.aspx

Edwards, J. E., & MacDonald, M. (n.d.). *Powerplant carbon capture with CHEMCAD*. Houston, TX. Chemstations. Retrieved May 23, 2010, from http://www.chemstations.com/content/documents/Technical_Articles/Power_Plant_Carbon_Capture_with_CHEMCAD.pdf

Energy Information Administration (EIA). (April 2, 2004). What are greenhouse gases? Retrieved June 18, 2010, from http://www.eia.doe.gov/oiaf/1605/ggccebro/chapter1.html

Energy Information Administration (EIA). (2009). Annual energy outlook 2009: With projections to 2030. Retrieved June 22, 2010, from www.eia.doe.gov/oiaf/aeo/

Energy Information Administration (EIA). (January 21, 2010). Electric power annual. Retrieved October 8, 2010, from http://www.eia.doe.gov/cneaf/electricity/epa/epates.html

Environmental Protection Agency (EPA). (April 2010a). *2010 U.S. greenhouse gas inventory report (3-1)*. (U.S. EPA # 430-R-10-006). Retrieved September 21, 2010, from http://epa.gov/climatechange/emissions/usinventoryreport.html

Environmental Protection Agency. (June 3, 2010b). National ambient air quality standards. Retrieved June 18, 2010, from http://www.epa.gov/air/criteria.html

Etheridge, M., Steele, L.P., Langenfelds, R.L., Francey, R.J.,Barnola, J.-M., & Morgan, V.I. (1998). Historical CO_2 records from the Law Dome DE08, DE08-2, and DSS ice cores. *Trends: A Compendium of Data on Global Change*. Carbon Dioxide Information Analysis Center, Oak Ridge National Laboratory, U.S. Department of Energy, Oak Ridge, TN. Retrieved August 28, 2010, from http://cdiac.ornl.gov/trends/co2/lawdome.html

Flame temperatures for various fuels [Schematic]. Retrieved June 17, 2010, from http://en.wikipedia.org/wiki/File:Cvft.jpg

Ganapathy, V. (Nov. 2001). Options for improving the efficiency of recovery steam generators. *Electric Energy Magazine,* Nov. 2001. Retrieved June 17, 2010, from http://www.electricenergyonline.com/?page=show_article&mag=2&article=14

Gottlicher, G., & Pruschek, R. (1997). Comparison of CO_2 Removal Systems for Fossil-Fuelled Powerplant Processes. *Energy Conservation and Management, 38, 173-178.* doi. 0196-8904/97

Intergovernmental Panel on Climate Change (IPCC). (2005). *Carbon dioxide capture and storage*. New York: Cambridge University Press: Metz, B., Davidson, O., Coninck, H., Loos, M., & Meyer, L. (Eds.).

International Energy Agency (IEA). (n.d.). Storing CO_2 in unminable coal seams. *IEA Greenhouse Gas R & D Programme*. Retrieved June 22, 2010, from http://www.ieaghg.org/docs/general_publications/8.pdf

Jensen, M. D., Musich, M. A., Ruby, J.D., Steadman, E. N., & Harju, J. A. (June 2005). Carbon Separation and Sequestration. *Plains CO_2 Reduction Partnership.* Retrieved June 23 2010, from http://www.netl.doe.gov/technologies/carbon_seq/partnerships/phase1/pdfs/CarbonSeparationCapture.pdf

Kawasaki Gas Turbine [Photograph]. Retrieved June 17, 2010, from http://www.directindustry.com/prod/kawasaki-gas-turbines/gas-turbine-17850-148941.html

Linde AG. (2008). *Cryogenic air separation: History and technological progress*. Retrieved June 24, 2010, from http://www.linde-engineering.com/process_plants/air_separation_plants/documents/L_History_e_100dpi_08.pdf

National Energy Education Development Project (NEED). (n.d.). *Natural Gas*. Retrieved October 3, 2010, from http://www.need.org/needpdf/infobook_activities/IntInfo/NGasI.pdf

National Energy Technology Laboratory (NETL). (April 2008). *Weyburn carbon dioxide sequestration project*. Retreived June 26, 2010, from http://www.netl.doe.gov/publications/factsheets/ project/Proj282.pdf

National Fuel Cell Research Center: University of California, Irvine. Energy tutorial: Gas turbines. Retrieved June 17, 2010, from http://www.nfcrc.uci.edu/EnergyTutorial/gasturbine.html

National Oceanic and Atmospheric Administration (NOAA). (September 8, 2010). Global trends in atmospheric carbon dioxide. Retrieved September 21, 2010, from http://www.esrl.noaa.gov/gmd/ccgg/trends/#global_data

Siemens AG. (2008a). *Siemens steam turbine-generator SST-5000 Series*. Orlando, FL: Siemens Power Generation, Retrieved June 18, 2010, from http://www.energy.siemens.com/hq/pool/hq/power-generation/steam-turbines/downloads/SST-5000.pdf

Siemens AG. (2008b). *Siemens gas turbine SGT6-5000F application overview*. Orlando, FL: Siemens Power Generation, Retrieved June 18, 2010, from http://www.energy.siemens.com/us/pool/hq/power-generation/gas-turbines/downloads/SGT6-5000F_ApplicationOverview.pdf

Singh, D., Croiset, E., Douglas, P. L., & Douglas, M. A. (2003). Techno-economic study of CO_2 capture from and existing coal-fired power plant: MEA scrubbing vs. O_2/CO_2 recycle combustion. *Energy Conservation and Management, 44, 3073-3091*. doi: 10.1016/S0196-8904(03)00040-2

Statoil. (2009). *Sleipner West*. Retrieved June 22, 2010, from http://www.statoil.com/en/ TechnologyInnovation/ NewEnergy/Co2Management/ Pages/SleipnerVest.aspx

Stine, W. & Geyer, M. (Creators). (October 2004). Simple Rankine cycle [Graphic]. Retrieved September 21, 2010, from http://www.powerfromthesun.net/

Turns, S. (2000). *An introduction to combustion: Concepts and applications* (Second ed.). Boston, MA: McGraw Hill.

U.S. Department of Energy Genome Programs. (Creator). (Sept. 24, 1999). Simplified representation of the global carbon cycle [Graphic]. Retrieved June 18, 2010, from http://genomicscience.energy.gov/benefits/simple.shtml

APPENDIX

Table 9

CHEMCAD Powerplant Model Specifications

Unit ID	Component	Input Value	Range or Factor	Units
1	Stream Divider	Flow Ratio	varies	-
2	Turbine Expander	Pressure Ratio	0.0625	atm
		Efficiency	0.85	%
3	Pump	Outlet Pressure	174	atm
		Efficiency	0.85	%
4	Turbine Expander	Pressure Ratio	0.0625	atm
		Efficiency	0.85	%
5	Stream Mixer	-	-	-
6	Turbine Expander	Pressure Ratio	0.0625	atm
		Efficiency	0.85	%
7	Compressor	Outlet Pressure	16	atm
		Efficiency	0.9	%
8	Stream Mixer	-	-	-
10	Gibbs Reactor	Thermal Mode	adiabatic	-
11	Heat Exchanger	Heat Duty	varies	MW
		Pressure Drop	0.01	atm
12	Compressor	Outlet Pressure	16	atm
		Efficiency	0.9	%
14	Gibbs Reactor	Thermal Mode	adiabatic	-
16	Stream Mixer	-	-	-
18	Turbine Expander	Pressure Ratio	0.058824	-
		Efficiency	0.9	%
20	Turbine Expander	Pressure Ratio	0.058824	-
		Efficiency	0.9	%
25	Heat Exchanger	Exhaust Stream Outlet Temperature	444.261	K
		Steam Cycle Stream Outlet Temperature	866.483	K
26	Stream Mixer	-	-	-
28	Stream Divider	Flow Ratio	0.5/0.5	-
29	Pump	Outlet Pressure	87	atm
		Efficiency	0.85	%
31	Cooling Tower	Outlet Temperature	299.817	K
		Pressure Drop	-1	atm

Table 10

CHEMCAD ASU Model Specifications

Unit ID	Component	Input Parameter	Range or Factor	Units
1	Compressor	Outlet Pressure	3.0	atm
		Efficiency	0.9	%
2	Compressor	Outlet Pressure	9.0	atm
		Efficiency	0.9	%
3	Valve	Outlet Pressure	5.0	atm
4	Distillation Column	Distillate Component Mole Fraction	0.98	% N_2
			0.996	% O_2
		Bottom Component Mole Fraction	7	-
			0.05	kg /s
		Side Product Stage	1	atm
		Side Product Liquid Mass Flow	1	atm
		Top Pressure	35	-
		Bottom Pressure	5	-
		No. of Stages	30	-
		Top Feed Stream Stage		
		Bottom Feed Stream Stage		
5	Valve	Outlet Pressure	1	atm
6	Controller	Adjust Inlet Stream Total Mass Rate Until Stream 11 is Specified	varies	-
7	Valve	Outlet Pressure	1	atm
8	Stream Mixer	-	-	-
9	Pump	Outlet Pressure	3	atm
		Efficiency	0.9	%
10	Stream Mixer	-	-	-
11	Cooling Tower	Pressure Drop	2	atm
		Exit Temperature	298	K
12	Distillation Column	Distillate Component Mole Fraction	0.99	% N_2
			0.5	% O_2
		Bottom Component Mole Fraction	5	atm
			20	-
		Top Pressure	15	-
		No. of Stages		
		Feed Stream Stage		
13	Heat Exchanger	Cooling Stream Output Temperature	300	K
			350	K
		Air Output Temperature	0.1	atm
		Pressure Drop		
16	Multi-Stream Heat Exchanger	Output Stream Temperatures	300	K
		Pressure Drop	0.01	atm

Table 11

CHEMCAD Amine Scrubber Model Specifications

Unit ID	Component	Input Value	Range or Factor	Units
1	Pump	Outlet Pressure	3	atm
		Efficiency	0.9	%
2	Compressor	Outlet Pressure	1.01	atm
		Efficiency	0.85	%
3	Stream Divider	Flow Ratio	0.33 / 0.66	-
4	Distillation Column	Top Pressure	1.00074	atm
		Column Pressure Drop	0.13422	atm
		No. of Stages	16	-
		Top Feed Stage	1	-
		Middle Feed Stage	3	-
		Bottom Feed Stage	16	-
5	Heat Exchanger	Stream Pressure Drops	0.01	atm
		Cooling Loop Outlet Temperature	305	K
		Exhaust Gas Stream Outlet Temperature	329	K
8	Heat Exchanger	Stream Pressure Drops	0.197385	atm
		Rich Amine Stream Outlet Temperature	378.15	K
11	Heat Exchanger	Lean Amine Stream Outlet Temperature	323	K
14	Distillation Column	Top Pressure	1.64	atm
		Column Pressure Drop	0.296077	atm
		Bottom Pump Pressure	1.97385	atm
		No. of Stages	20	-
		Feed Stream Stage	2	-
		Distillate Temperature	310.95	K
		Reboiler Duty	380	MW
		Side Product Liquid Mole Flow	0.9311	kg / s
		Side Product Stage	1	-
16	Pump	Pressure Increase	2.46731	atm
		Efficiency	0.7	%
17	Pump	Pressure Increase	1.97385	atm
		Efficiency	0.7	%
20	Stream Mixer	-	-	-
22	Stream Divider	Flow Ratio	0.33 / 0.66	-
28	Unit Controller	Set Input Heat Duty of Unit 30 Equal to Unit 14 Condenser Heat Duty	-	-
29	Cooling Tower	Output Temperature	298	K
		Pressure Drop	2	atm
30	Heat Exchanger	Pressure Drop	0.01	atm
		Heat Duty (Controlled by Unit 28)	varies	MW

Table 12

CHEMCAD CO_2 Drying and Compression Model Specifications

Unit ID	Component	Input Value	Range or Factor	Units
1	Valve	Output Pressure	1	atm
2	Compressor	Output Pressure	3	atm
		Efficiency	0.9	%
3	Compressor	Output Pressure	15	atm
		Efficiency	0.9	%
4	Compressor	Output Pressure	40	atm
		Efficiency	0.9	%
5	Flash Separator	Flash Mode - Use inlet T and P	-	-
6	Pump	Outlet Pressure	3	atm
		Efficiency	0.9	%
7	Stream Mixer	-	-	-
8	Flash Separator	Flash Mode - Use inlet T and P	-	-
10	Heat Exchanger	Pressure Drops	0.01	atm
		CO_2 Stream Outlet Temperature	310	K
11	Heat Exchanger	Pressure Drops	0.01	atm
		CO_2 Stream Outlet Temperature	310	K
12	Heat Exchanger	Pressure Drops	0.01	atm
		CO_2 Stream Outlet Temperature	300	K
13	Cooling Tower	Pressure Drop	2	atm
		Outlet	301	K
14	Heat Exchanger	Pressure Drops	0.01	atm
		Cooling Loop Stream Outlet Temperature	300	K
		CO_2 Stream Outlet Temperature	300	K
15	Flash Separator	Flash Mode - Use inlet T and P	-	-
16	Flash Separator	Flash Mode - Use inlet T and P	-	-
18	Stream Mixer	-	-	-
19	Pump	Outlet Pressure	3	atm
		Efficiency	0.9	%